



The CMS Pixel detector - from Physics to Technology

Caterina Vernieri, Fermilab

26 August 2016

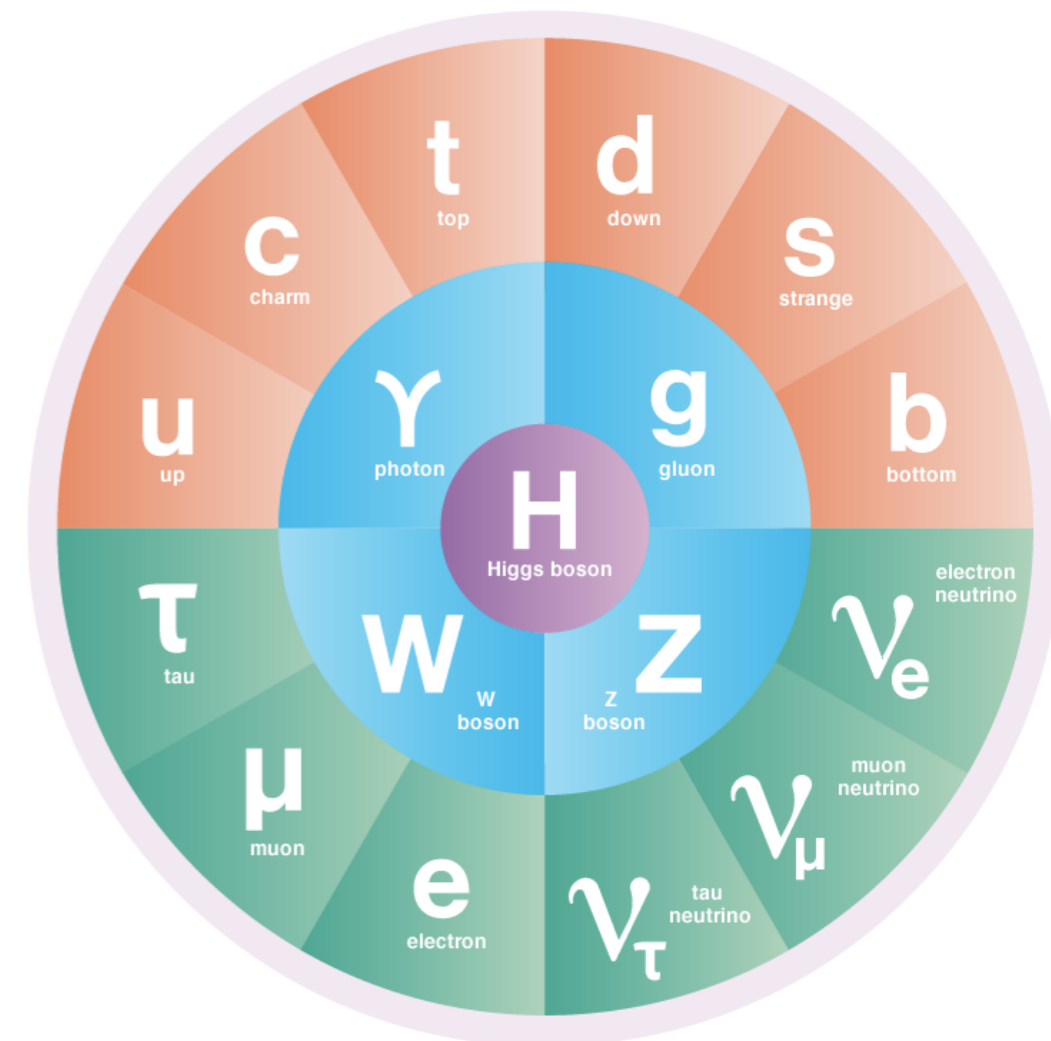
Outline

- LHC and its physics
 - an example, b quark reconstruction
- Semiconductor detectors
- CMS pixel detector and its evolution
- R&D for HL-LHC

Standard Model and Beyond at the LHC

- An important part of the **LHC** physics program is
 - to perform precision measurements of top quark and Higgs boson properties
 - it will provide a **crucial test for the Standard Model**
 - to look for **physics beyond the SM** (BSM)
- The **Higgs** boson is the only fundamental scalar
- The **top** quark is the SM particle most strongly coupled to the Higgs.
- New **BSM** states can generically couple preferentially to the Higgs and top sector [*]
- **b-tagging plays a critical role**
 - important for measurements of SM processes ($t \rightarrow Wb$, $H \rightarrow b\bar{b}$) and **searches for new physics**
 - to identify high p_T top and Higgs in new physics searches

[*] <https://arxiv.org/pdf/1110.6670v2.pdf>
<https://arxiv.org/abs/0804.1954>
<https://arxiv.org/abs/hep-ph/9905221>



The LHC

Proton-proton collider (27 km)

2010-2013, first collisions at **7** and **8 TeV**

~29fb⁻¹ delivered by the end of Run I

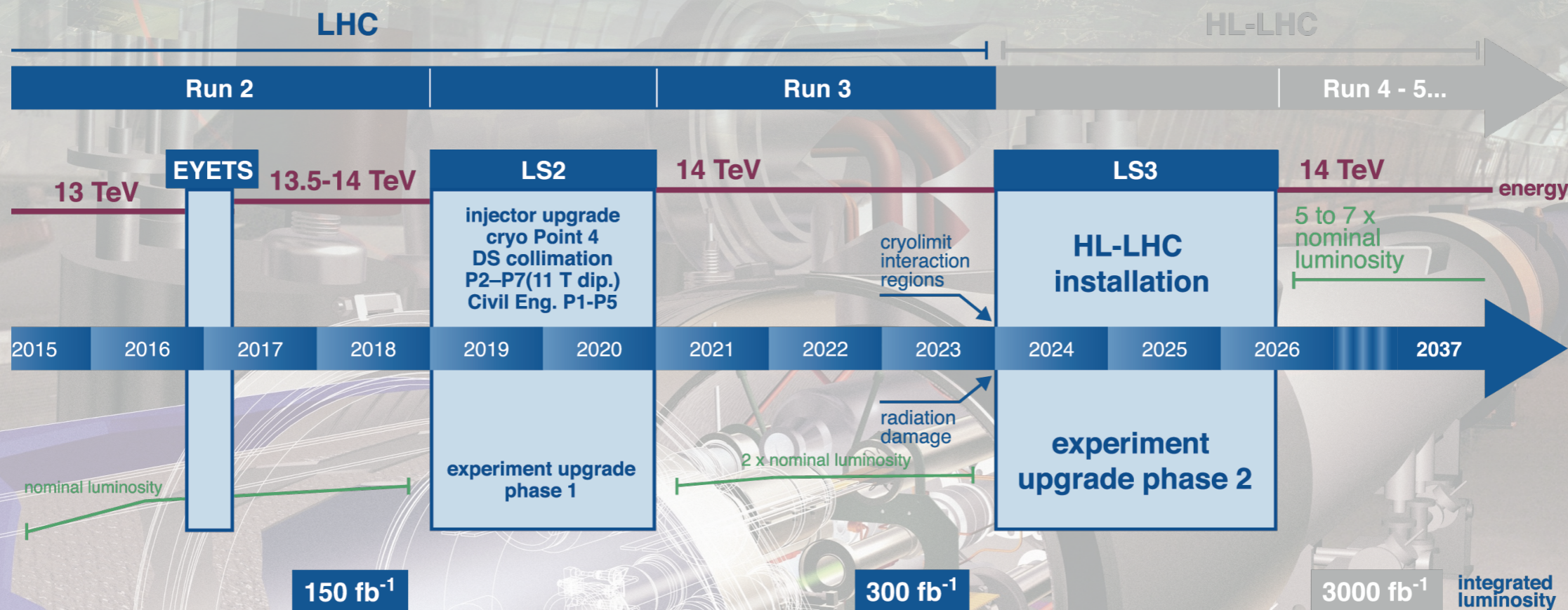
On average ~**10-20** p-p interactions per bunch crossing (**pileup**)

2015-2016, ~28 fb⁻¹ delivered in Run II at **13 TeV**

the last big jump in energy for a while, on average ~**30-40 pileup**

2018, up to **80 pileup**

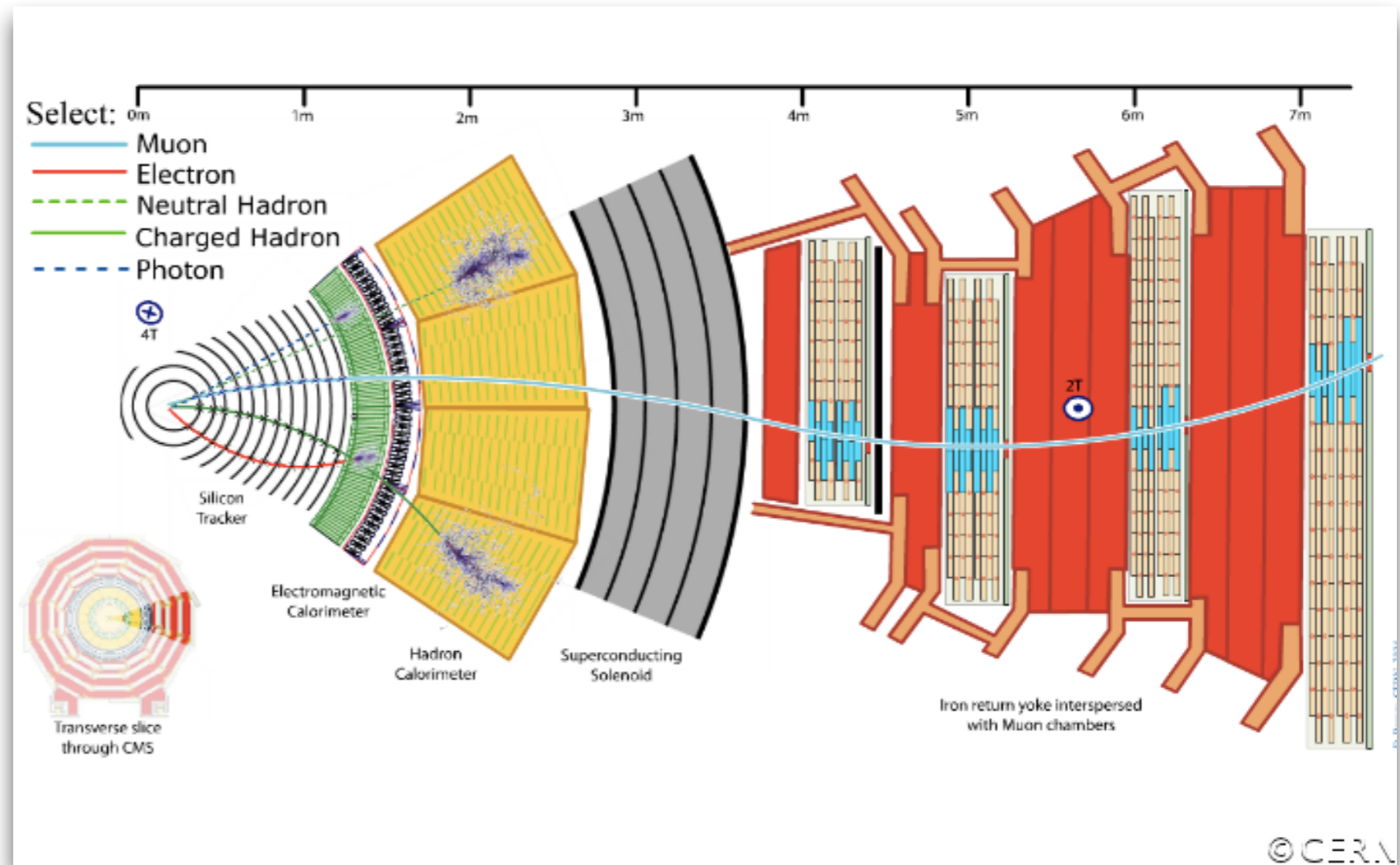
2025, **140-200 pileup**



Detectors for LHC

A **general purpose detector** :

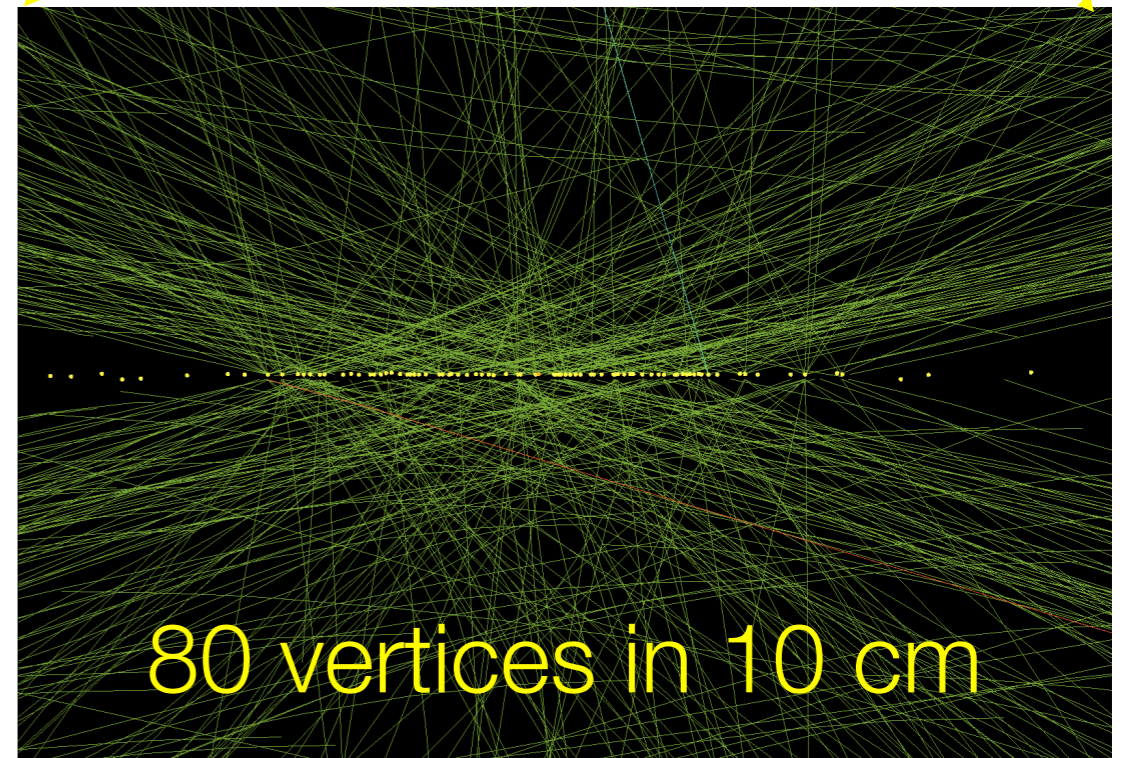
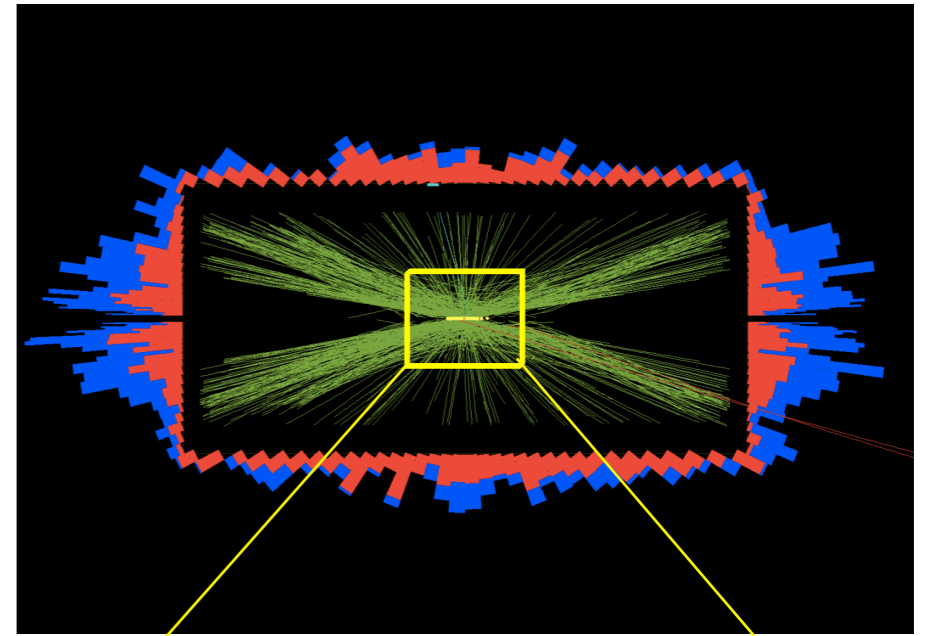
- * high granularity vertex detector
- * magnetic field
- * tracking system
- * electromagnetic and hadronic calorimeters
- * muon detectors



- * Charged and neutral particles produced in each p-p interactions are reconstructed as signal in one or more sub detectors
- * Neutrinos are partially reconstructed assuming energy conservation
- * In CMS there is a Level 1 trigger (based on muon and calorimeters) which filters events
 - * The rate is reduced from 40 MHz to ~100 kHz
 - * Then by using also the information from the tracking system it is further reduced in HLT to ~1kHz

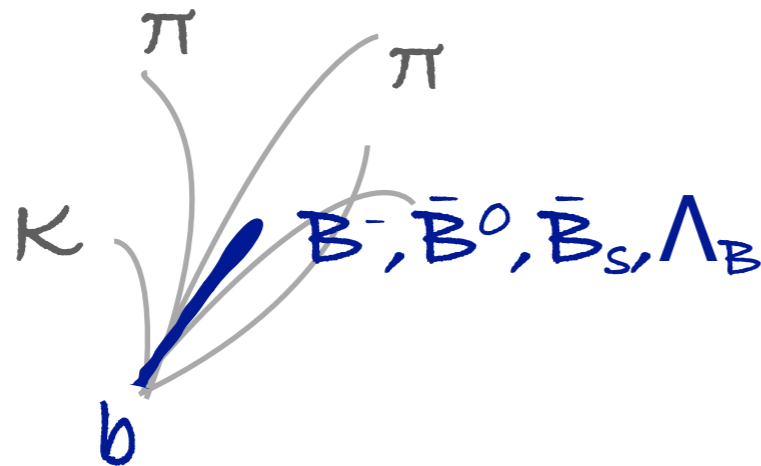
Pileup

- The **instantaneous luminosity will be increasing** creating more challenging experimental environments
- As the instantaneous luminosity of the LHC increases, we will be inundated with additional pp interactions on top of our process of interest
- Narrow beams produce a **narrow interaction region**
 - $\sim 15\text{-}20\ \mu\text{m}$ wide for 2012 data taking
- The beam spot does not tell us where along the beam axis the interaction point is (z-axis)
- Because of several collisions per crossing, information on the **z position is critical** to identify the primary vertex
 - **High resolution vertex detector** is needed



B properties useful for its tagging

b quarks hadronize



- **Measurable lifetime**

$$c\tau \sim 500 \mu\text{m} \rightarrow \beta\gamma c\tau \sim 5\text{mm} @ 50 \text{ GeV}$$

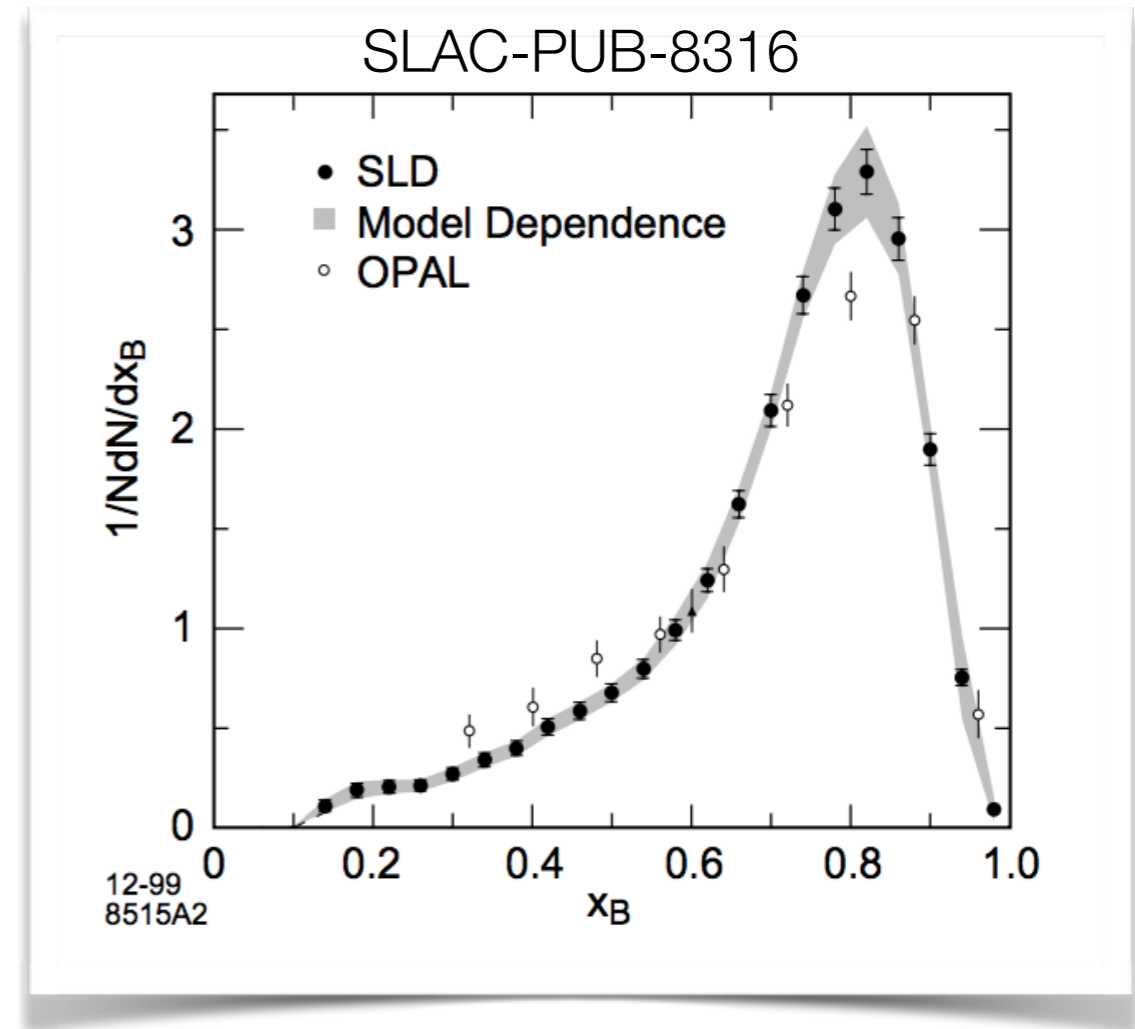
- **Large mass** ($\sim 5 \text{ GeV}$)

- **High momentum transferred** to the B-hadron

- The **weak b-decay** often produces leptons

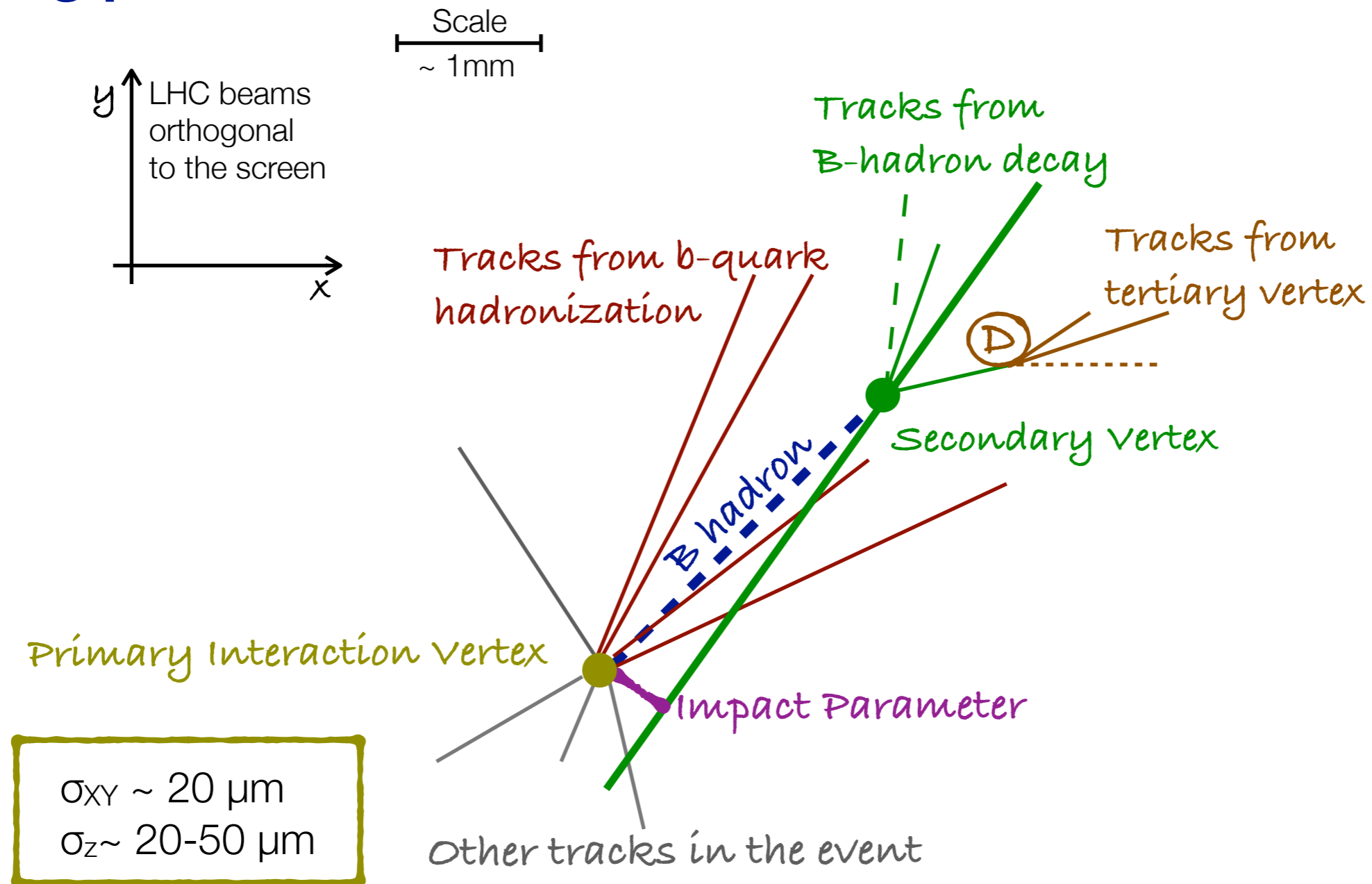
$$\text{BR: } B \rightarrow \ell + \nu + X \quad \sim 25\%$$

$$B \rightarrow D \rightarrow \ell + \nu + X' \quad \sim 20\% \text{ tertiary vertex}$$

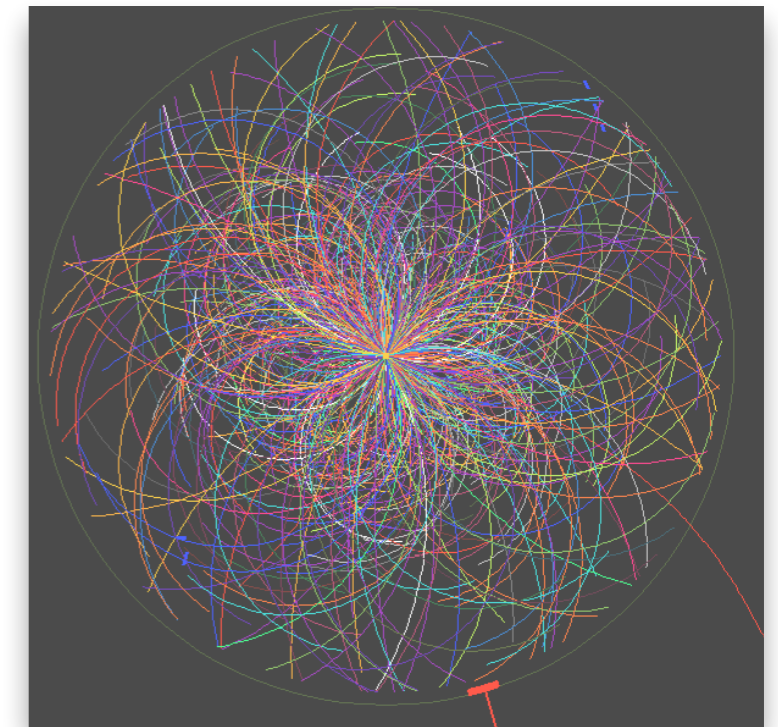
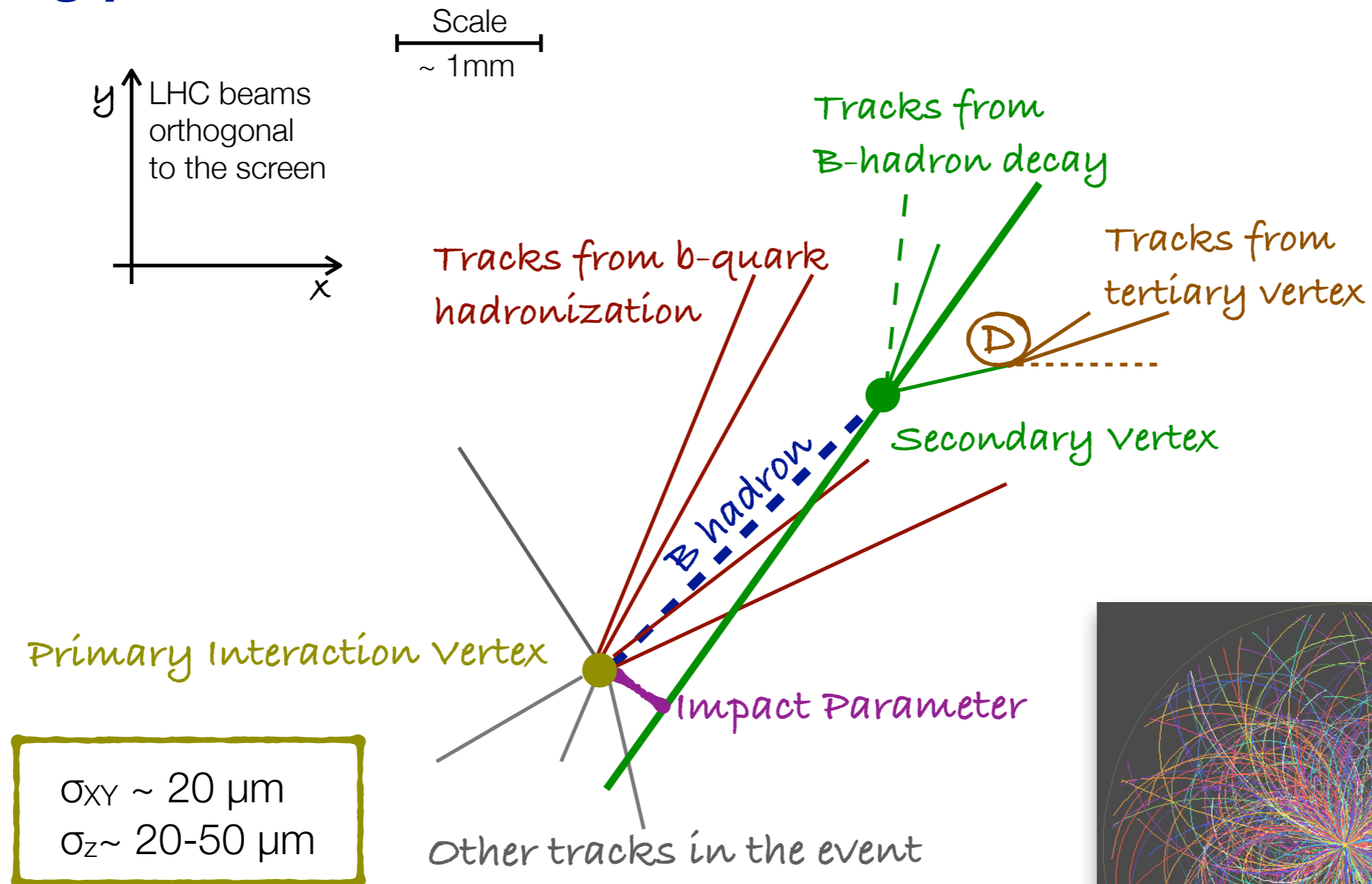


Fraction of momentum carried by the B, $\langle x_B \rangle \sim 0.7$

The B tag picture



The B tag picture

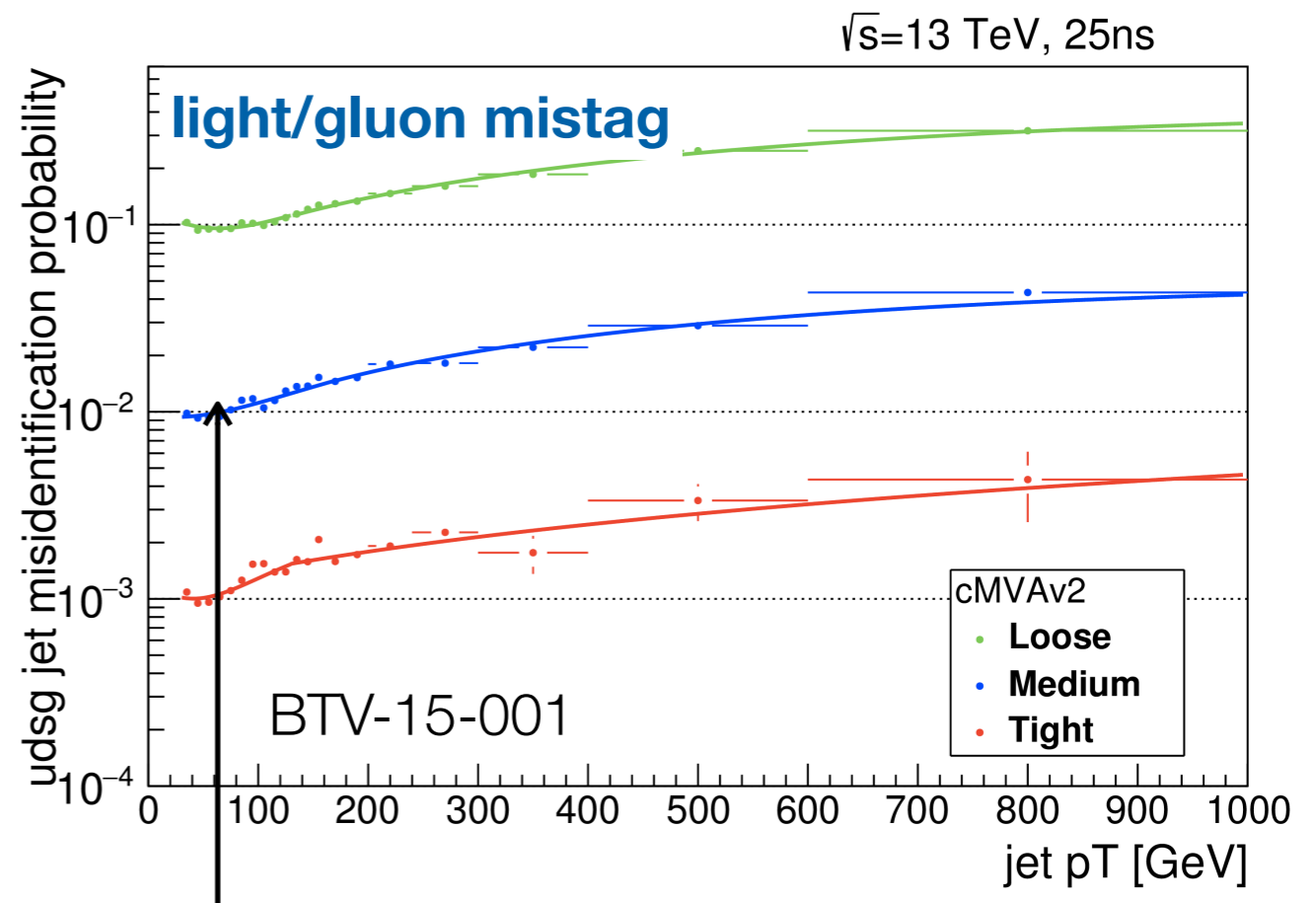
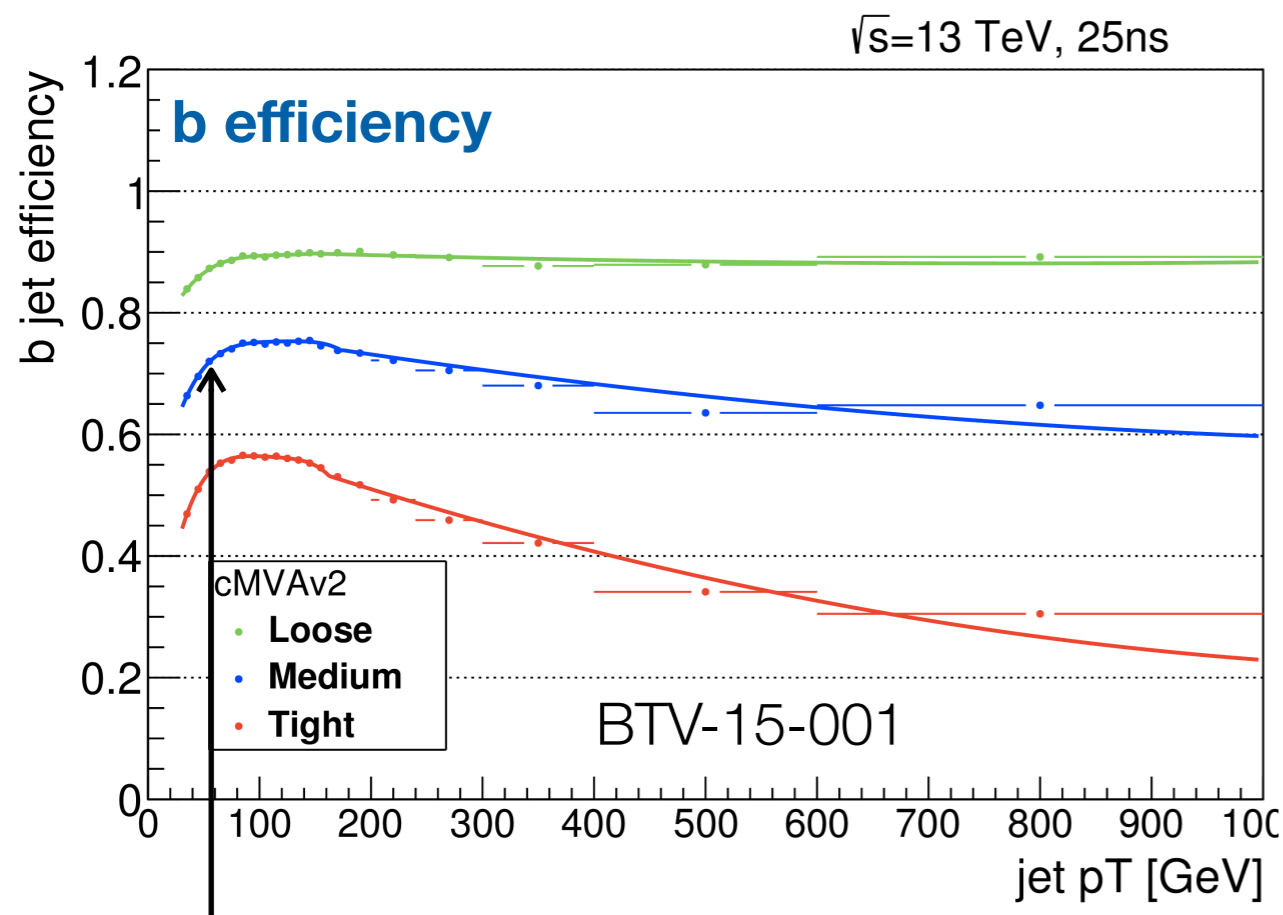


In reality there are **several collisions per crossing**
it makes quite challenging to identify the primary vertex

b-tagging in CMS

b-tagging algorithms use the information from:

- **impact parameter** significance of charged-particle tracks
- the presence and properties of reconstructed **decay vertices**
 - mass, energy ratio, number of charged tracks at the secondary vertex
- the presence of a **lepton** in the jet and its p_T relative to the jet



for an **H to $b\bar{b}$** search a typical **operating point** has 70% b efficiency and 1% mistag probability

Tracking particles

- **Tracking** is fundamental to reconstruct and measure:
 - trajectories of charged particles
 - long lived particles decay
 - momentum of charged particles
- **Resolution** on the momentum is:

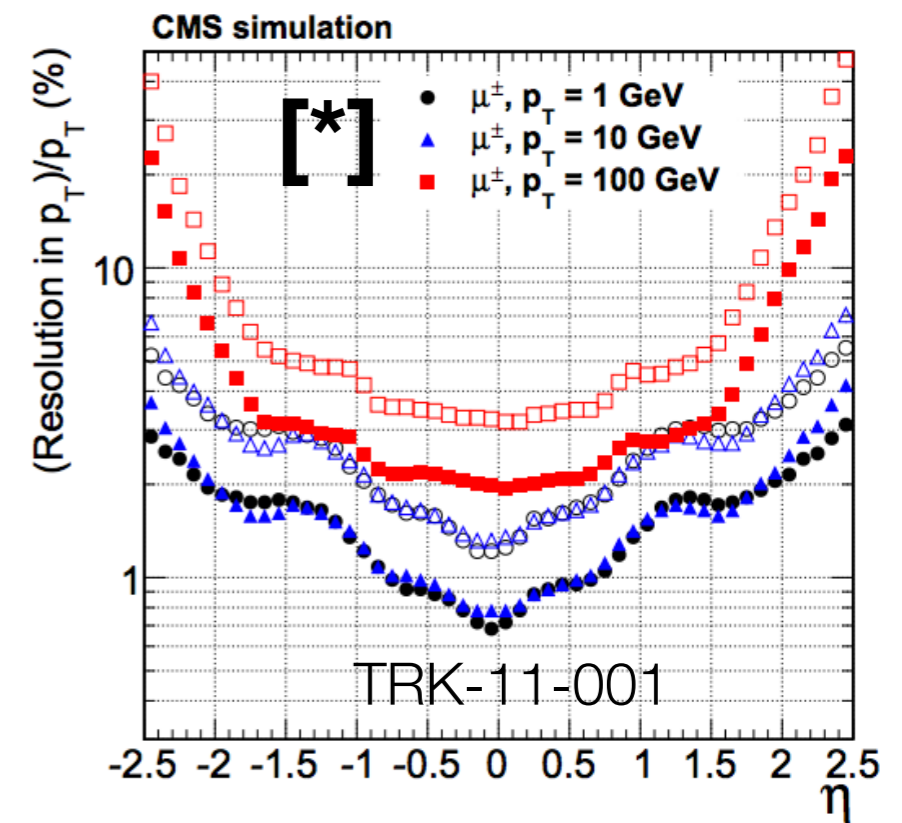
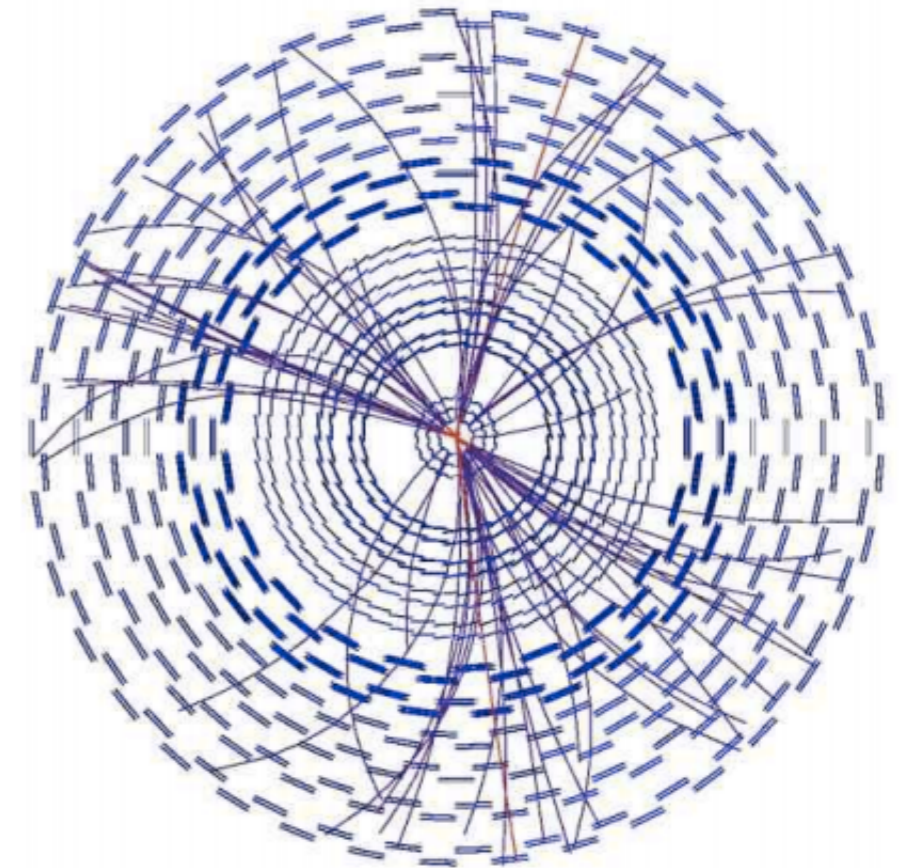
$$\left(\frac{\sigma_{p_T}}{p_T}\right)^2 \propto c_1 \cdot \left(\frac{p_T}{BL^2} \sqrt{\frac{720}{N+4}}\right)^2 + c_2 \cdot \left(\frac{1}{B\sqrt{LX_0}}\right)^2$$

curvature
multiple scattering

- The error in measuring momenta is :
 - **proportional to momentum**
 - inversely proportional to the bending power
 - weakly dependent on the number of measurements
 - at small momentum limited by the multiple scattering

for CMS $B = 3.8$ T and $L = 1.2$ m and $N > 10$

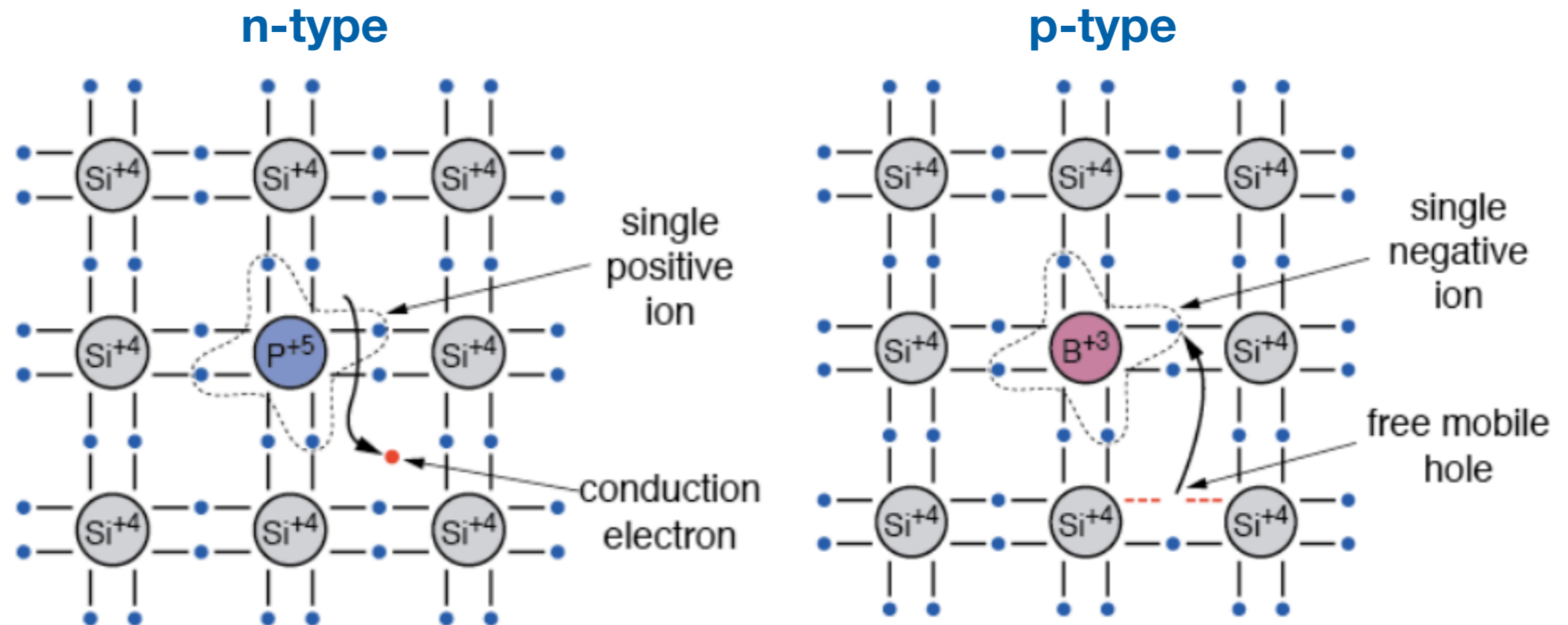
The resolution for isolated muons of p_T 100 GeV is approximately $\sim 3\%$



Semiconductor detectors

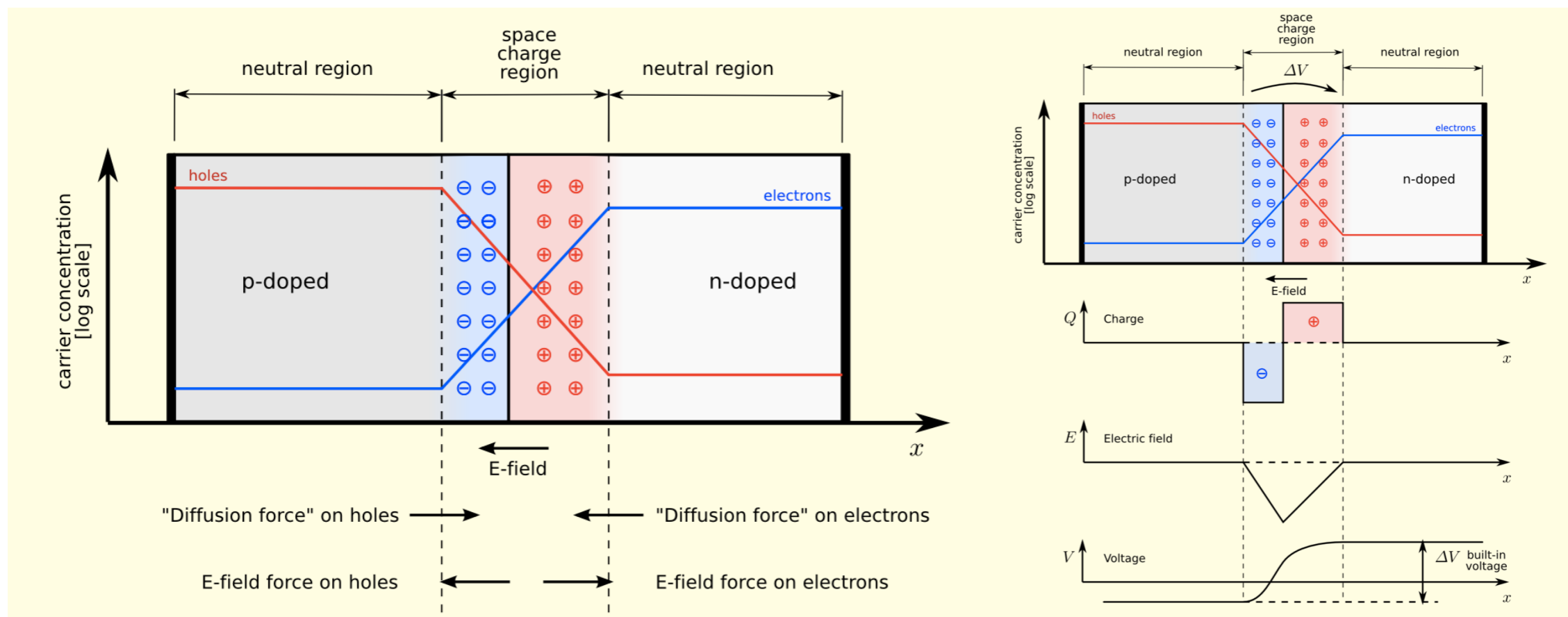
Silicon

- Silicon is the **second most abundant** element on earth and it is the basic material for modern electronic.
- **Production** of silicon crystals and wafers is an extremely **well defined process**.
- Semiconductors are ‘doped’:
 - penta-valent element \Rightarrow **n-type** silicon \Rightarrow **electrons** are loosely bound and are ‘majority’ **carriers**.
 - tri-valent element \Rightarrow **p-type** silicon \Rightarrow the **holes** are the majority **carriers**.
- The central element of a silicon detector is **p-n junction** where two types of material meet.

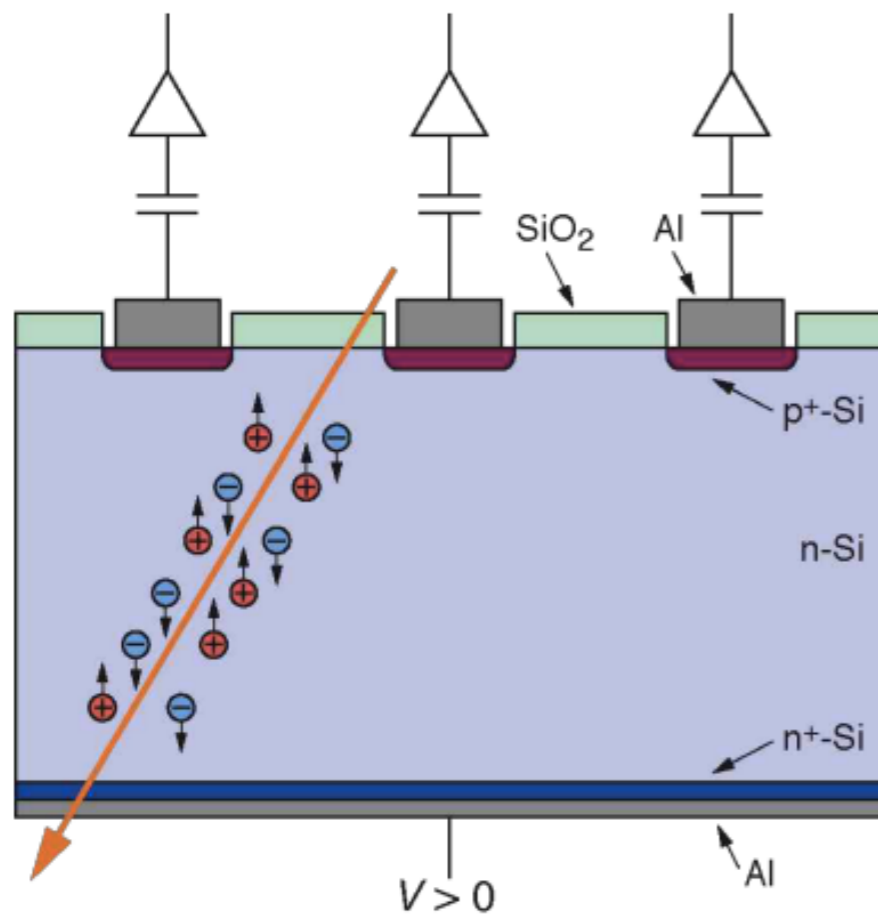


Silicon pn-junction

- In an **unbiased** p-n junction diode majority carriers migrate from one side to the opposite side, until the potential difference - ΔV (0.6 V) – due to the charge distribution halts the process.
- Then at the junction there is on either side a **depletion region** where the number of free carriers is at the intrinsic level.
- By applying a **reverse bias**, electrons and holes are pulled out of the depletion zone.
 - the depletion region increases and the (leakage) current across the junction is very small
 - This is the way we operate **semiconductor detectors**



Silicon Trackers

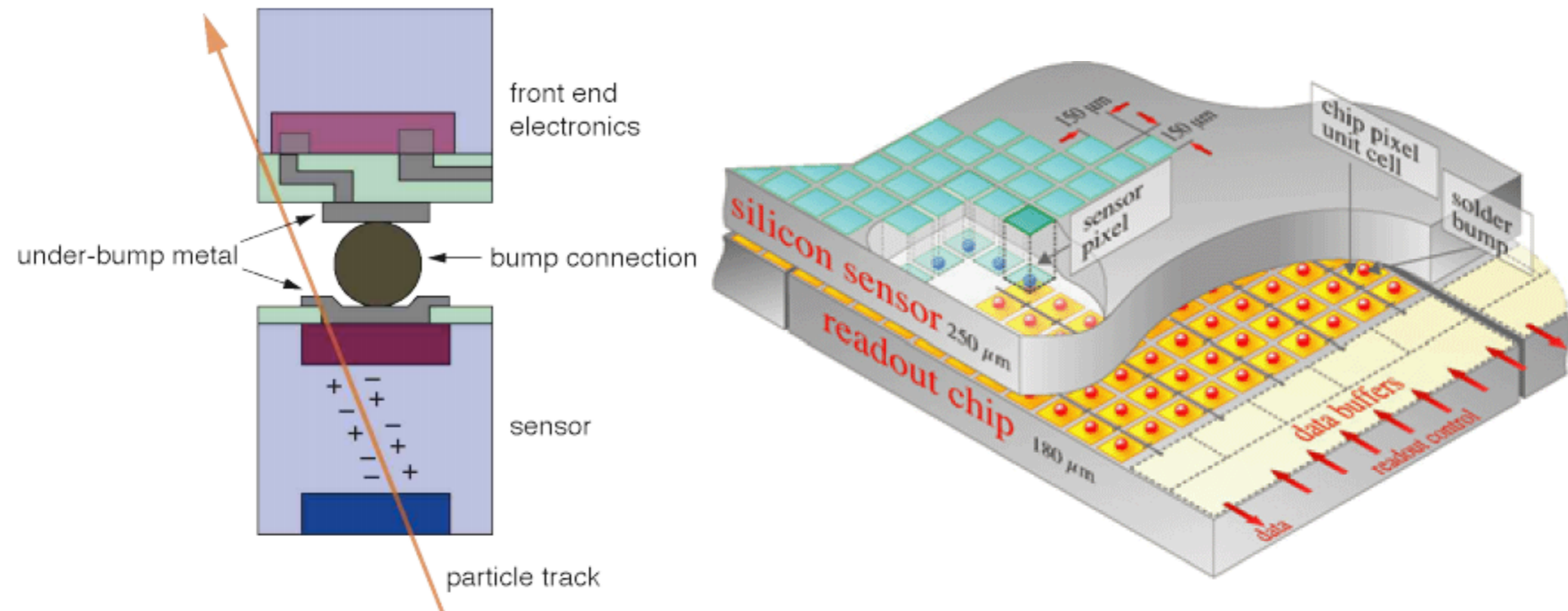


The semiconductor detector functions as an ionization chamber:

- particles lose part of their energy ionizing the Silicon atoms in the reticule
 - electrons and holes drift inside the lattice according to the applied electric field
 - electron and holes are collected at the electrodes (that can be segmented in different ways)
 - pixels / strips / pads
-
- When **reverse voltage** is applied, then the silicon bulk becomes fully depleted, with only a small leakage current flowing.
 - A **particle traversing the silicon** creates electron-hole (e/h) pairs in the depleted volume
 - The energy to generate an e-h pair is 3.62 eV
 - a minimum ionizing particle will generate **~80 e-h pairs per μm** (24000 e-h for 300 μm Si)
 - a fast current pulse will flow to the electronic readout
 - The integrated charge is proportional to the absorbed energy

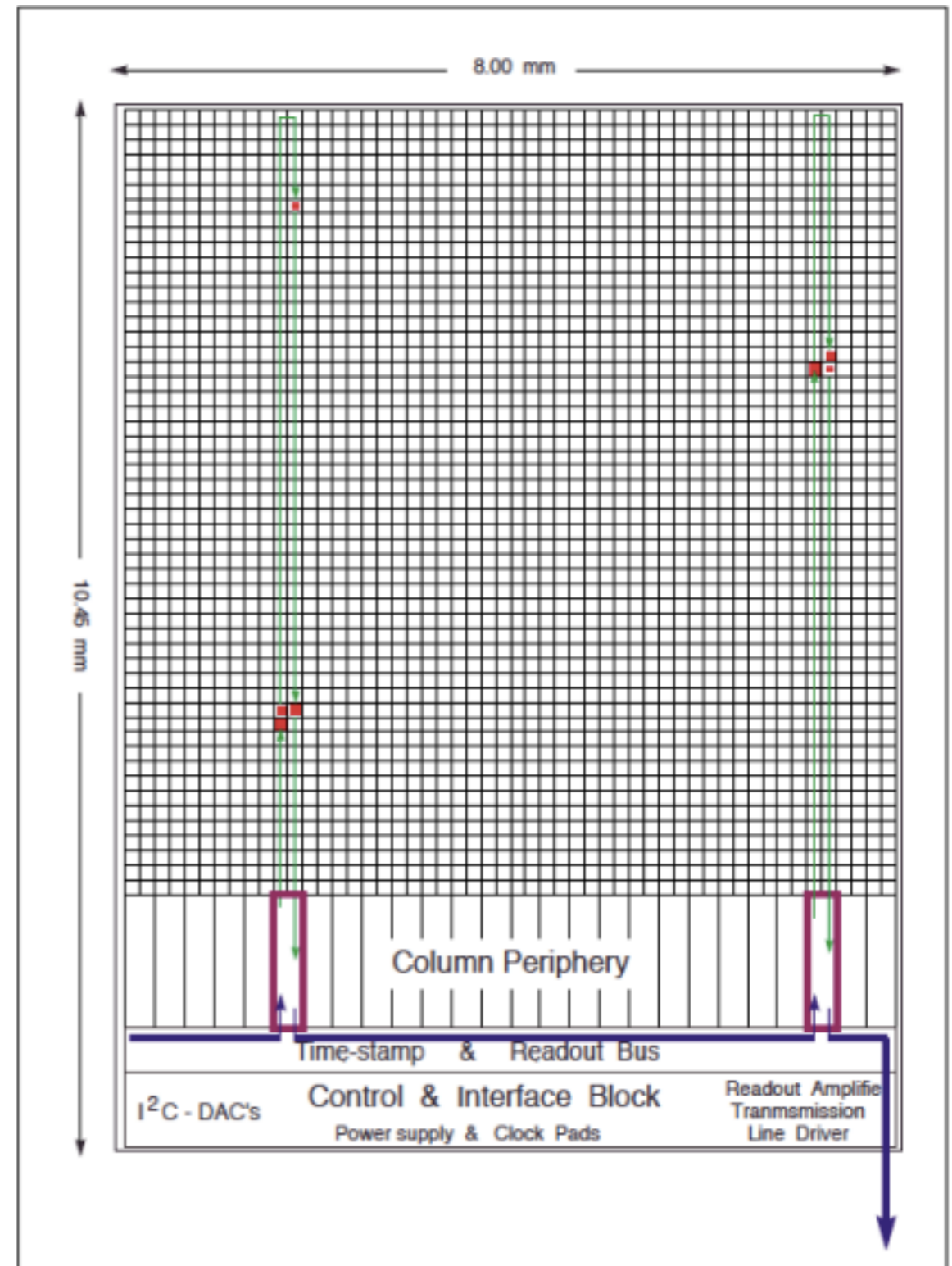
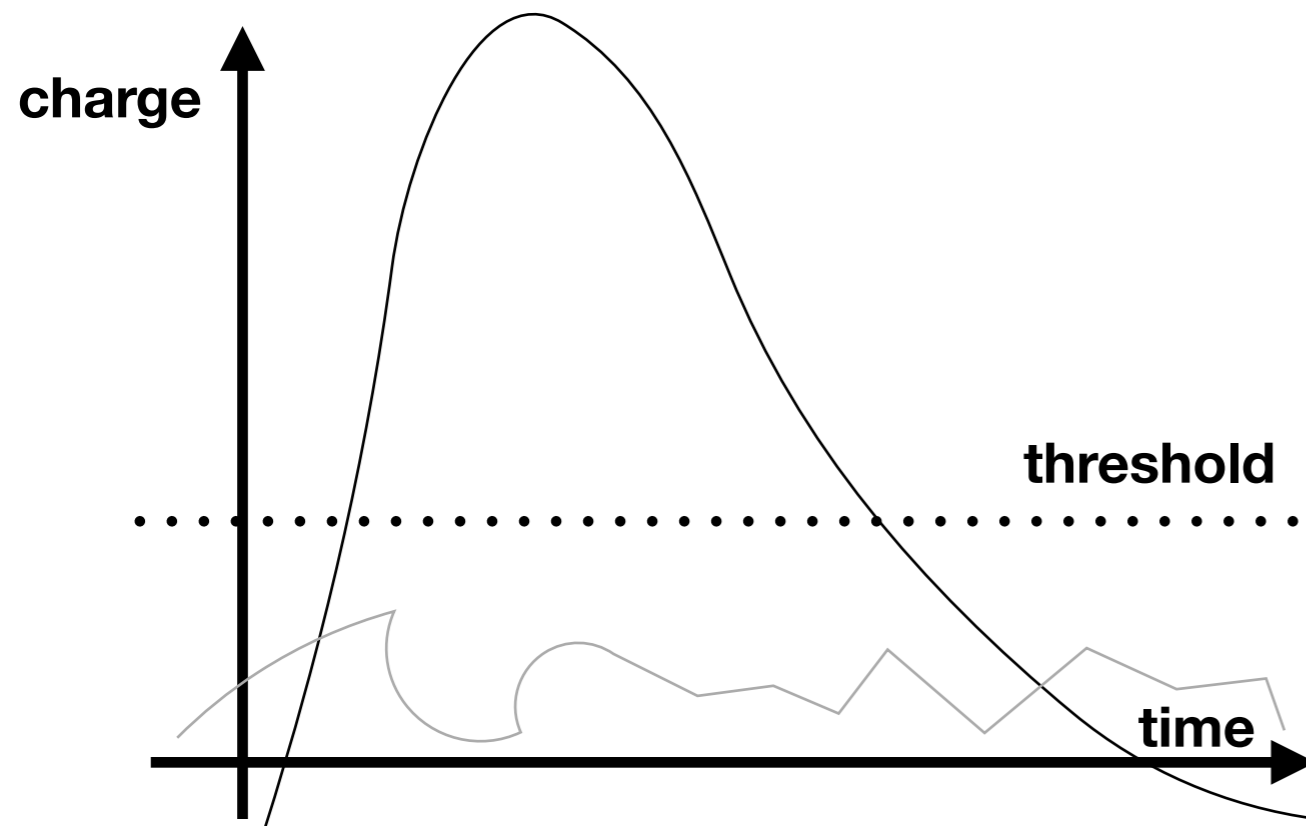
Pixelation in Silicon Detectors

- Basic idea is to divide the silicon sensor into small cells and readout each cell individually.
 - The **CMS** pixel detector has pixels that are $100 \times 150 \mu\text{m}^2$
- The **sensor** electrodes (pixel) are **coupled directly to the readout electronics** (ASIC).
- The interconnections are made with bump bonds (PbSn, In, etc)
 - pitches varying from mm to $\sim 50 \mu\text{m}$.



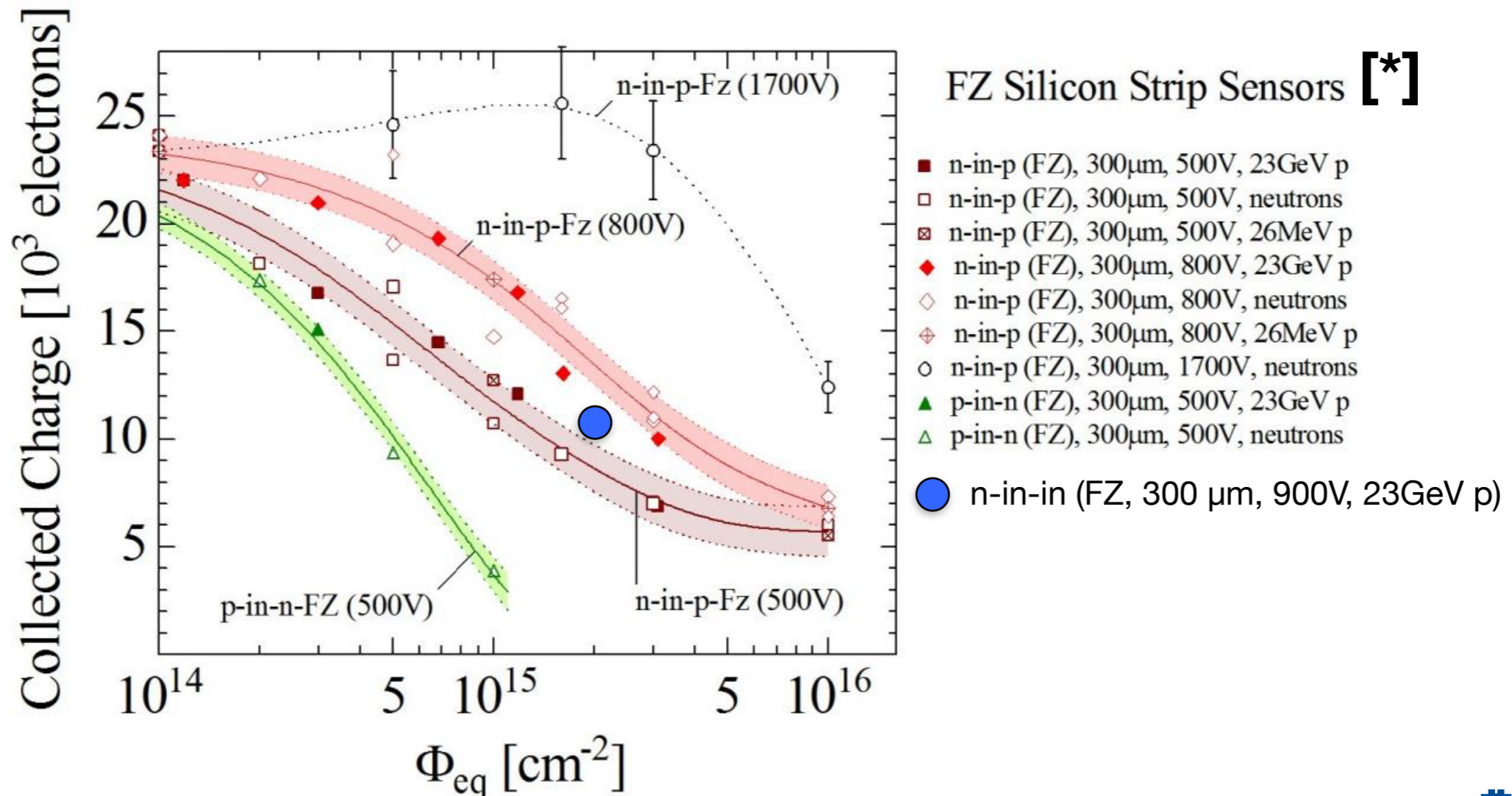
Readout of a pixel detector

- In **CMS** there are **60 million pixels**
⇒ extracting all the pixel information off detector at the bunch crossing rate and at the LHC luminosity is impossible
- The first level of data reduction is the **zero-suppression**
 - Only pixel with signal above threshold are stored (waiting for L1 trigger) on local buffers in the readout ASIC.
- Then, only data confirmed by the L1 trigger are readout from the ASIC to the off-detector electronics



Radiation Damage

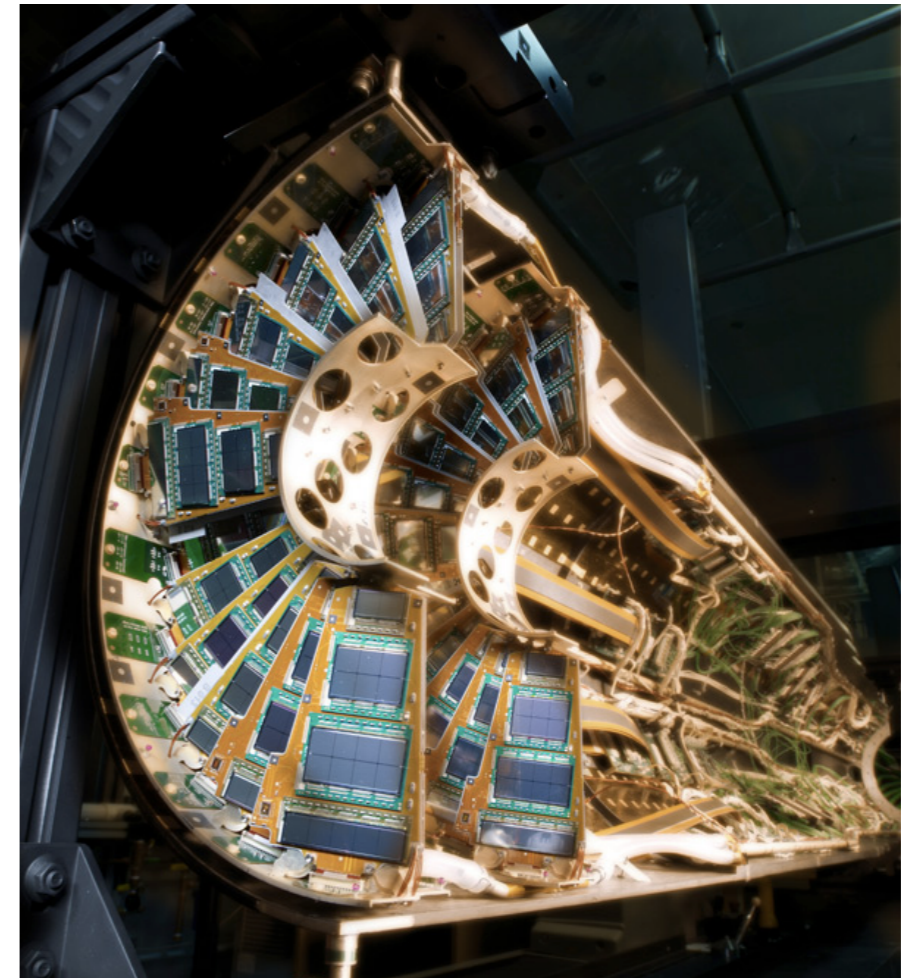
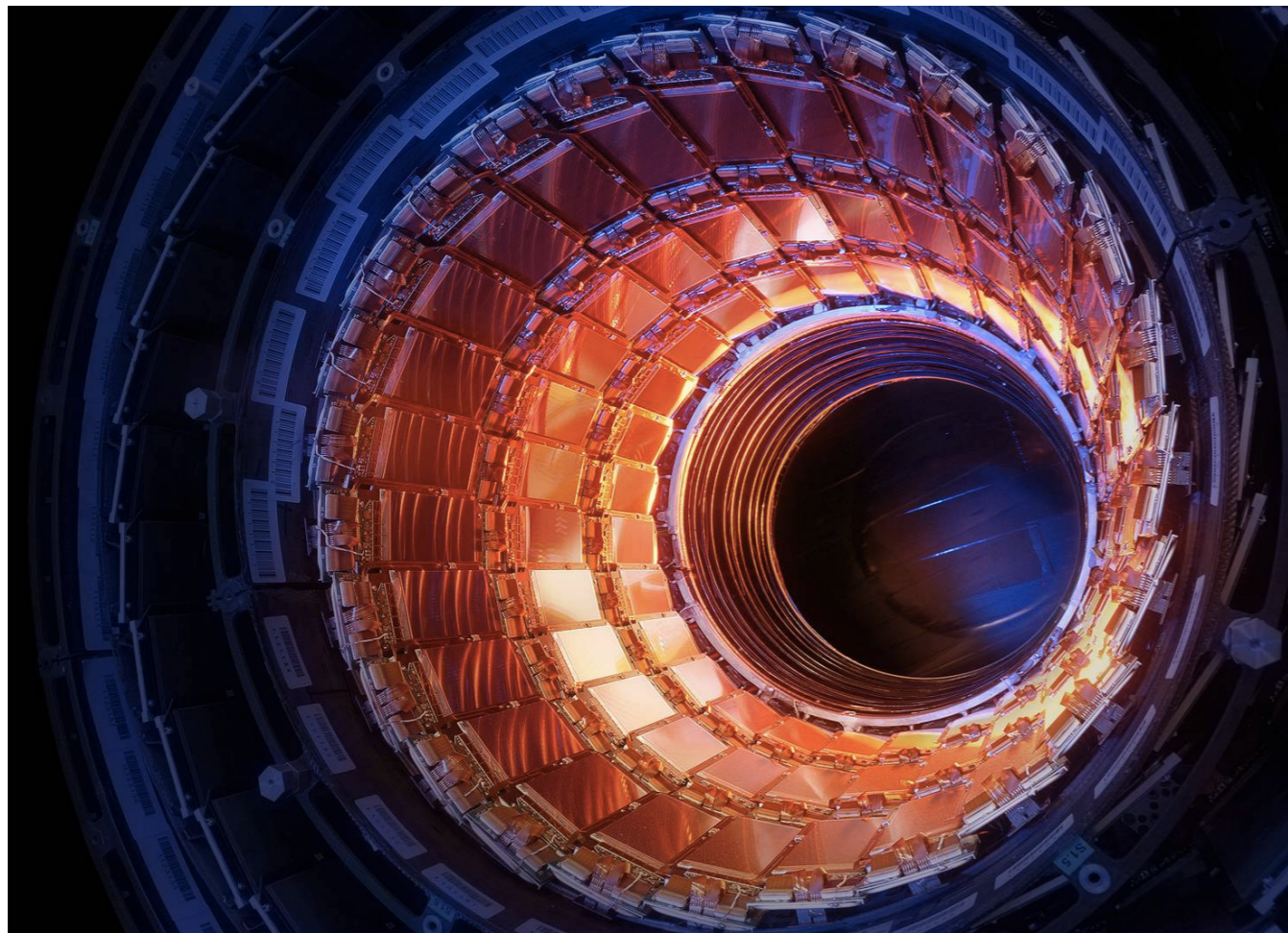
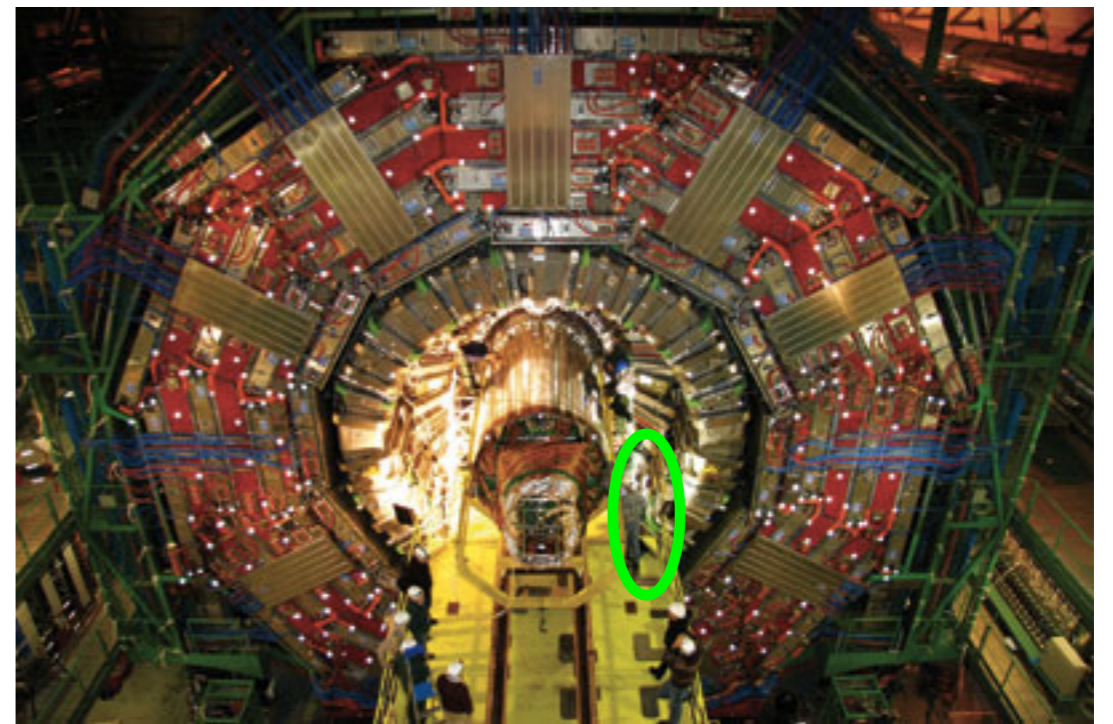
- The principle source of radiation damage in silicon sensors is from **non-ionizing-energy-loss** (NIEL).
 - It is normally expressed in terms of 1 MeV neutron equivalent for silicon
- Effects are additional defects which increase effective dopant concentration with p-type like
 - ⇒ **increased depletion voltage**
- Increase in the **number of traps** ⇒ **increase in leakage current**
 - ⇒ **reduced charge collection efficiency**



CMS pixel detector and its evolution

CMS tracking detector

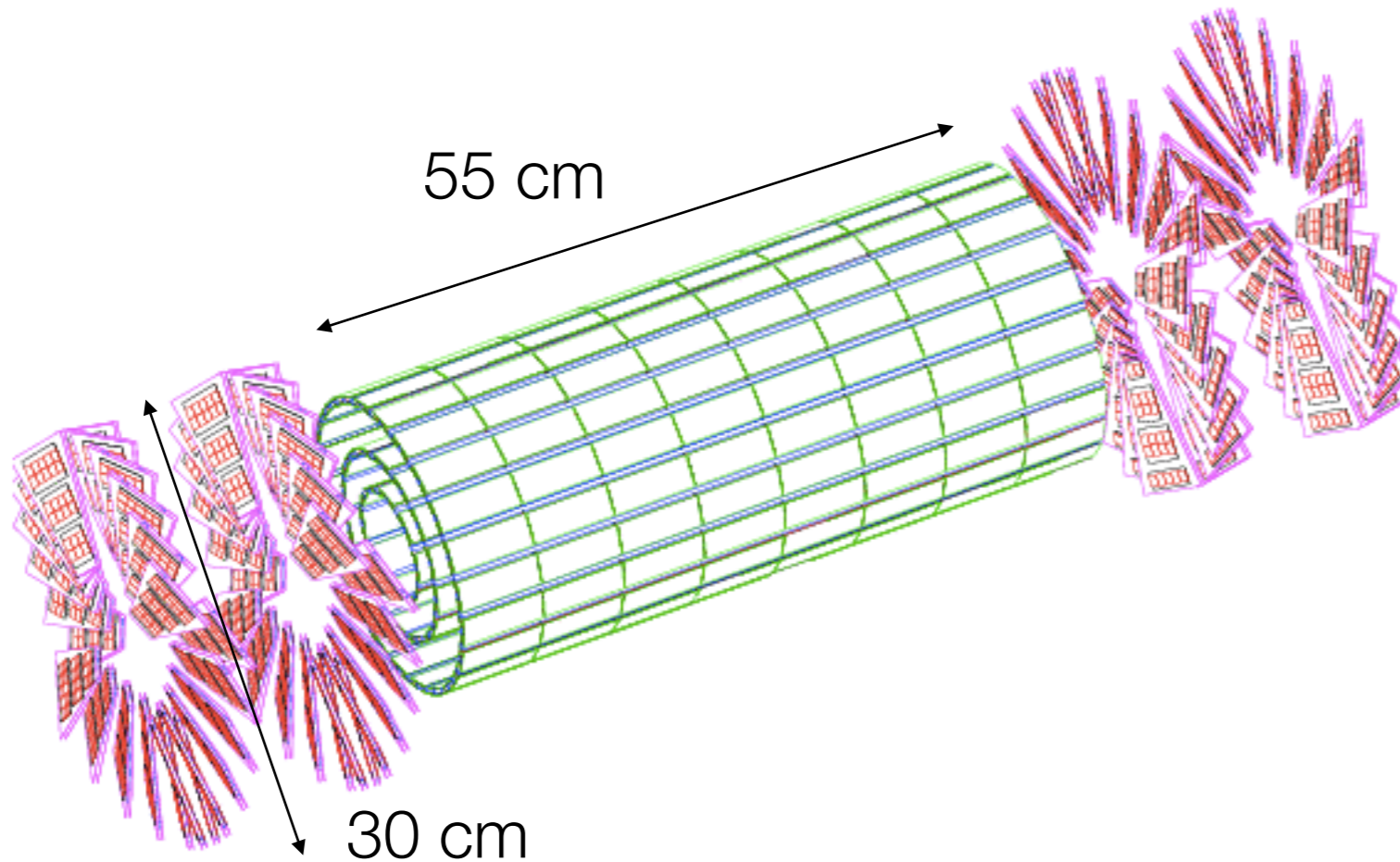
- Full silicon tracking system
 - **biggest** silicon detector ever built
 - Inner pixel detector (**1 m²** n-in-n silicon)
 - Outer strip detector (**200 m²** n-in-n silicon)
- Operated in a 3.8T magnetic field



CMS Pixel detector - Phase 0

Excellent resolution and efficiency

Designed for a maximum peak luminosity of $10^{34} \text{ cm}^{-2}\text{s}^{-1}$



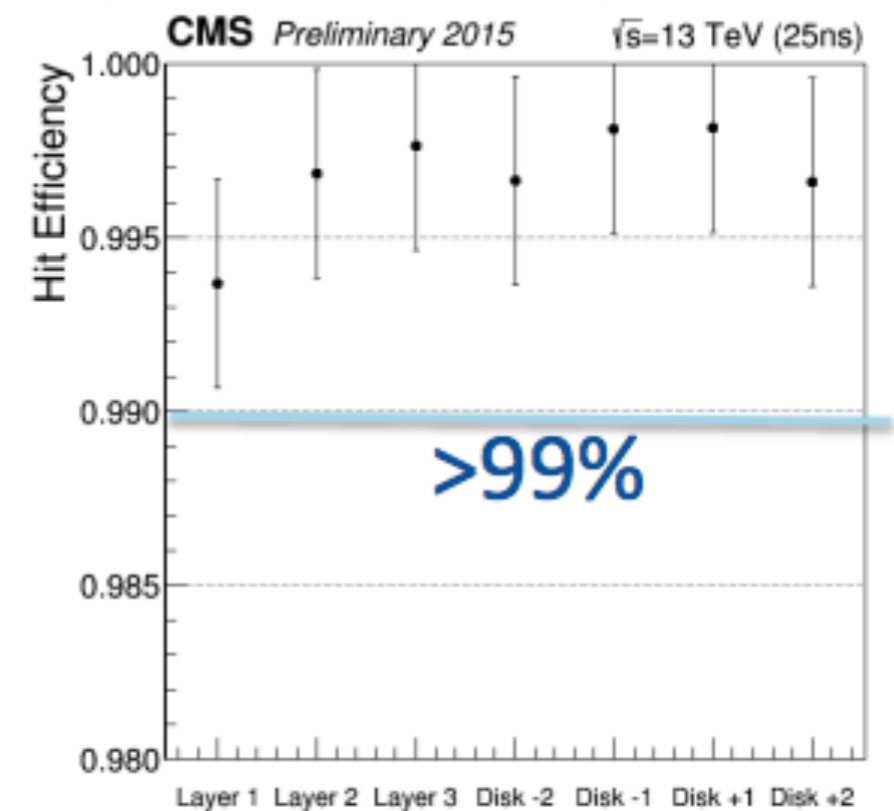
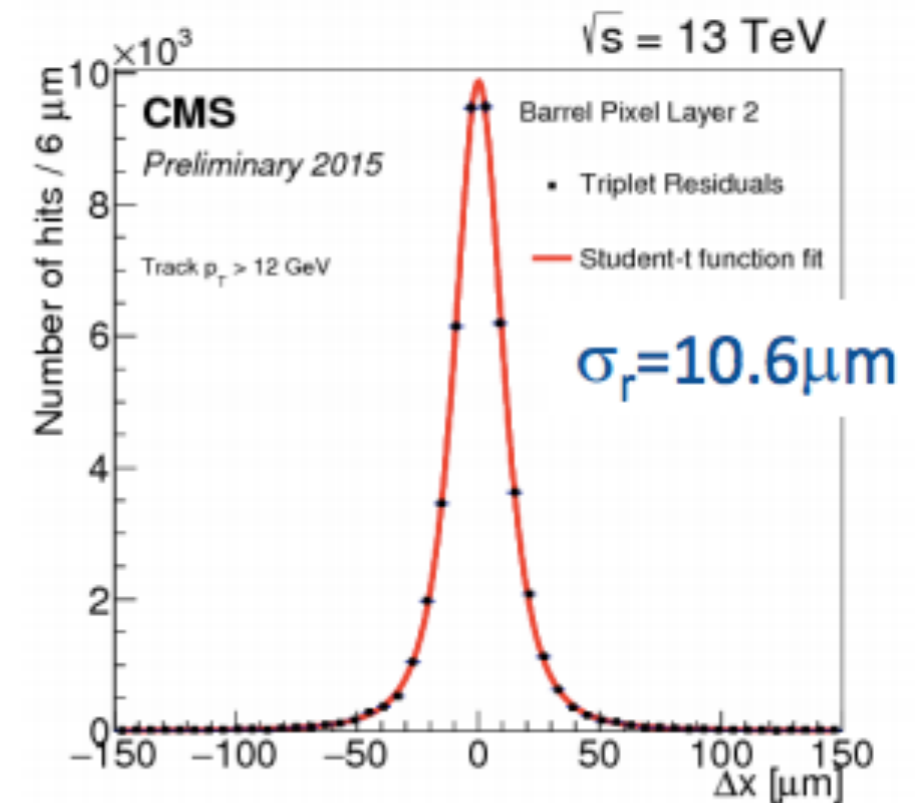
Barrel Pixel: 3 barrel layers at r of 4.3, 7.3, 10.4 cm

11520 chips (48 million pixels)

Forward Pixel: 4 disks at z of ± 35.5 and ± 46.5 cm

4320 chips (18 million pixels)

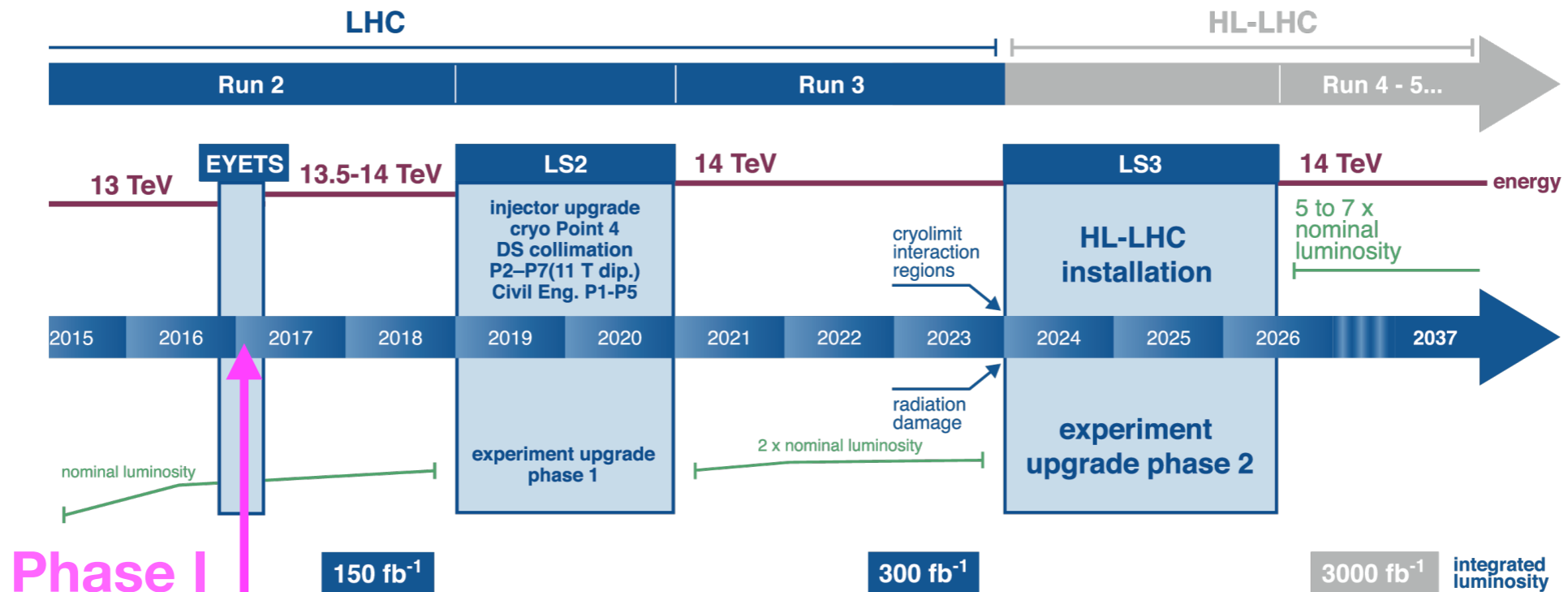
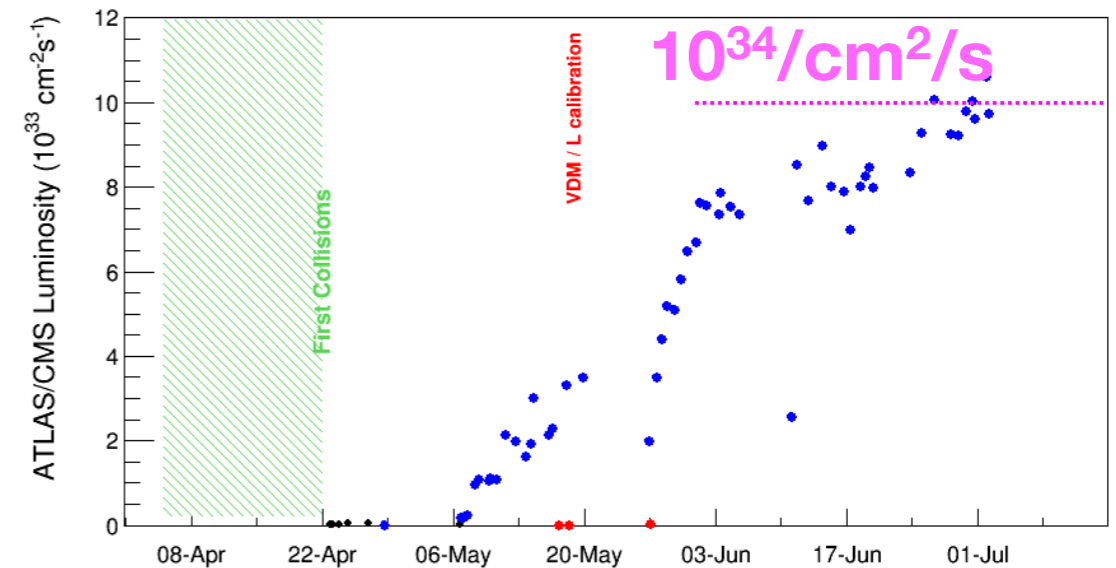
Modules tilted by 20° for better charge sharing



CMS Pixel detector - Phase I

- Current detector could not sustain luminosity higher than $10^{34} \text{ cm}^{-2}\text{s}^{-1}$
 - **readout inefficiency**
- To fully profit from the higher instantaneous luminosities foreseen in 2017 (hit rates of $\sim 600\text{MHz}/\text{cm}^2$) a new pixel detector will be installed in February'17
- detector need to be operational at $2 \times 10^{34} \text{ cm}^{-2}\text{s}^{-1}$
- an **ultra low mass system** with four barrel layers and three disks on either end

Design luminosity: achieved!



Phase I

150 fb⁻¹

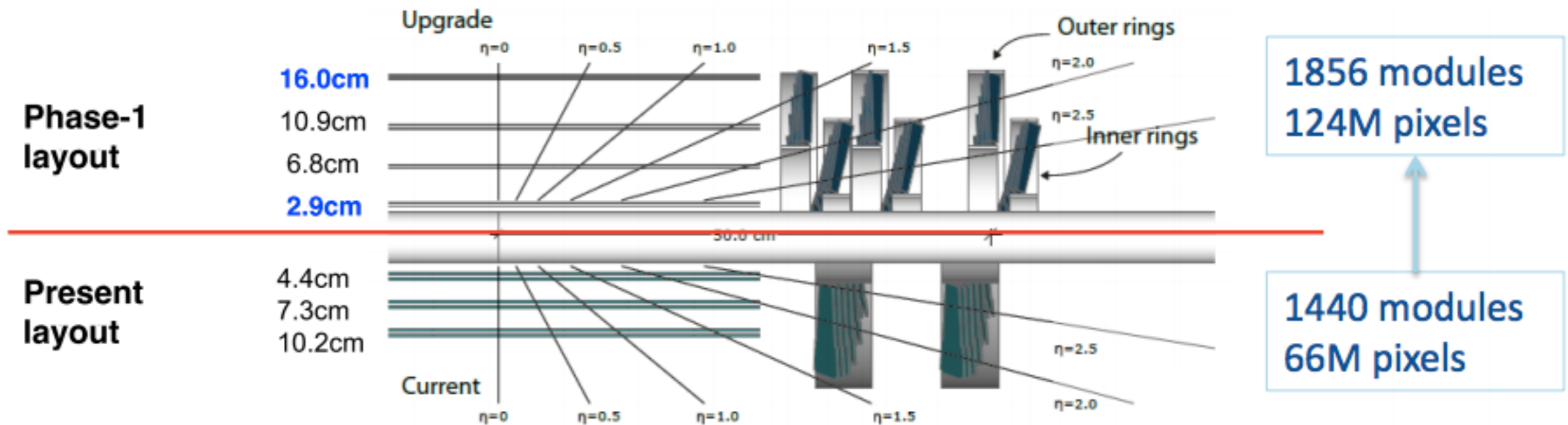
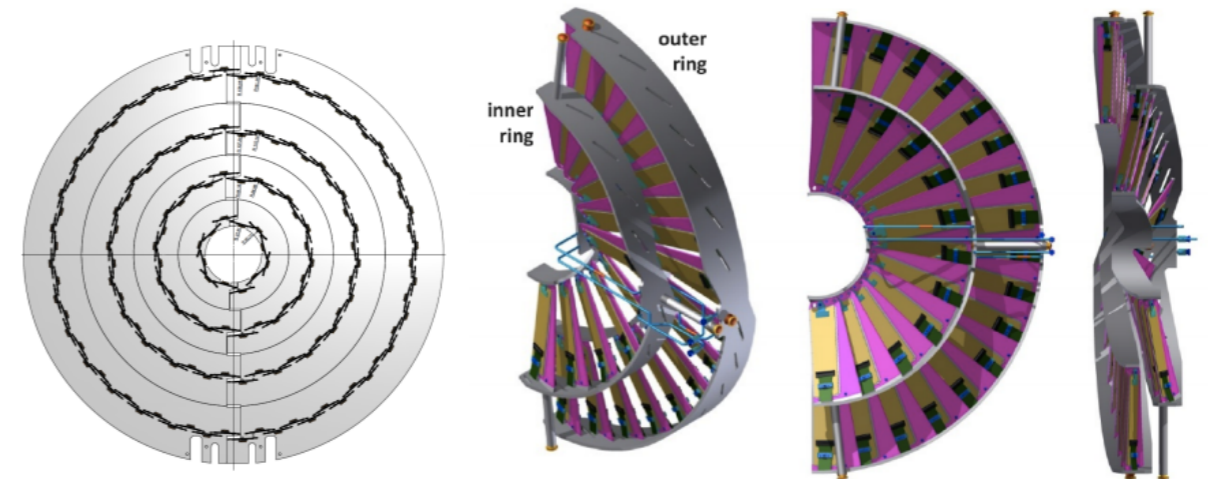
300 fb⁻¹

3000 fb⁻¹

integrated luminosity

CMS pixel detector - Phase I

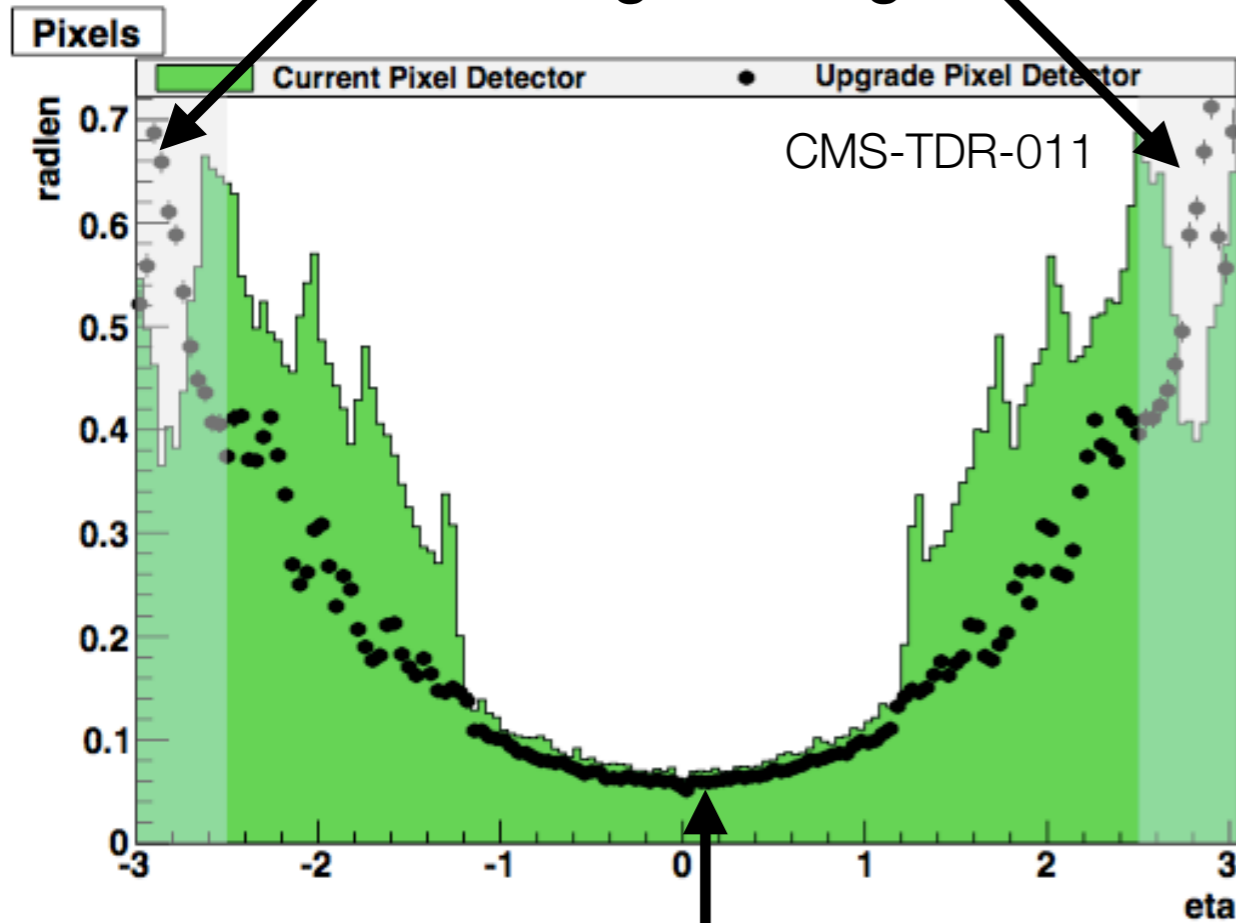
- Move **from 3- to 4-hit coverage** to increase redundancy and track finding efficiency
- Sensor technology, pixel size and module concept very similar to fit into existing infrastructure
- Move **from analog to digital readout chip (ROC)**
 - **reduced buffer overflow** and inefficiency
- **Barrel:** 1184 modules, 48M \Rightarrow 79M pixels
- **Forward:** 672 modules, 18M \Rightarrow 45M pixels



Phase I improved performance

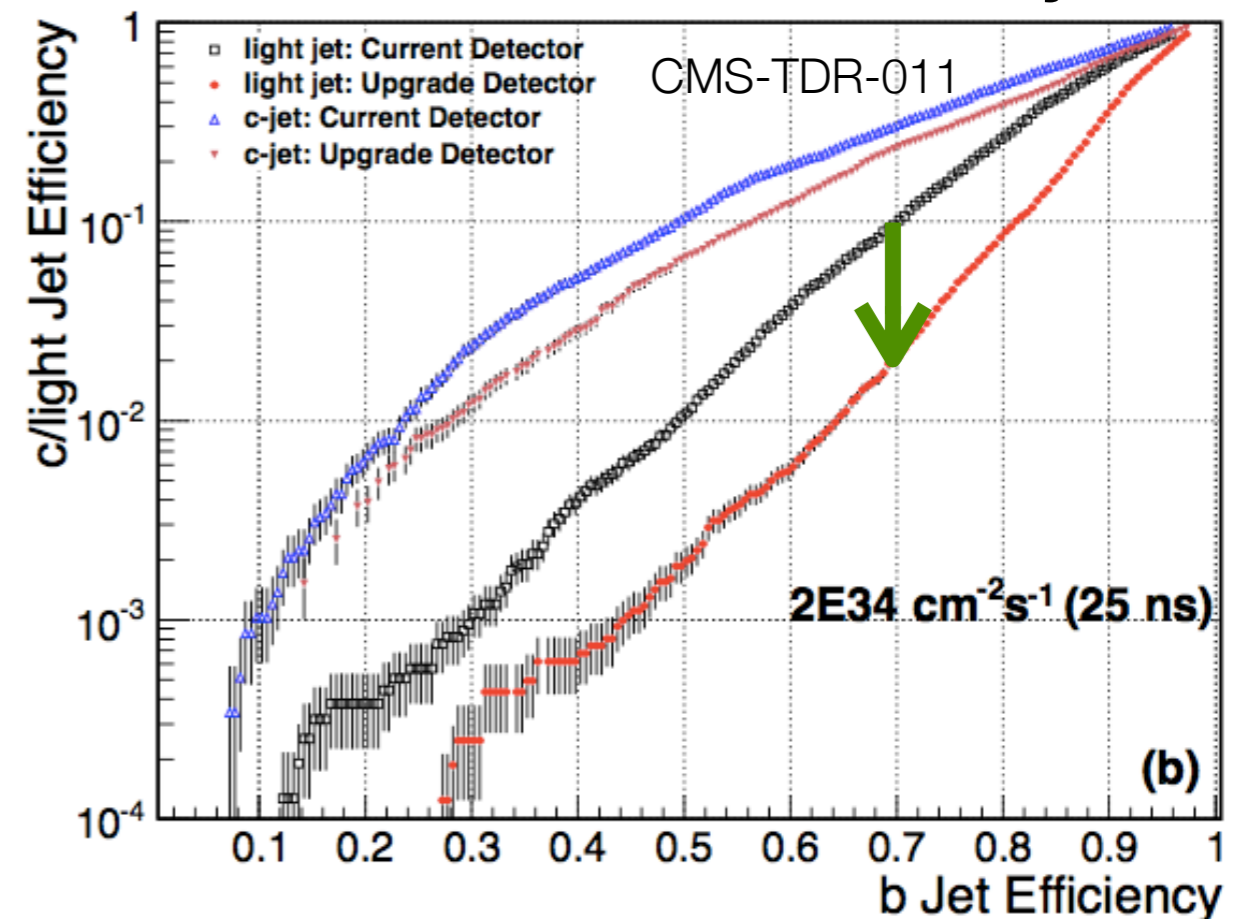
- Reduced mass by a factor two: from one-phase C_6F_{16} to two-phase CO_2 cooling system
- Improved **redundancy** \Rightarrow impacts **tracking efficiency** and purity
- Move **closer to beam** \Rightarrow improves **vertexing** and b-tagging

services moved outside the tracking coverage



but one more layer

factor 5 in reduction of mistag @70% b efficiency



R&D for HL-LHC

The upgrade of the CMS Tracker for HL-LHC

Radiation tolerance up to 3000 fb^{-1}

Keep the possibility to extract, repair and reinstall the pixel detector.

- 3000 fb^{-1} over 10 years \Rightarrow Radiation damage of the previous 10 years in only one year
- Non-ionizing energy loss: fluence up to $2 \times 10^{16} \text{ cm}^{-2} n_{\text{eq}}$ for innermost pixel layer

Operate up to 200 PU

Maintain occupancy at the $\sim 1\%$ level \rightarrow higher granularity

DAQ compatible with higher Level 1 trigger rate and longer latency

100 kHz \rightarrow 750 kHz ; $3.2 \mu\text{s}$ \rightarrow $12.8 \mu\text{s}$

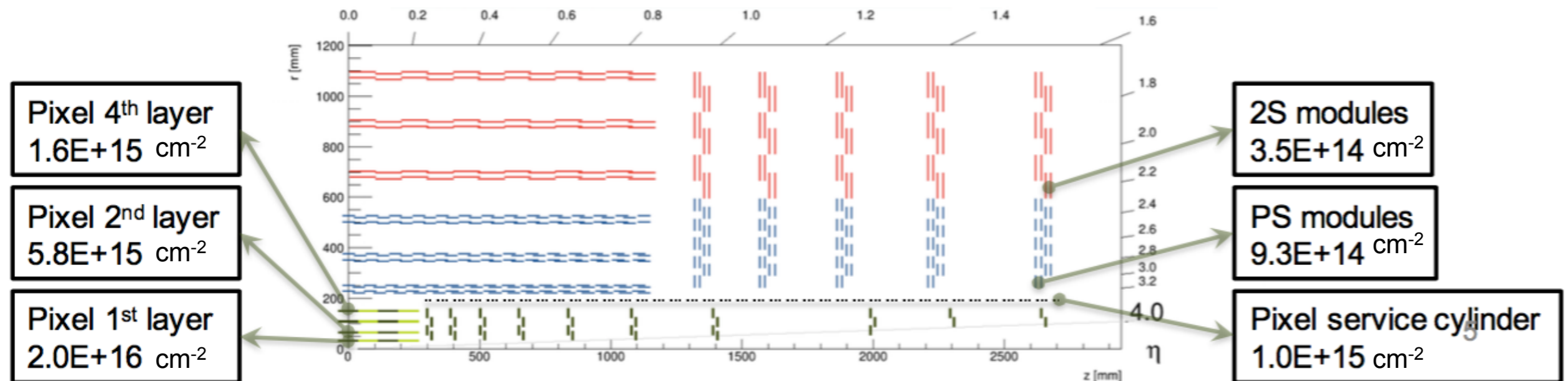
Contribution to the Level 1 trigger decision

p_T discriminating modules in the Outer Tracker

Extended tracking acceptance

Up to $\eta \sim 4$ (by adding more pixel disks in the forward detector)

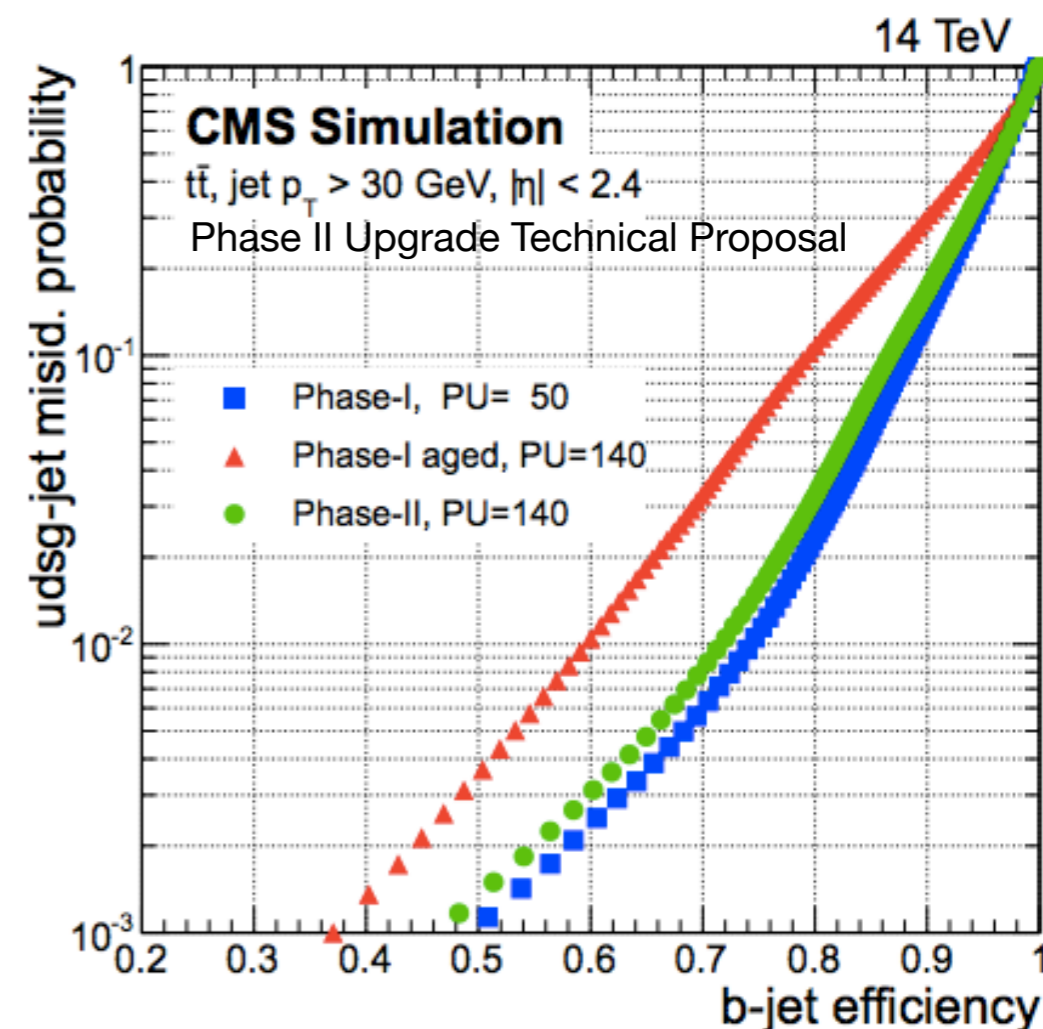
Reduce material in the tracking volume



Phase-II-Pixel upgrade

Ongoing R&D plan to develop a new pixel tracking system to operate at HL-LHC

- To maintain a high tracking and b-jet identification efficiency at luminosities up to $5 \cdot 10^{34} \text{ cm}^{-2}\text{s}^{-1}$
- It will extend the η coverage from the present $\eta = 2.5$ to $\eta = 4$
- main requirement is to match jets to vertices in the forward region
- Different lines of investigation for Phase-II:
 - **Better acceptance**/hermeticity \Rightarrow **slim edge sensors**
 - to reduce the dead area in between sensors
 - similar to ATLAS IBL
 - Higher instantaneous luminosity \Rightarrow **high granularity** \Rightarrow **small pitch sensor**
 - Higher integrated luminosity \Rightarrow **high radiation tolerance** \Rightarrow **thinner sensors**



ongoing R&D

Three different lines of the investigations for the inner parts of the pixel detector:

1. planar pixel sensors in n-in-n

2. 3D pixel sensors

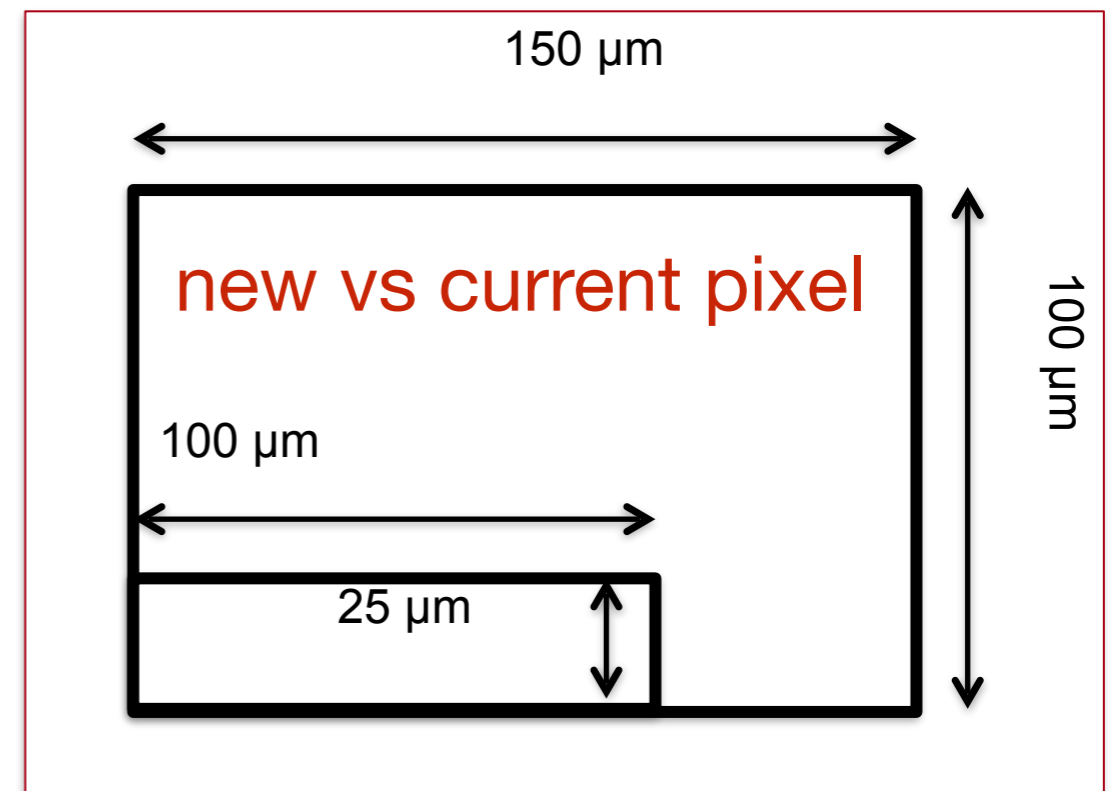
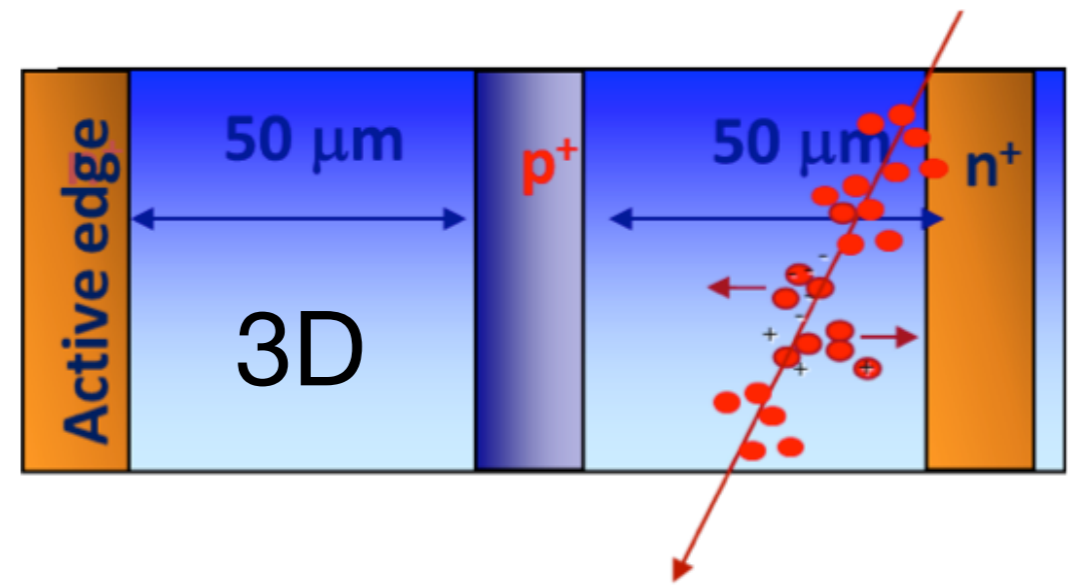
- small pitch sensors investigated by CNM (Spain) and FBK/INFN (Italy)
- thinner wafers (200 μm)

3. thin planar pixel sensors in n-in-p

- **single sided** process favored
 - More vendors, **cost effective**
- 6" n-in-p FZ with 150 μm thickness
 - submission of small pitch pixel sensors
 - pixel sizes of 25 μm x100 μm and 50 μm x50 μm under investigations

Common advantages:

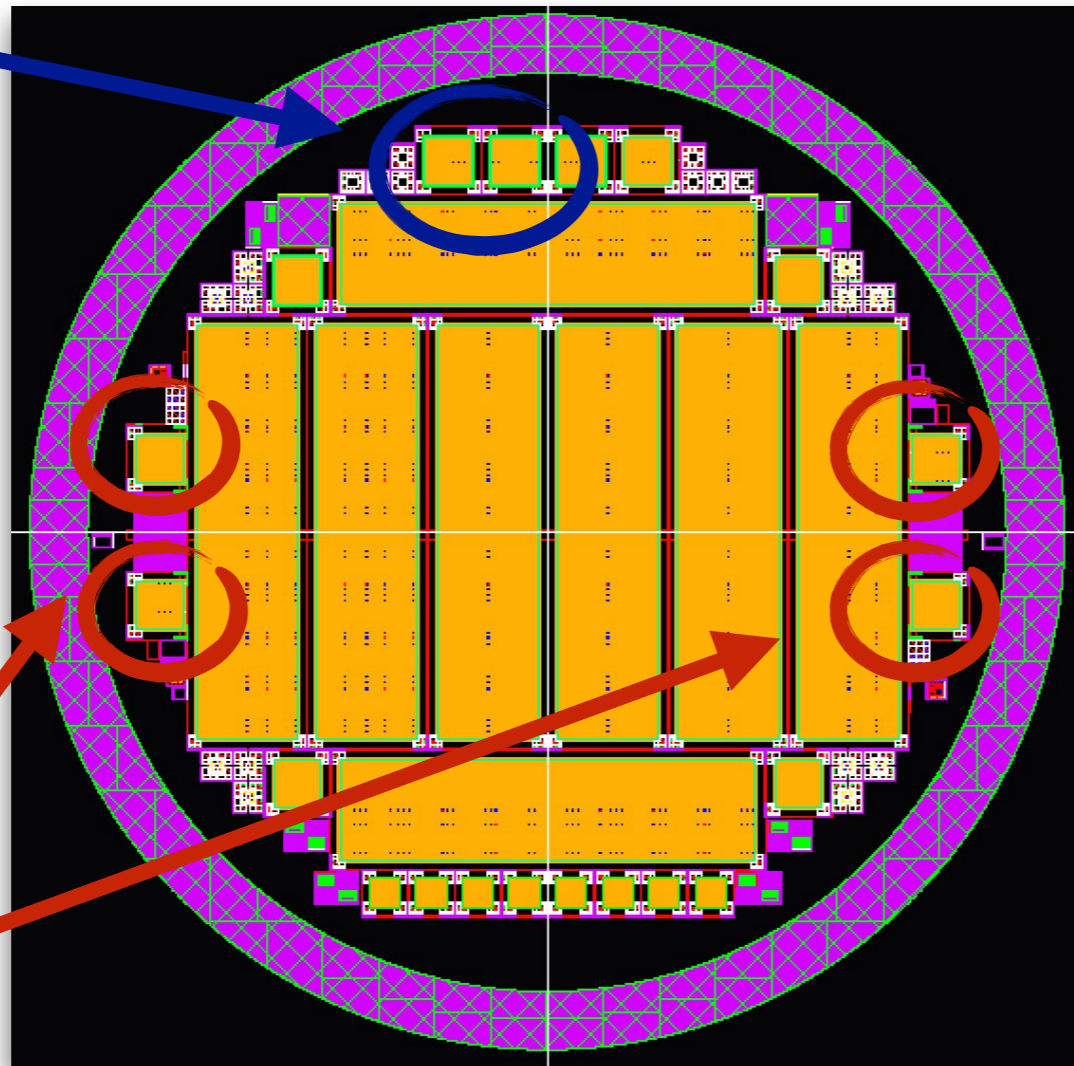
- Short drift path
- Higher field at same V_{bias}
- Lower operation voltage



n-in-n, take advantage of the Phase-I production

The pixel sensors of the CMS Forward Pixel detector were fabricated by Sintef

Small pitches



Slim edge

The technology

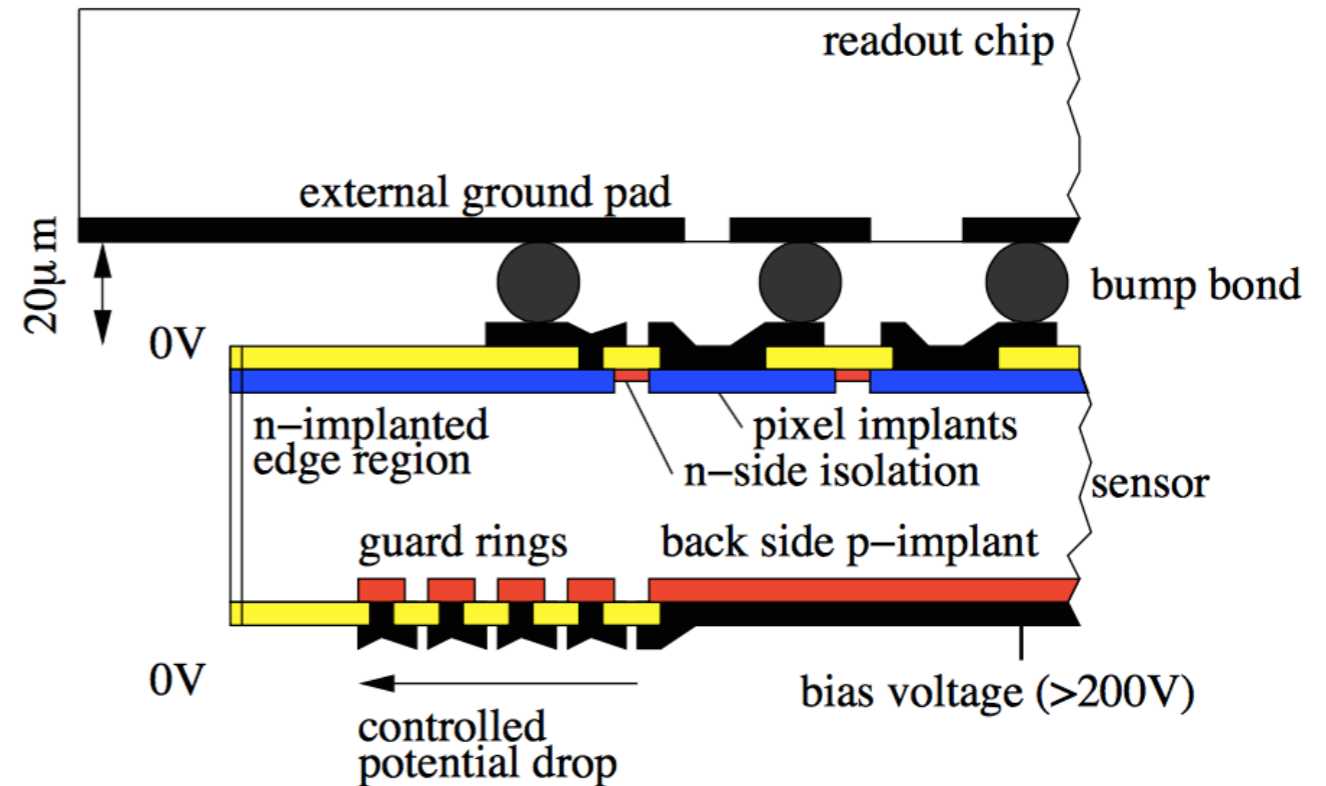
- n-in-n
- double sided
- symmetric 10 masks process (5 masks per side)
- 300 μ m thick
- FZ, 3-5 k Ω cm

The approach:

- Saves money
- Relies on a established process

R&D for n-in-n

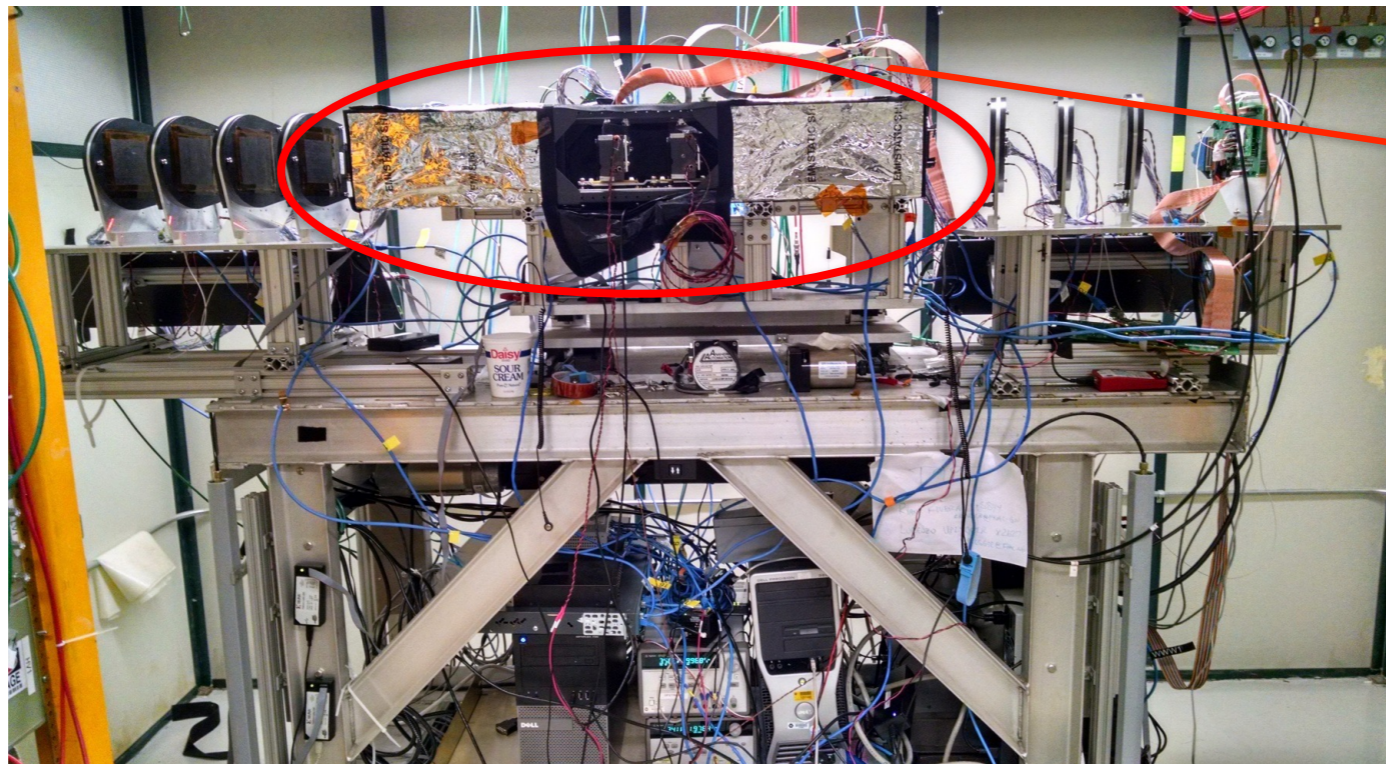
- Development and characterization of **n-in-n prototypes** silicon sensors for this upgrade
- Understanding the performance of **small pitches** and **slim edges** devices
 - Stand-alone DC characterization
 - Test beam measurements
 - Efficiency
 - Resolution
 - Charge Collection
- Evaluation of the degradation induced by radiation damage



The Fermilab MTest beam facility

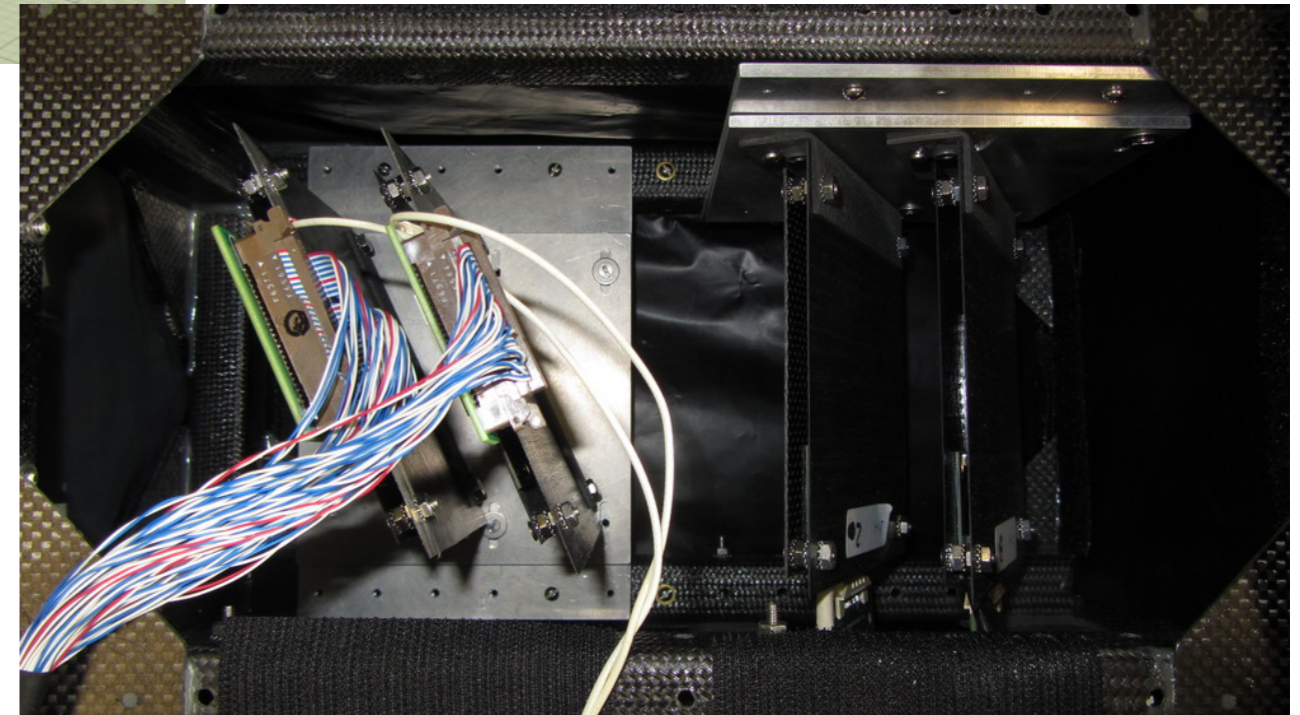
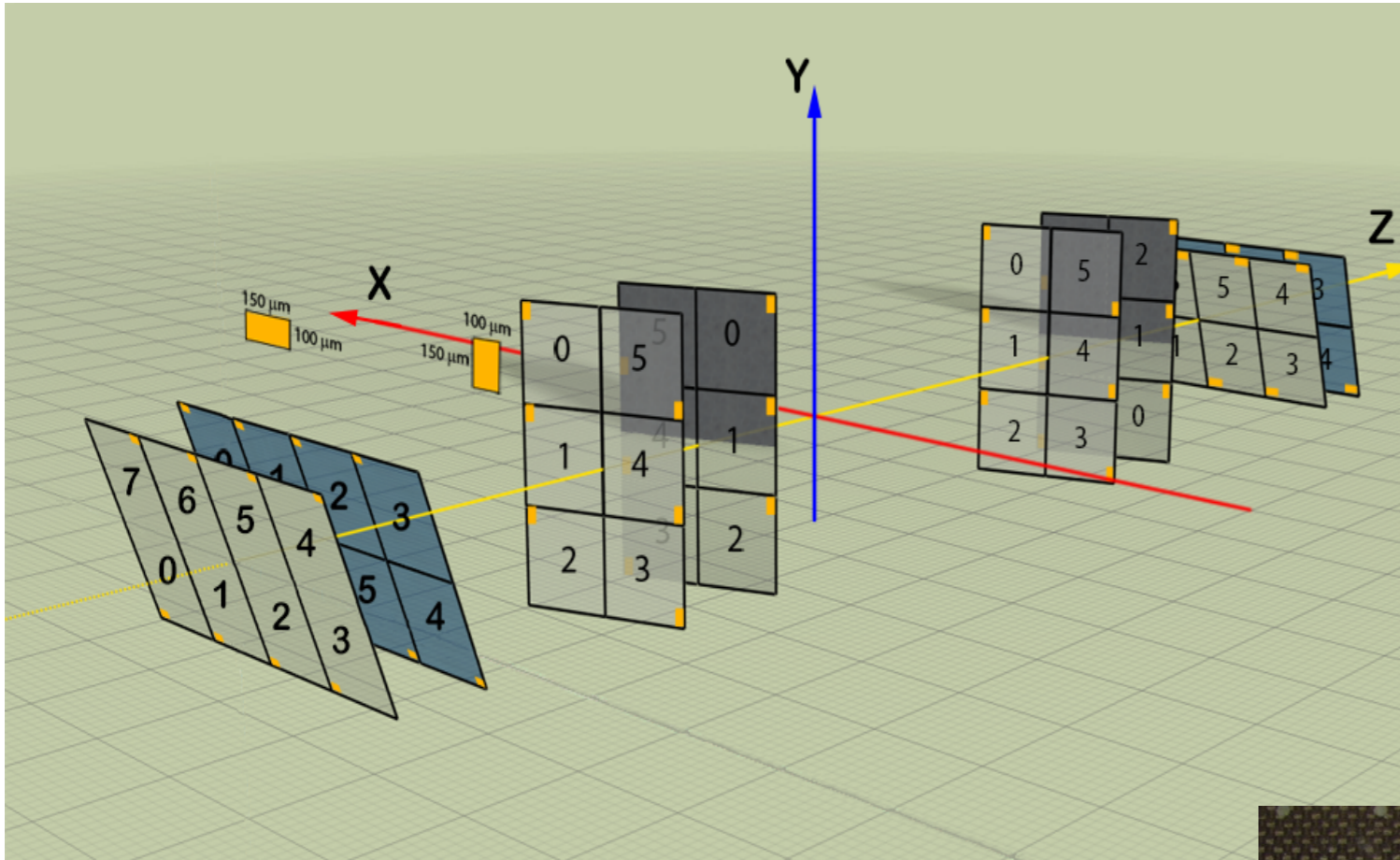
Fermilab Test Beam Facility provides **120 GeV protons** from Main Injector

- At present 2 independent tracking telescopes are installed:
 - The legacy **pixel telescope** built using leftover CMS modules
8 pixel planes
readout based on PSI46 analog chip (Phase 0)
(100x150 μm^2 pixel cell for 80 rows and 52 columns)
~8 μm resolution on each coordinate
 - The new strip based telescope (being commissioned now)



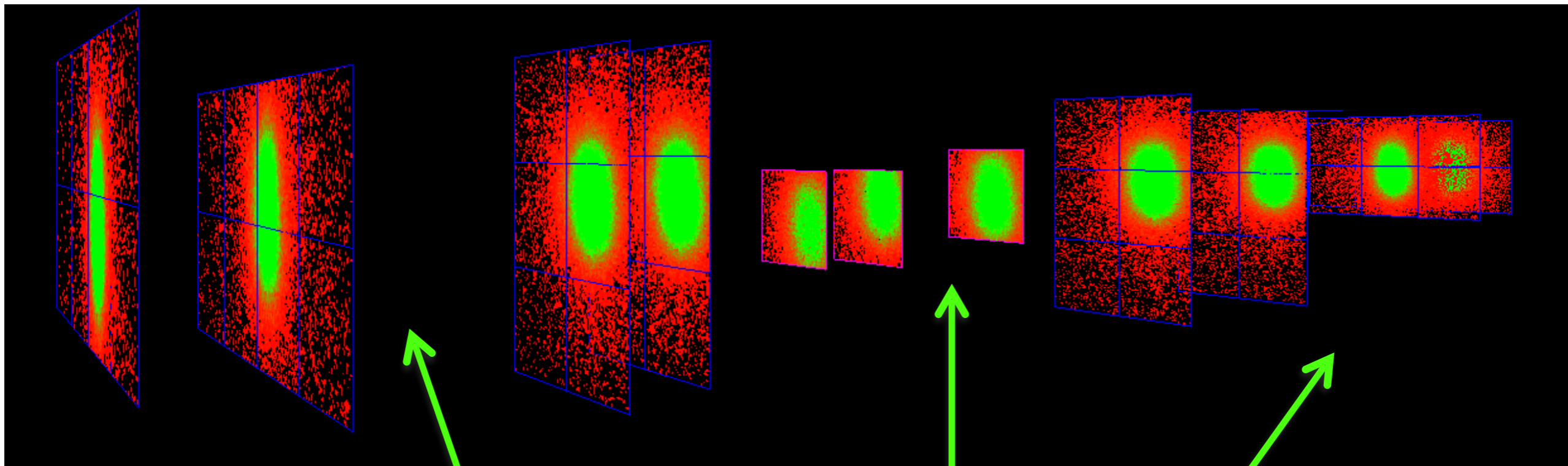
Pixel Telescope

Pixel telescope planes



- 8 modules tilted at 25° to maximize charge sharing
- Coverage area only $1.6 \times 1.6 \text{ cm}^2$
- Resolution on the detector under test of $\sim 8 \text{ } \mu\text{m}$

Online data taking

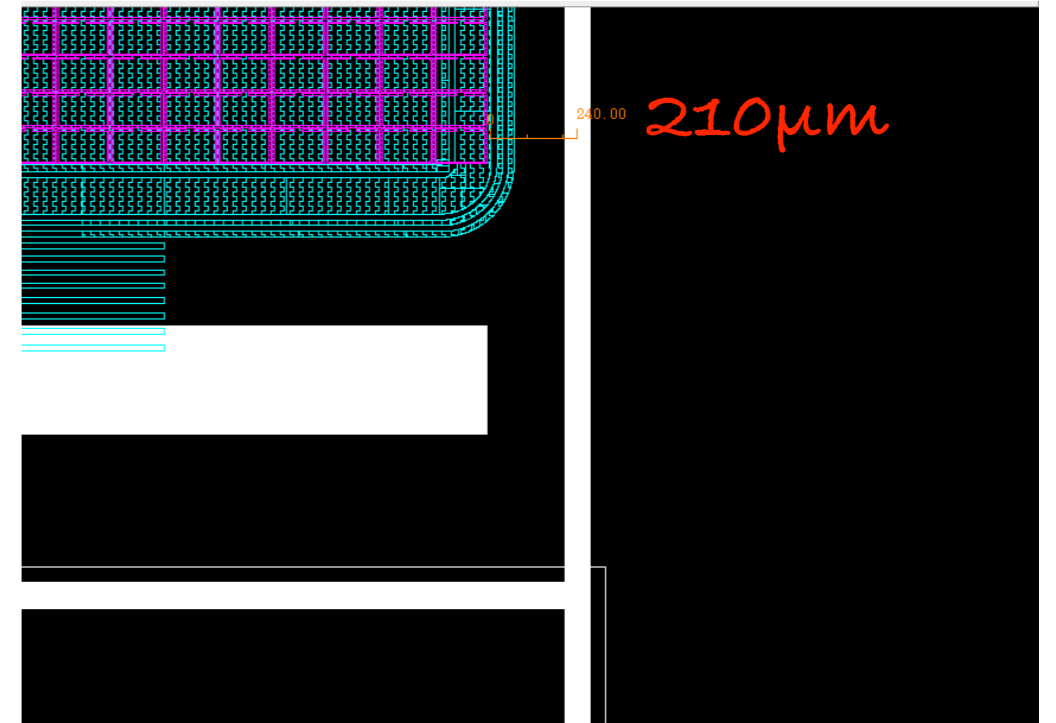


3 detectors under test

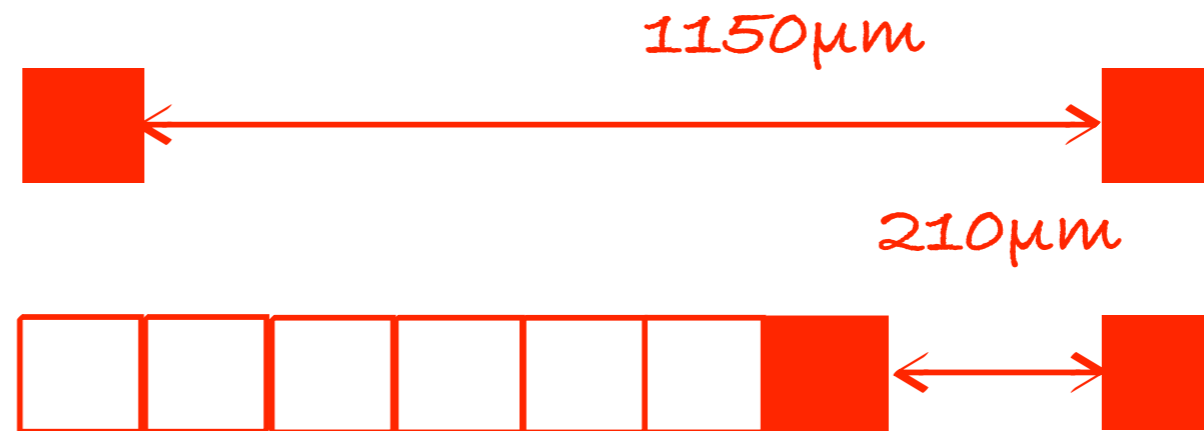
Pixel telescope

Slim Edge

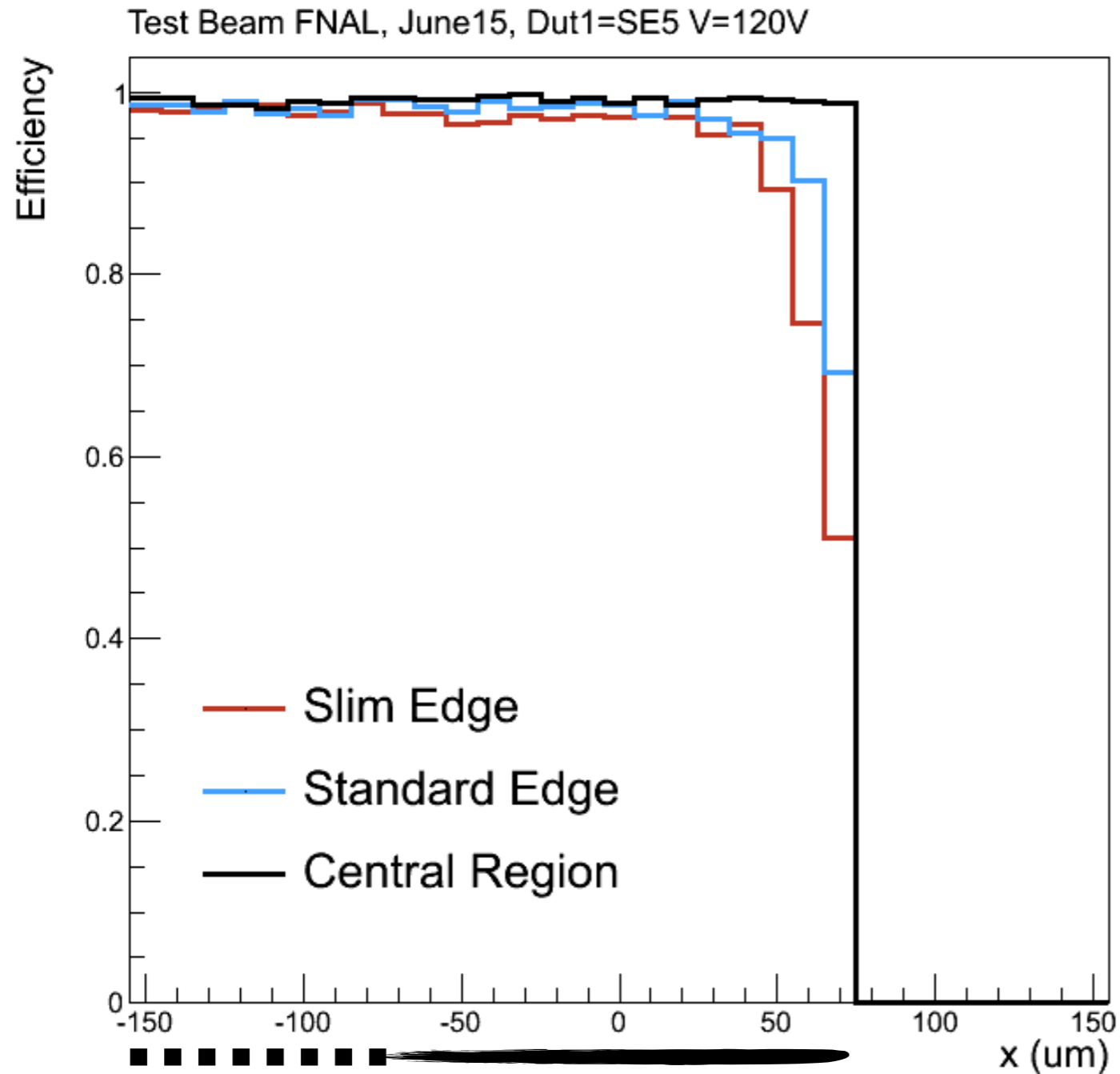
- Aim at minimizing the dead region at the physical edge of the sensor itself
- The efficiency of the pixels closely located to the edge depends on the geometry of the guard-rings on the opposite side (p-side).
- The pixel array (active area) normally ends at 1.15 mm from the dicing edge.
 - In these prototypes such distance has been reduced down to only 210 μm .
 - The reduction is of $\sim 950 \mu\text{m}$



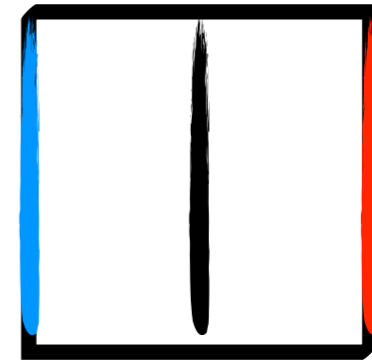
type3, full CCE up to 210 μm



Slim-Edge, efficiency



col: 0 25 51



- * Loss of efficiency on the edge due to error on the track extrapolation
- * Right and left edge behave similarly
- * Slight worse efficiency for the Slim edge
 - * effect on the last 15 μm ,
 - * but 950 μm are gained (~6 pixels)

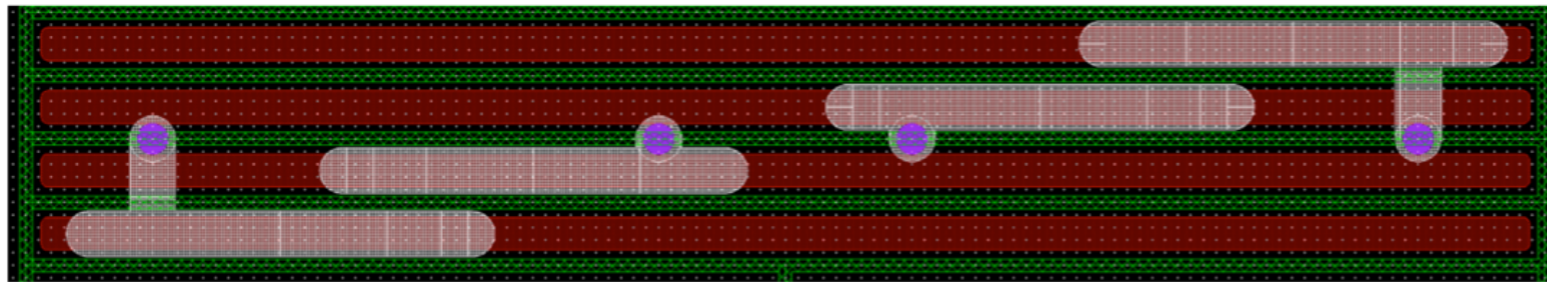
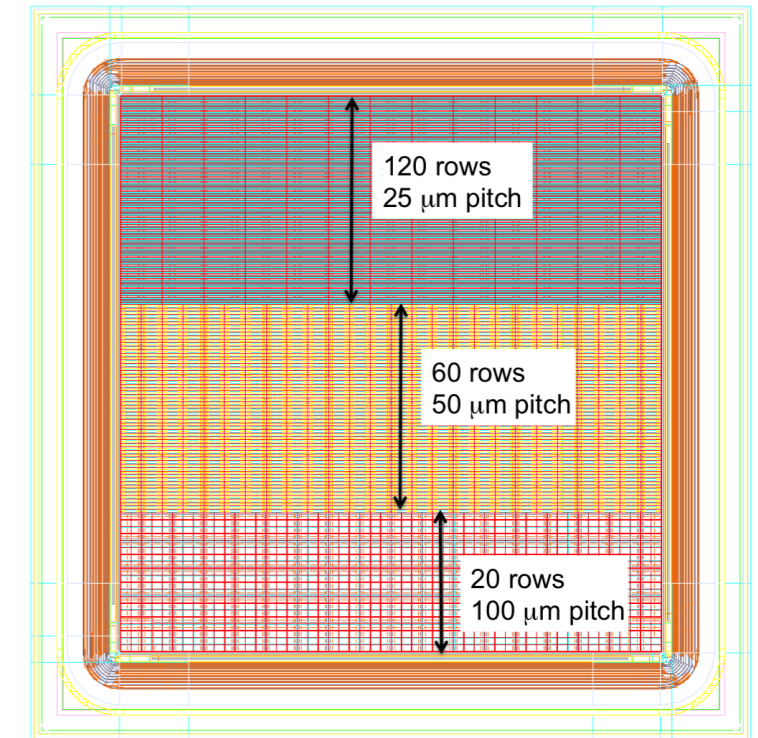
col: 1 24 50 0 25 51

Small pitch sensors

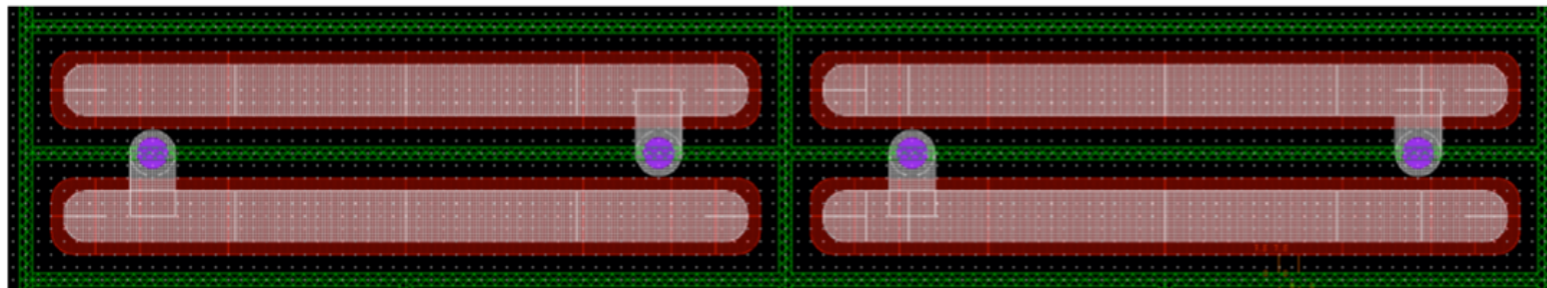
Require bump-bonding patterns compatible to PSI46 ROC

Maintained the same pixel area $100 \times 150 \mu\text{m}^2$ that is implemented in the Phase-I design

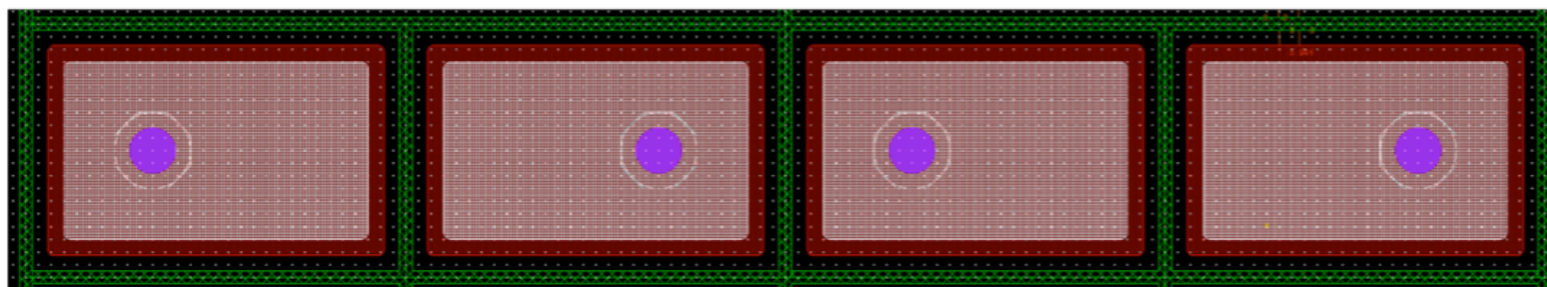
Single ROC sensors split in 3 regions with 3 different pitches



n+	→ 13 μm
gap	→ 3.5 μm
p+	→ 5 μm
gap	→ 3.5 μm
Pitch	→ 25 μm



n+	→ 30 μm
gap	→ 7.5 μm
p+	→ 5 μm
gap	→ 7.5 μm
total	→ 50 μm



n+	→ 83 μm
gap	→ 6 μm
p+	→ 5 μm
gap	→ 6 μm
total	→ 100 μm

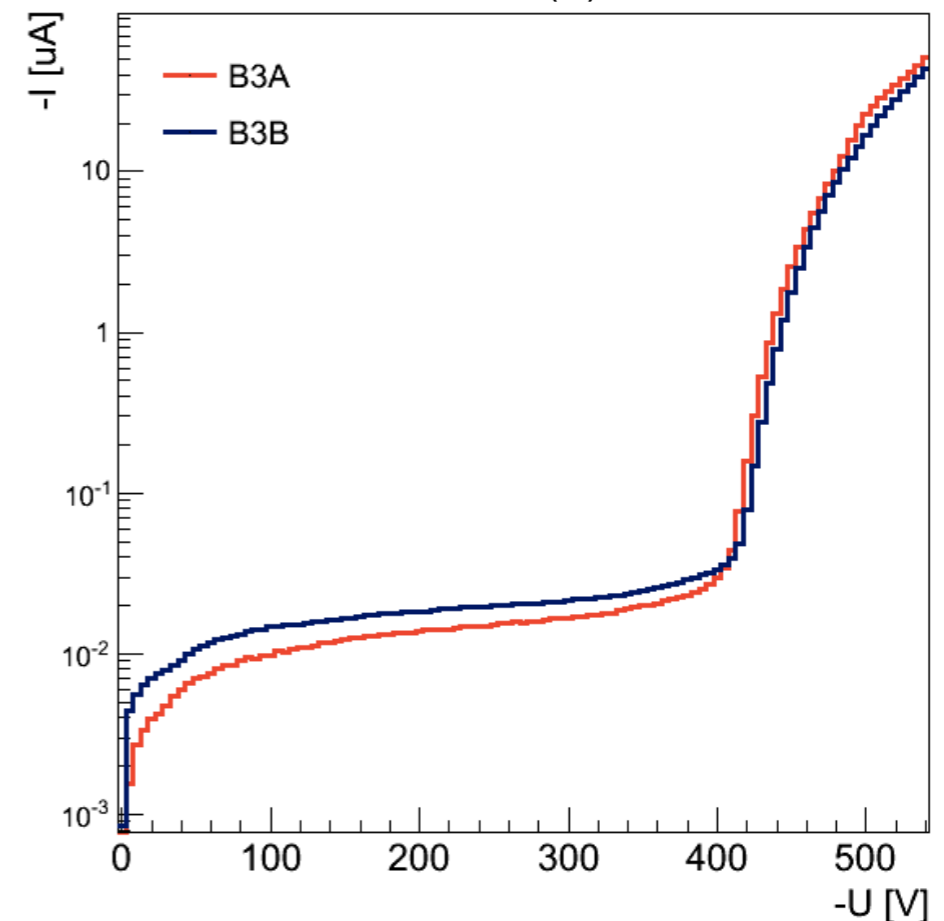
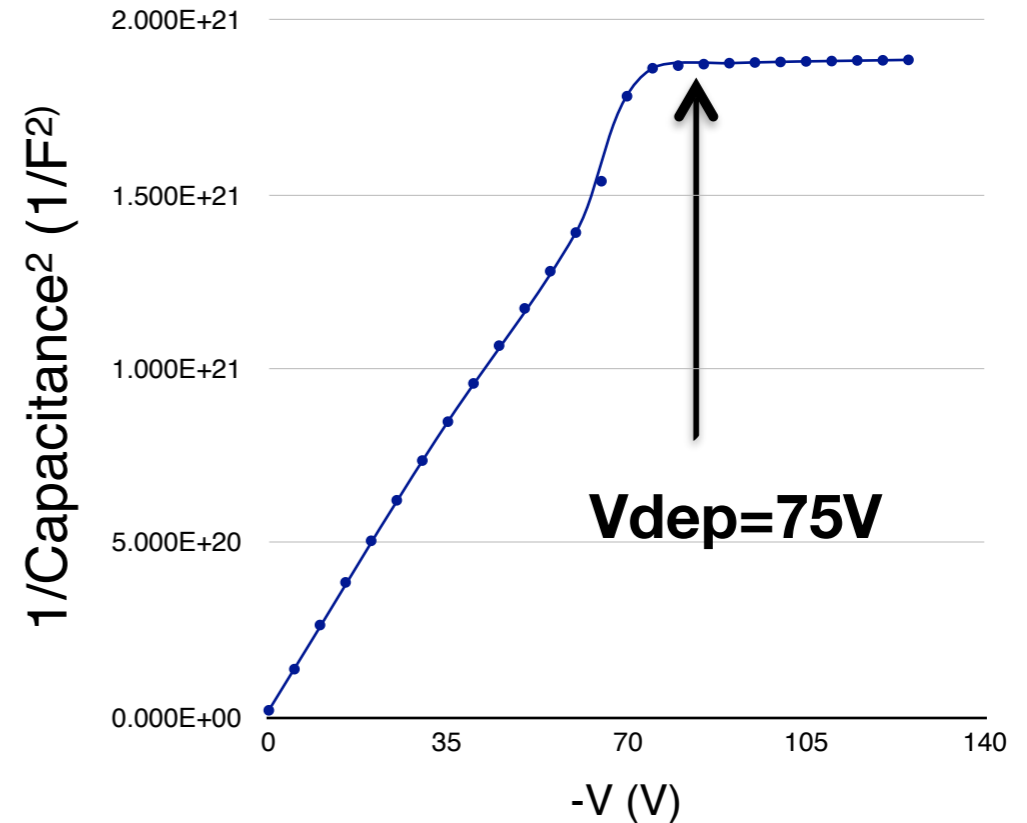
Small pitch, DC characterization

Depletion voltage is measured from CV curve to be $\sim 75\text{V}$

Breakdown voltage is well above the depletion voltage

Sensors were mounted on board post bumping, tested and they are functional with similar IV performance.

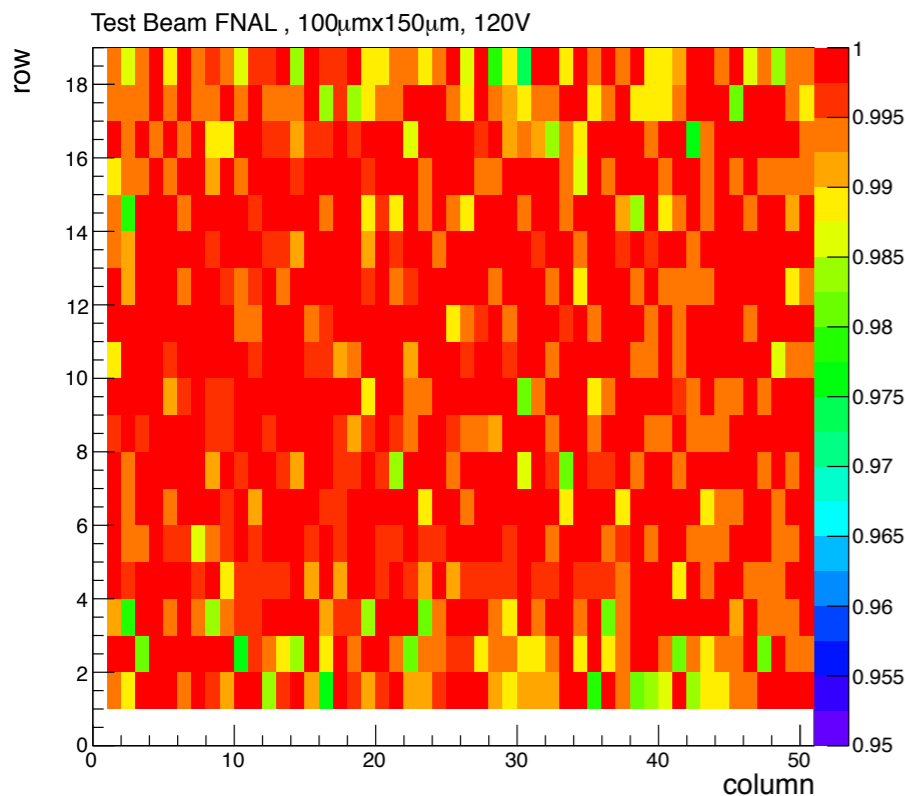
Total leakage current of 20nA in 0.64 cm^2 (very low)



Small pitch, efficiency

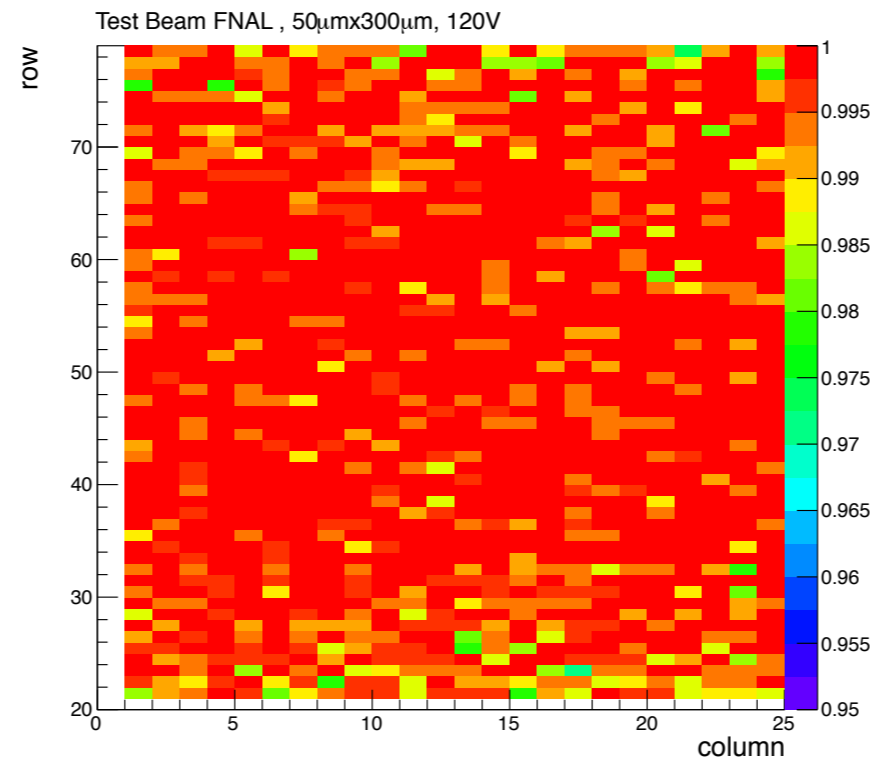
- Analysis is performed separately for each zone
- Efficiency is computed by requiring that either the cell pointed by the track or one of its neighboring cells has an hit

100x150



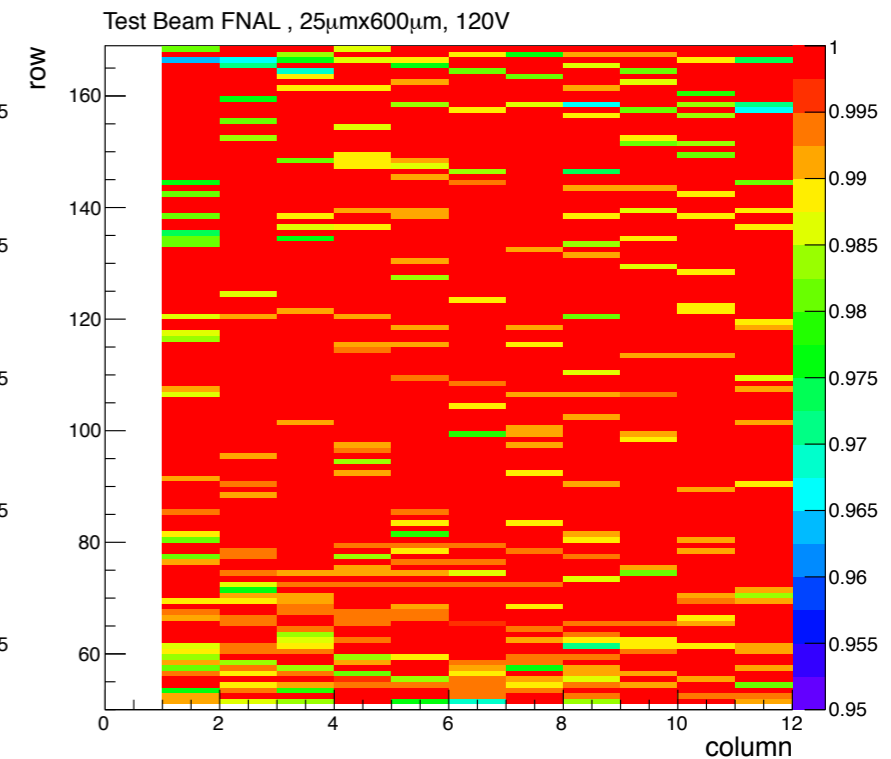
99.7%

50x300



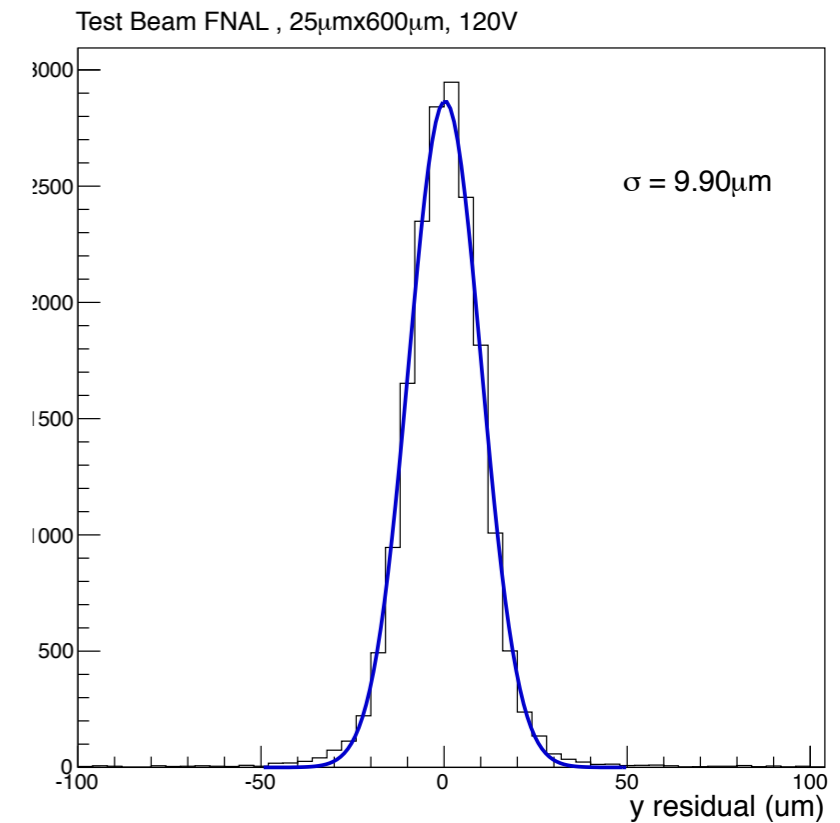
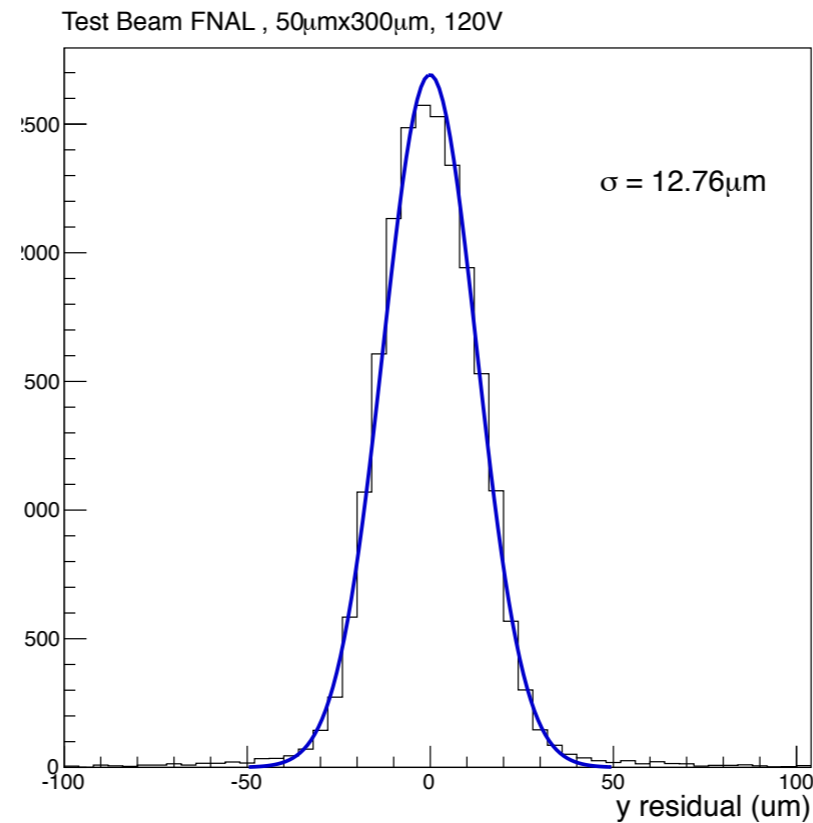
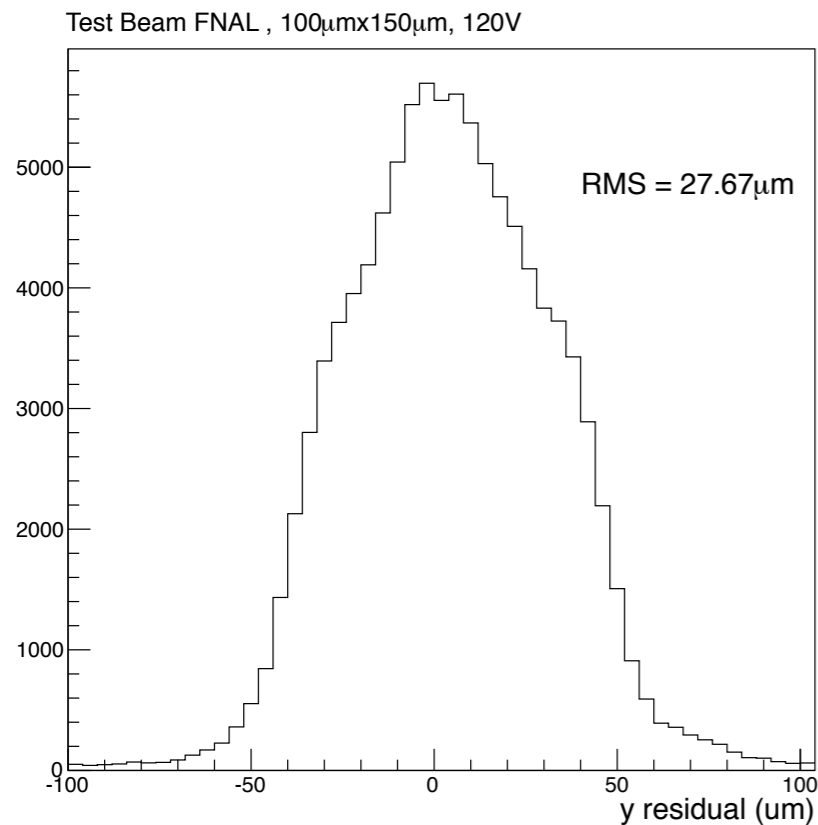
99.7%

25x600



99.6%

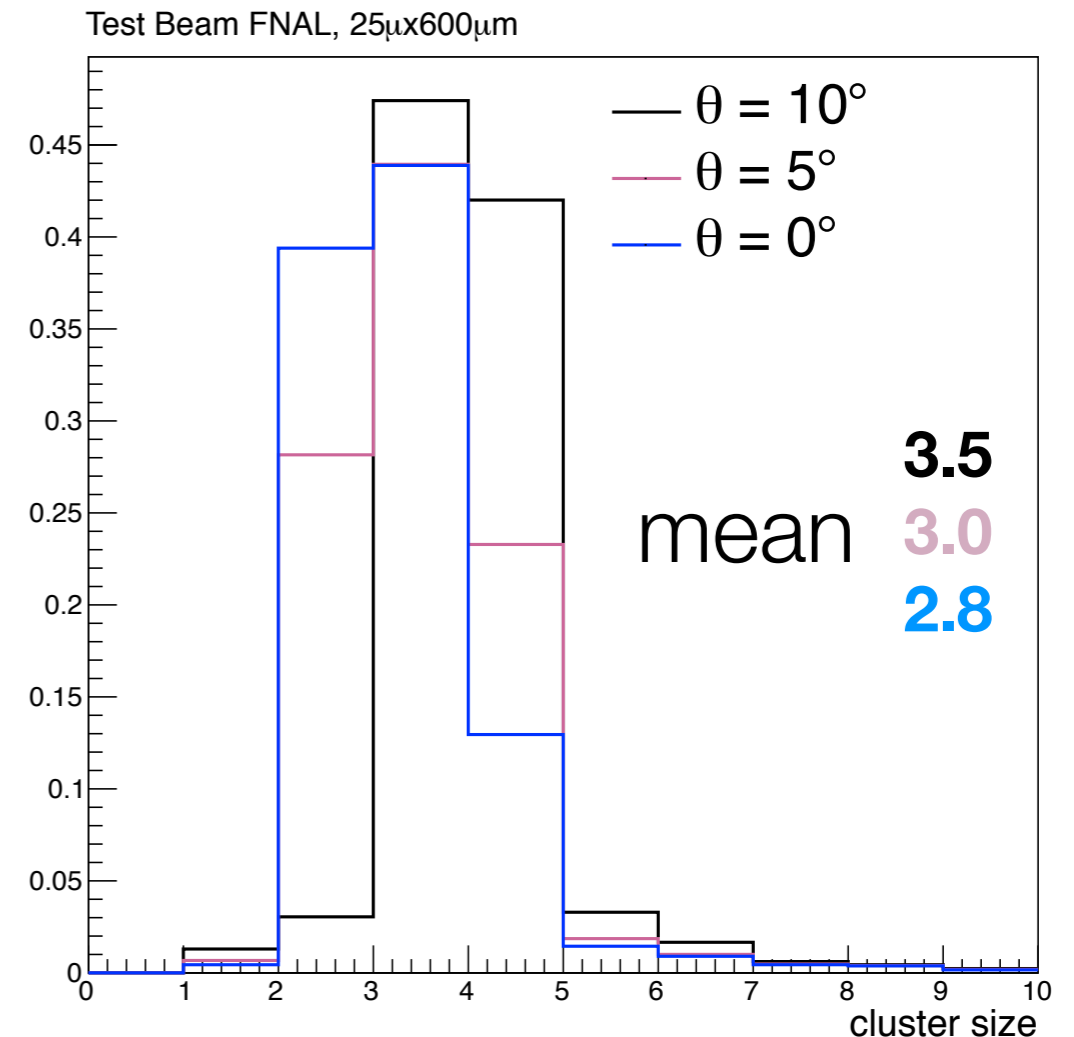
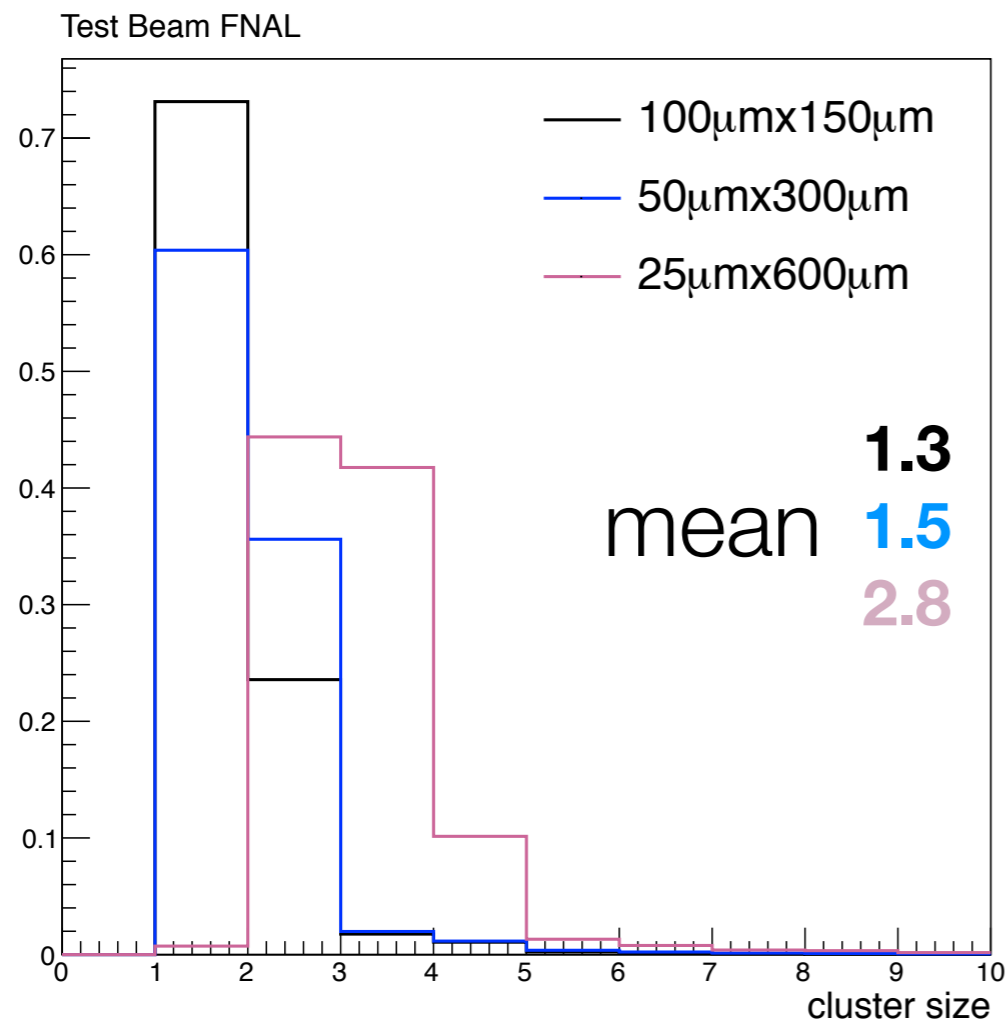
Variable pitch, resolution



Spatial resolution :

- * Position on detector under test is determined using the cluster's center of mass
 - * $< 9.9\mu\text{m}$ for 25 μm pitch even if all clusters are considered
 - * 12.8 μm for 50 μm pitch
 - * 27.7 μm for 100 μm pitch
- * Taking into account the telescope resolution of 8 μm , the hit **resolution is 5.8 μm** for **25 μm pitch pixels**

Variable pitch, cluster size



Cluster size increases as pixel pitch decreases.

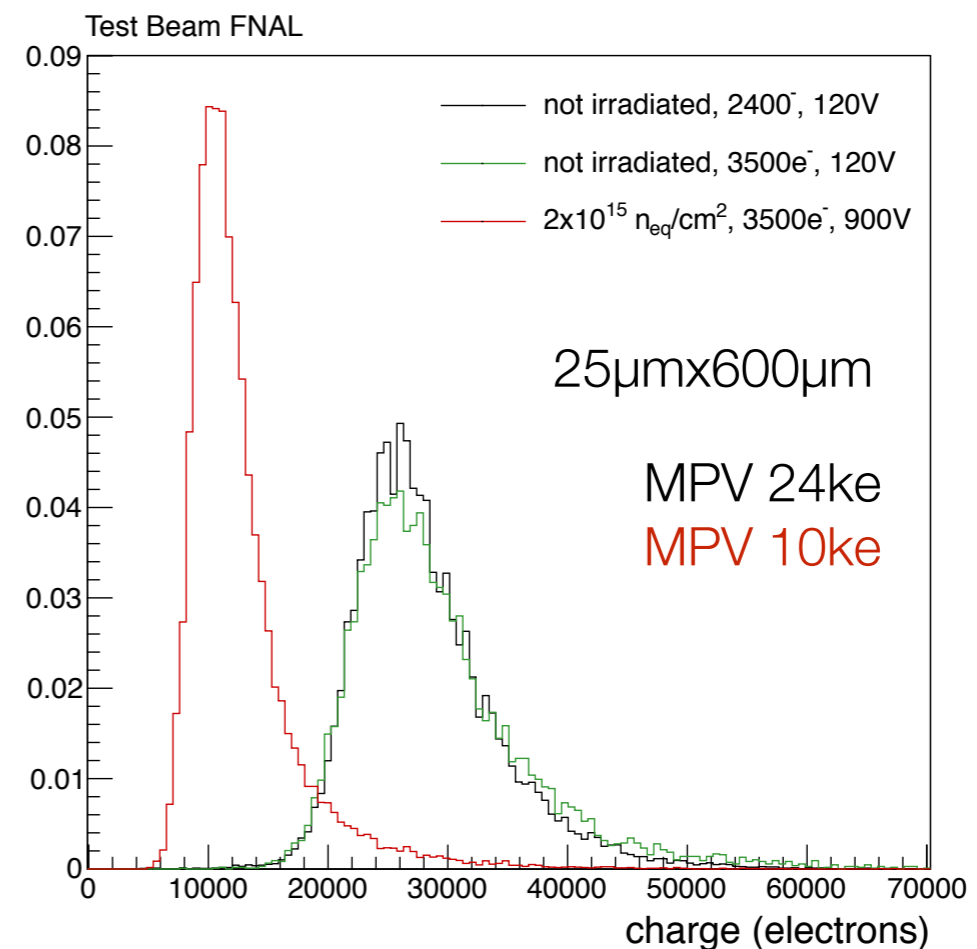
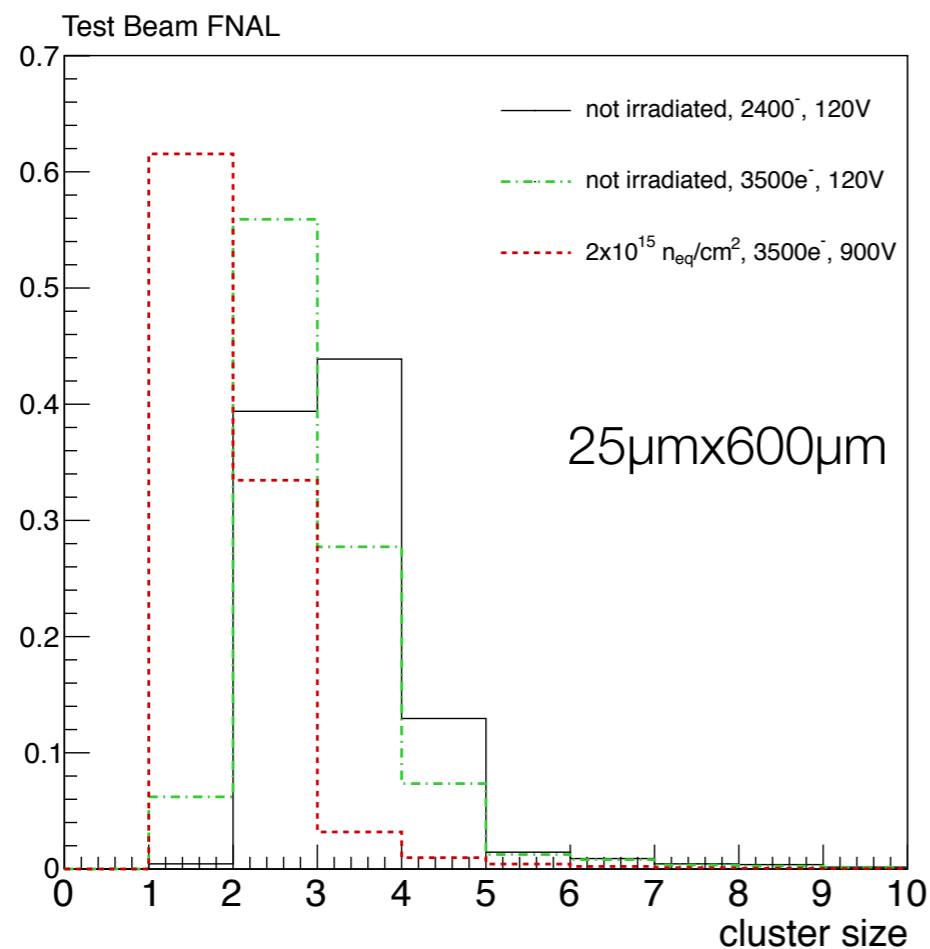
100 and 50 µm pitch pixels behave according to expectations

For the 25 µm pitch:

- No more single pixel clusters.
- Several clusters of size 4
- Cluster size increases for rotation along the short pitch

Small pitch, after irradiation

- We have irradiated (CERN PS, 23 GeV p) some of these devices at different fluences:
 - 2×10^{15} , 4×10^{15} and 6×10^{15} 1MeV Neutron equivalent
- Sensors irradiated at 6×10^{15} 1MeV Neutron equivalent were not operable anymore as we integrated more than 200 MRad reaching ROC's limits
- We have operated these devices at FTBF at -20C at 900V



We report a reduction of the cluster size and of the collected charge

Next on Irradiation studies

- We were able to operate irradiated devices up to $2 \times 10^{15} \text{ cm}^{-2} n_{\text{eq}}$
 - As we integrated more than 200 MRad reaching ROC's limits
- We are interested in much higher fluences for HL-LHC
- Currently we are limited by the PSI46 which cannot integrate more than 200 MRad
 - The PROC600 would integrate 500 MRad, it will be available soon
- Two possible alternative approaches to test sensor performance with the PSI46
 - **neutrons**
 - **cold bump bonding** and then **proton** irradiation
 - get the sensor irradiated first and then perform the cold bump-bonding
 - achieve uniform exposure by a scan of the sensor's area

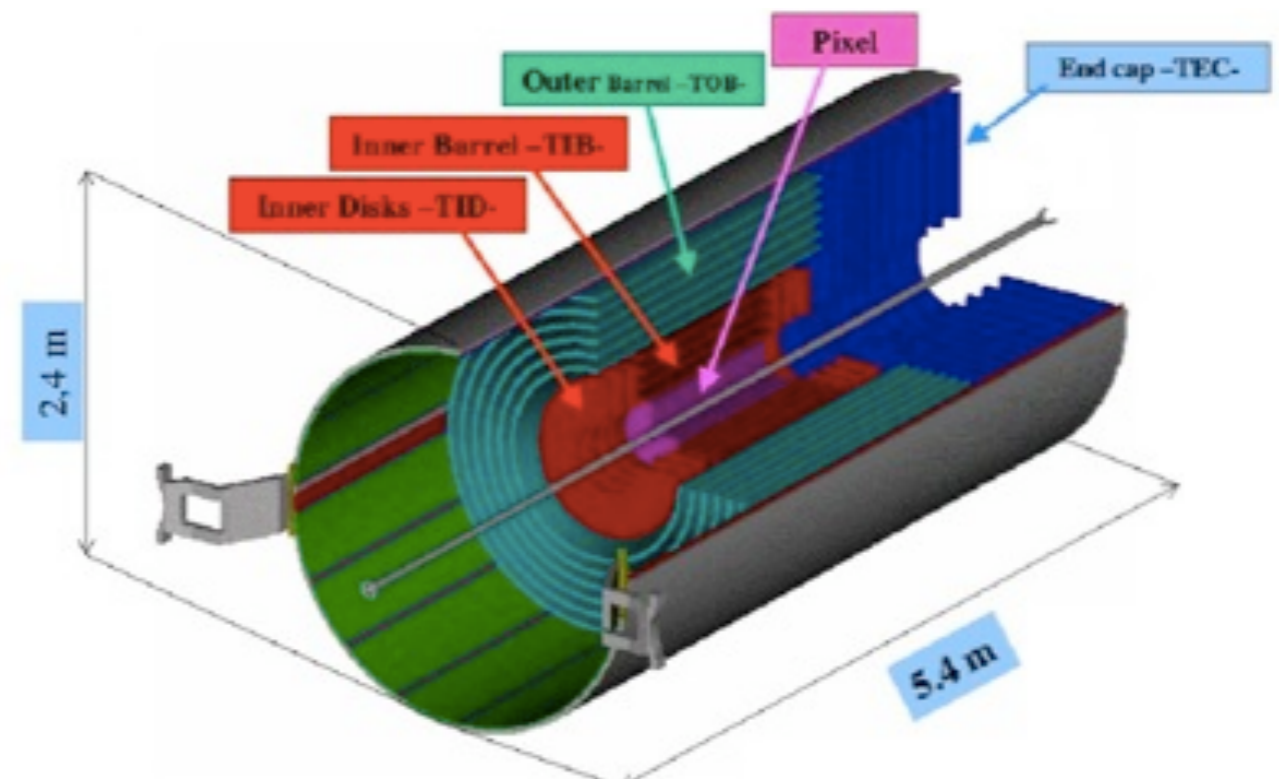
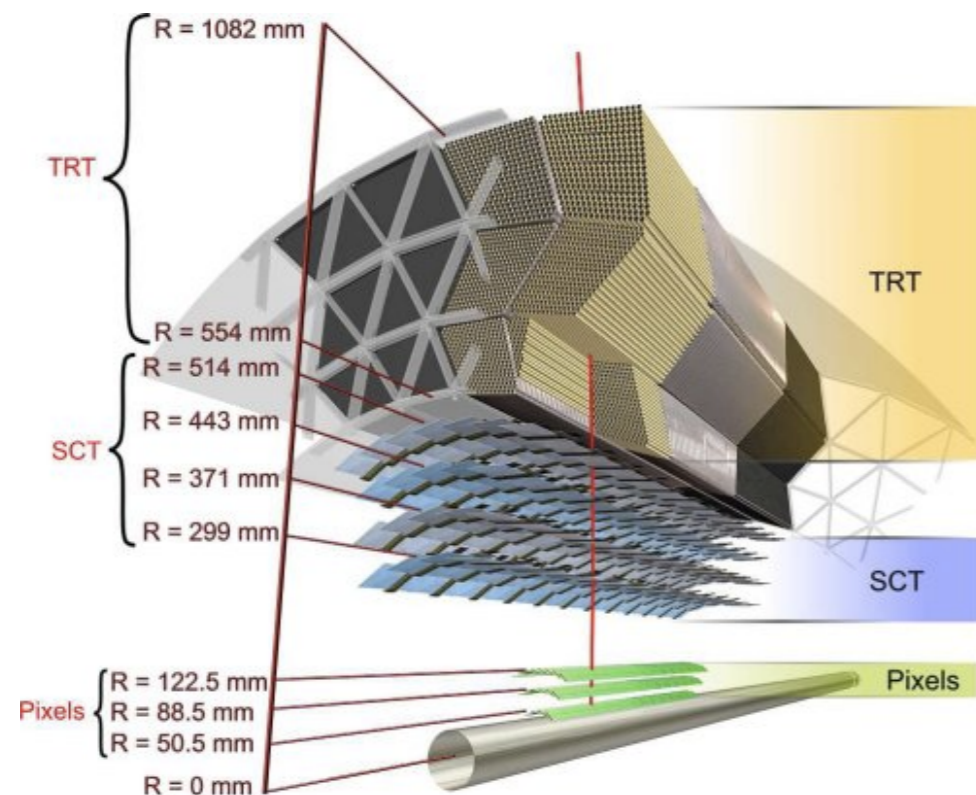
Conclusions & Outlook

- R&D for CMS HL-LHC upgrade is ongoing to achieve higher granularity and radiation tolerance
- Different technologies and prototypes are being investigated
 - 3D and thin pixel sensors with small pitches both in n-in-p and n-in-n
- Here presented the characterization of **n-in-n** prototypes silicon sensors :
 - **Small Pitch** sensors:
 - fully efficient independently of the pitch
 - resolution is as good as $\sim 6\mu\text{m}$
 - **Slim Edge** sensors:
 - fully efficient up to $300\mu\text{m}$ from the diced edge
 - not full charge collection efficiency for half of the last pixel
- Tools are in place to explore other sensors technologies and prototypes
 - This is a process that will continue for the next 1/2 decade and can be a great opportunity to learn the science behind particle detectors.

Additional Material

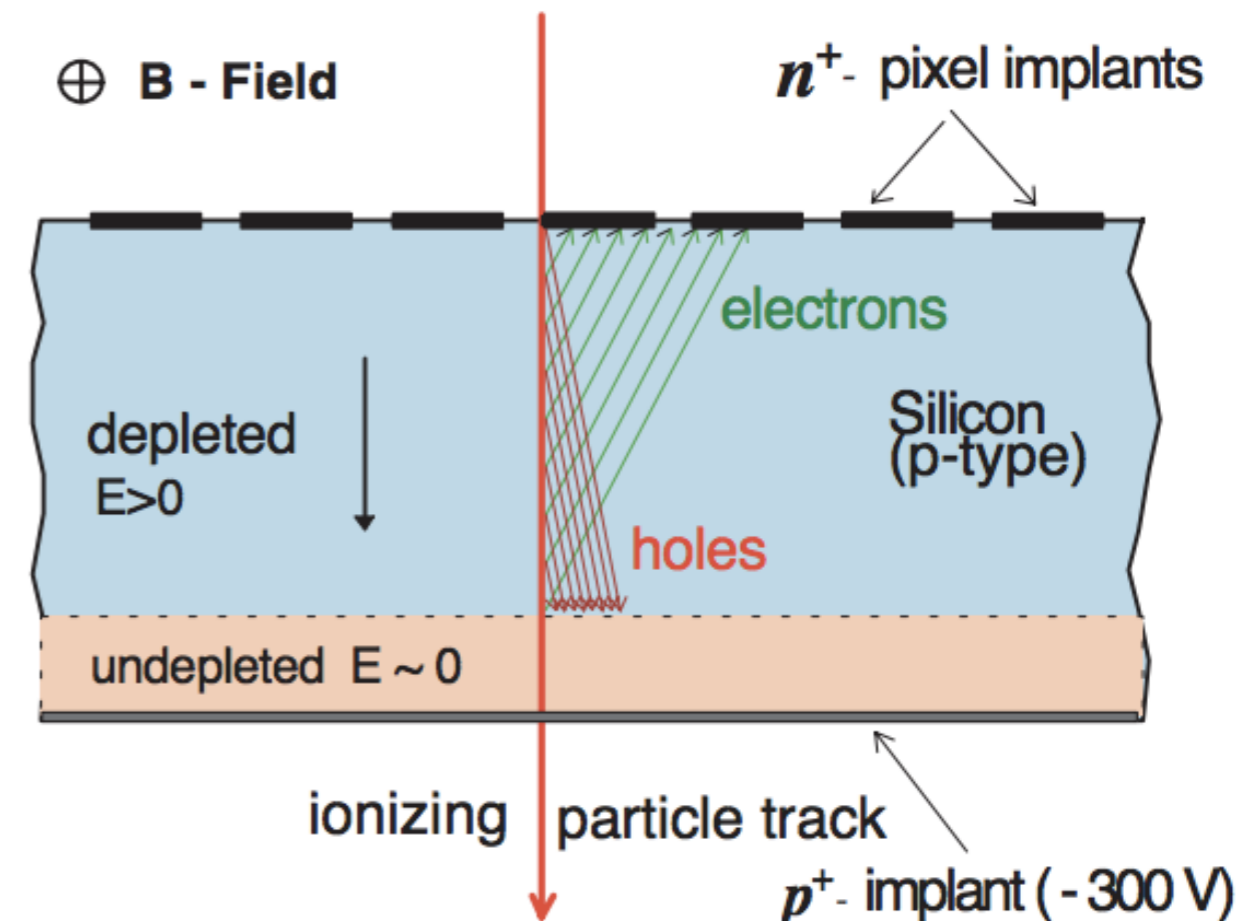
Atlas and CMS tracking systems

- Although CMS and ATLAS have the same scientific goals they use different technical solutions:
 - **Silicon pixels and strips+transition radiation tracker** vs. **full silicon tracker**
 - a different magnet-system design \Rightarrow different Lorentz angle
 - **2 T solenoid + toroid: 0.5 T (barrel), 1 T (endcap)** vs **3.8 T solenoid**
 - pixels: **50x400 μm** vs. **100x150 μm**
- Performance of CMS tracker and ATLAS trackers are in terms of momentum resolution
 - **$5 \times 10^{-4} p_T + 0.01$** vs. **$1.5 \times 10^{-4} p_T + 0.005$**
- Vertexing and b-tagging performances are similar



Lorentz shift

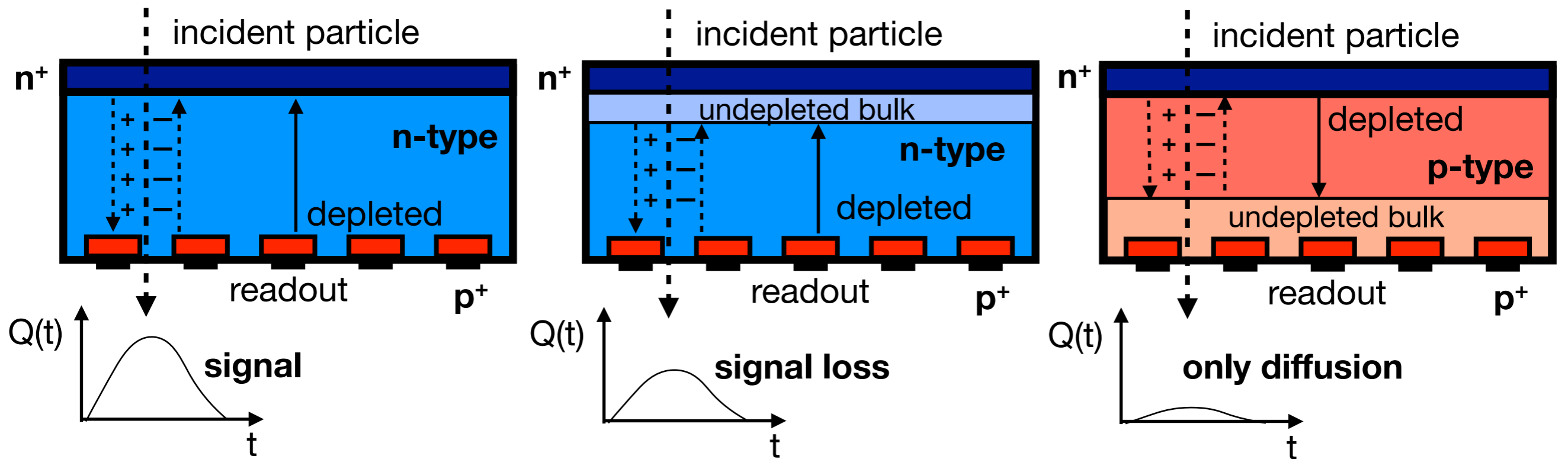
- The bending magnetic field not only bends the tracks but also bends the electrons and holes drifting within the silicon bulk.
- This Lorentz effect increases the number of cluster with multiple pixels
- and consequently (with the appropriate corrections) improve the spatial resolution of the detector.



for **CMS** Lorentz angles of ~ 30 for electrons in a silicon detector of $300\mu\text{m}$ thickness

p-in-n

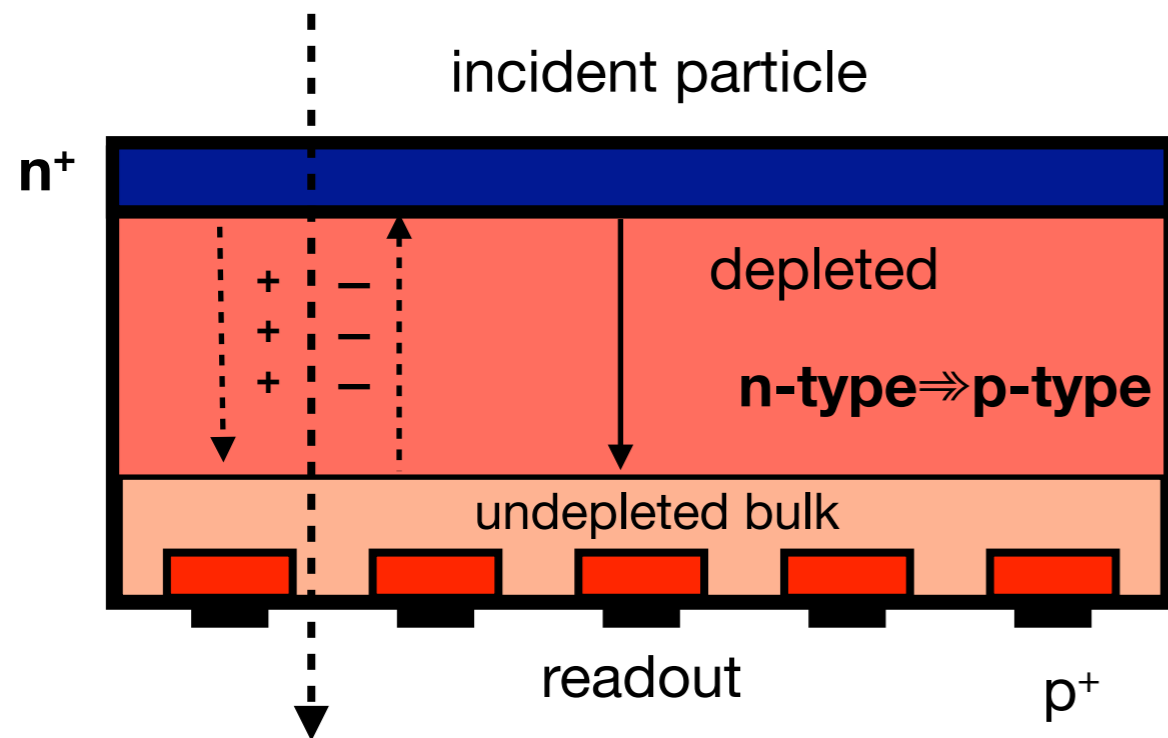
After irradiation (to a level implying type inversion) p-in-n does not function well if not fully depleted.



n-in-n vs p-in-n

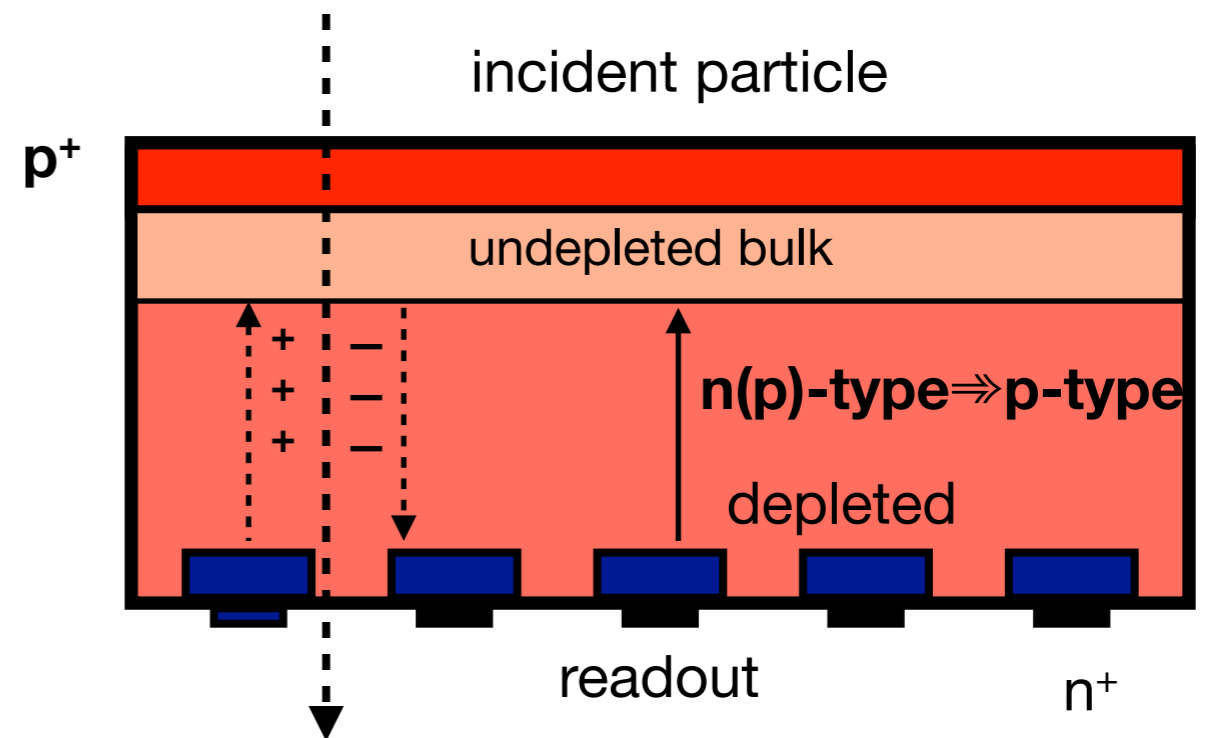
after irradiation and type-inversion

p-in-n



- signal loss
- resolution degradation due to charge spreading

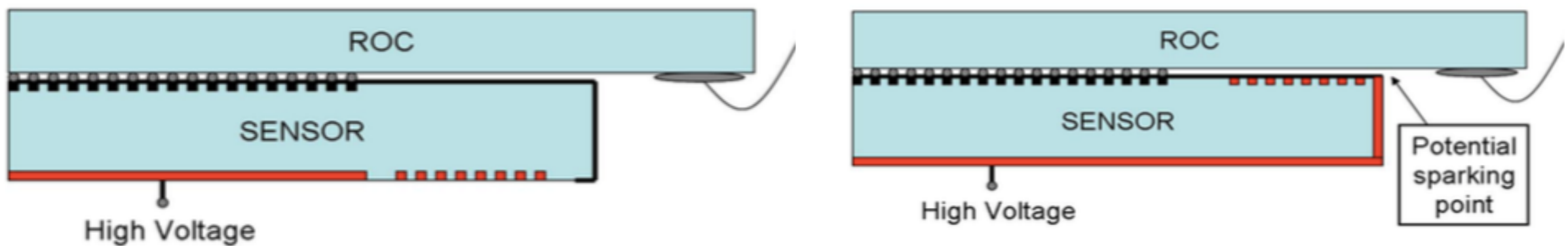
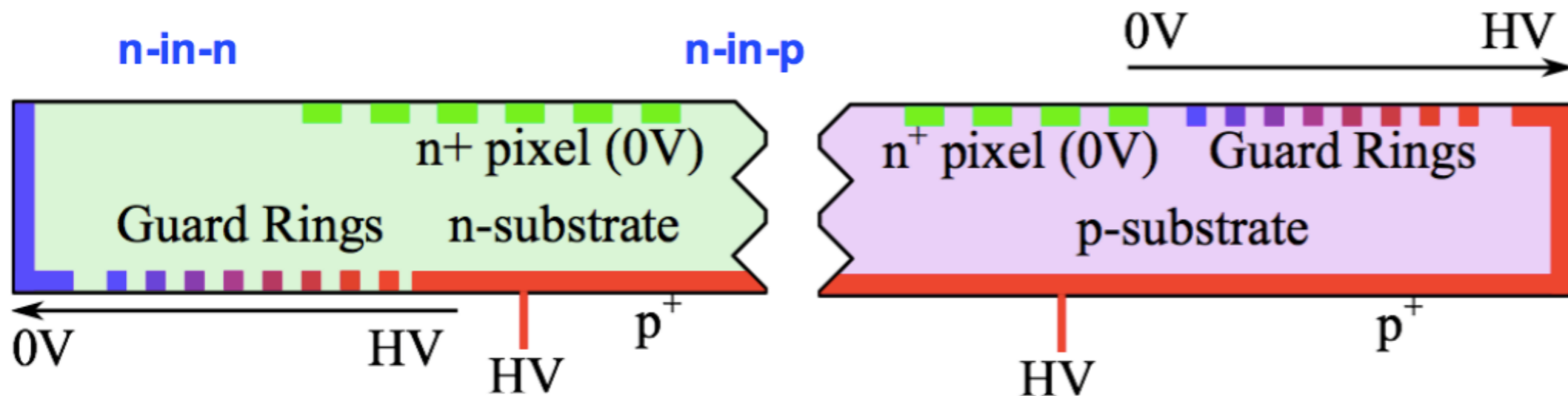
n-in-p or n-in-n



- faster charge collection
(drift for electron is larger)
- CCE degradation

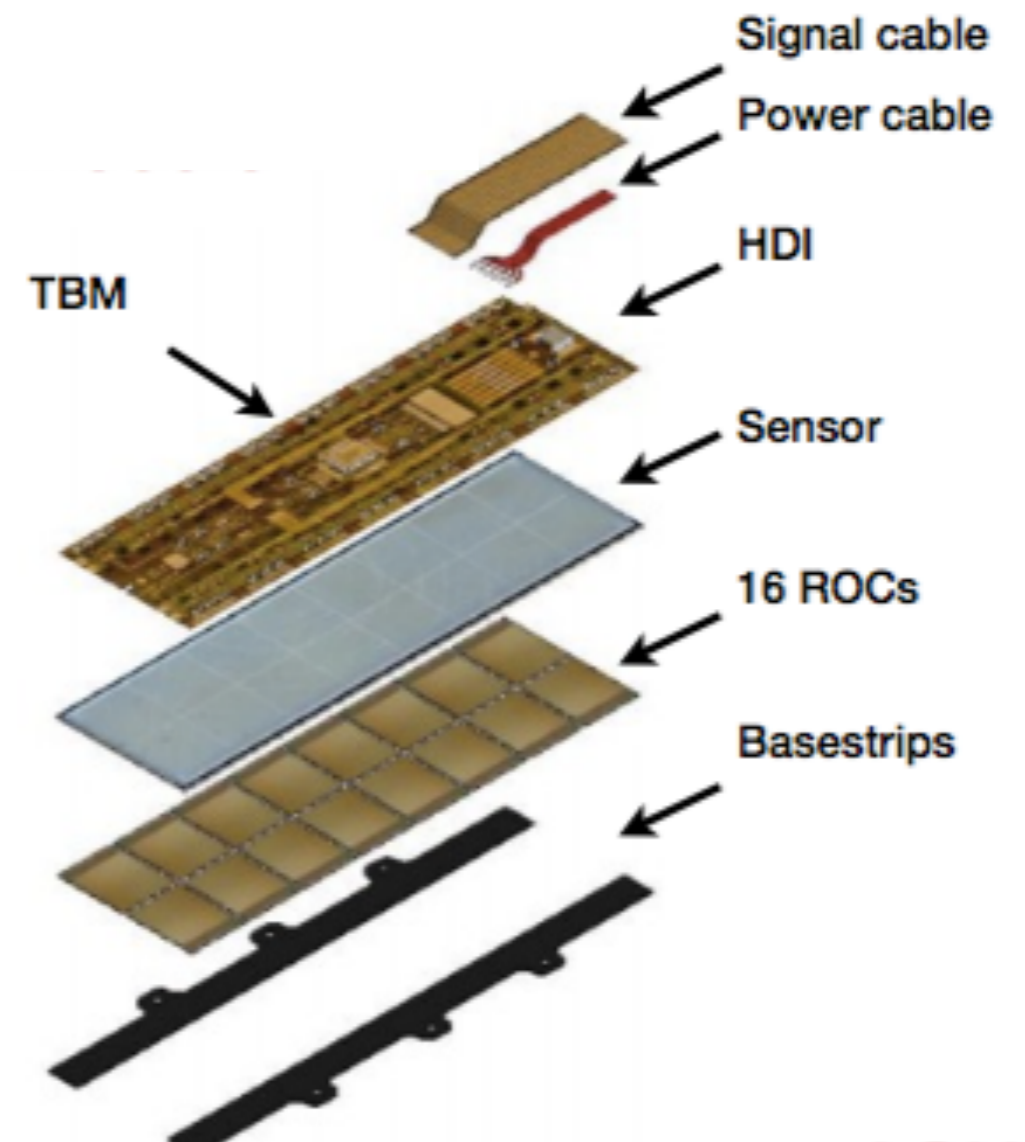
n-in-n vs n-in-p

double sided vs single sided



Modules for Phase I

- Module = ROCs + SiSensor + HDI
 - 1 ROC serves a 52x80 array of pixels
 - 16 ROCs \Rightarrow 66k pixels
- Digital readout chip based on present analog PSI46
 - 40MHz analog \Rightarrow 160 Mbits/s digital (8 bit ADC)
 - Zero suppression applied on ROC
 - better efficiency, resolution and longevity
- Token Bit Manager (TBM) located on High Density Interconnect (HDI)
 - Distributes clock and trigger to ROCs, manages ROC controls and readout



Full Size: 66.6 mm \times 25/21.6 mm (L2-4/L1)

Sensor size: 66.6 mm \times 18.8 mm

ROC size: 10.55 mm \times 8.02mm

Weight: < 3 g

Si sensor thickness: 285 μ m

ROC thickness: 75/175 μ m (L1/L2-4)

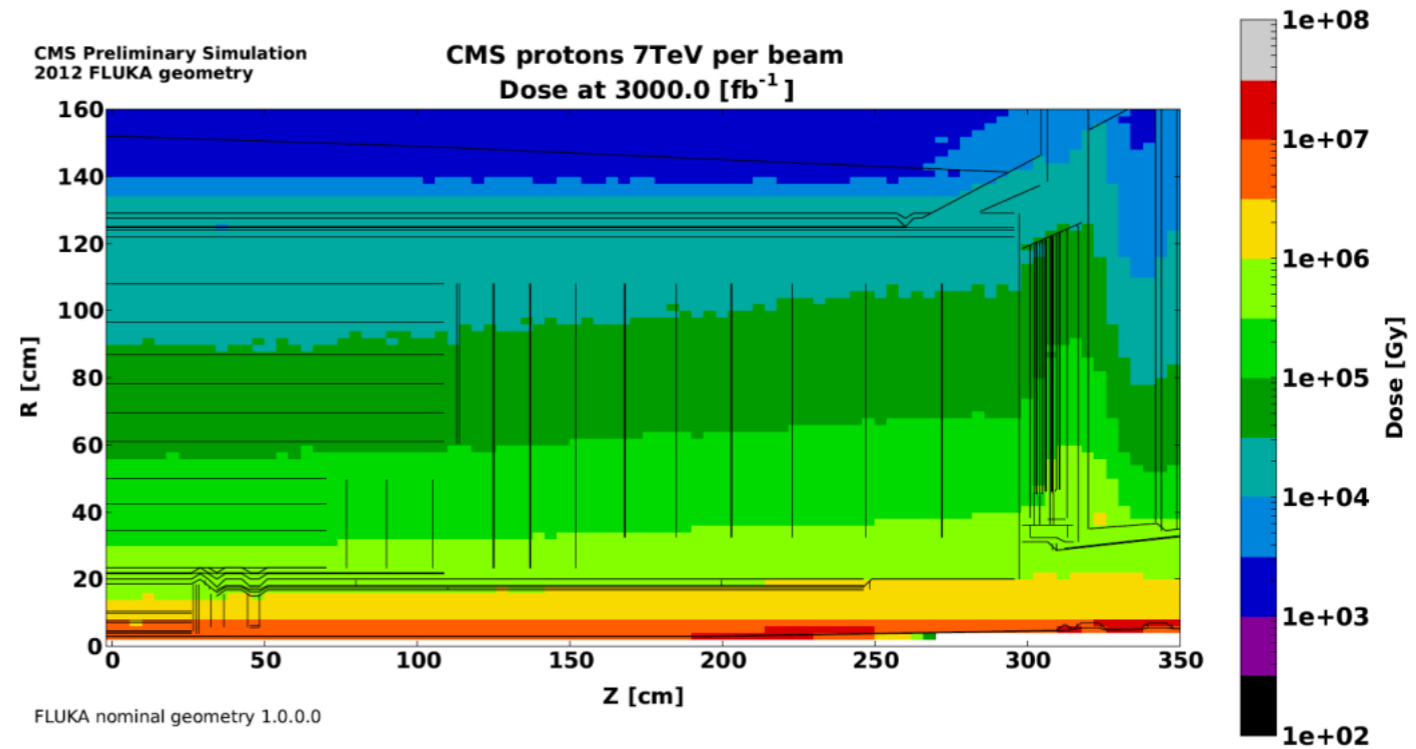
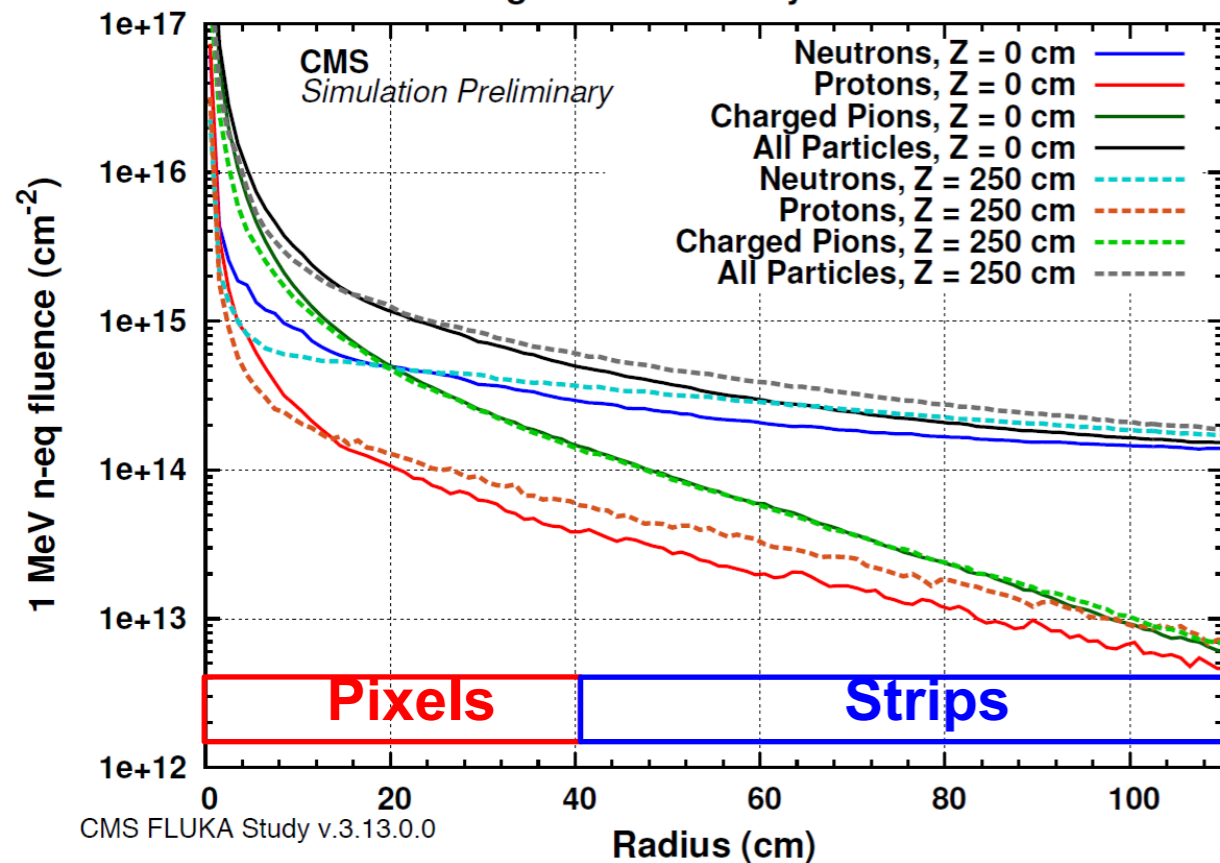
Segmentation: 16 \times 52 \times 80 = 66560 pixels

Power: 2.0 W

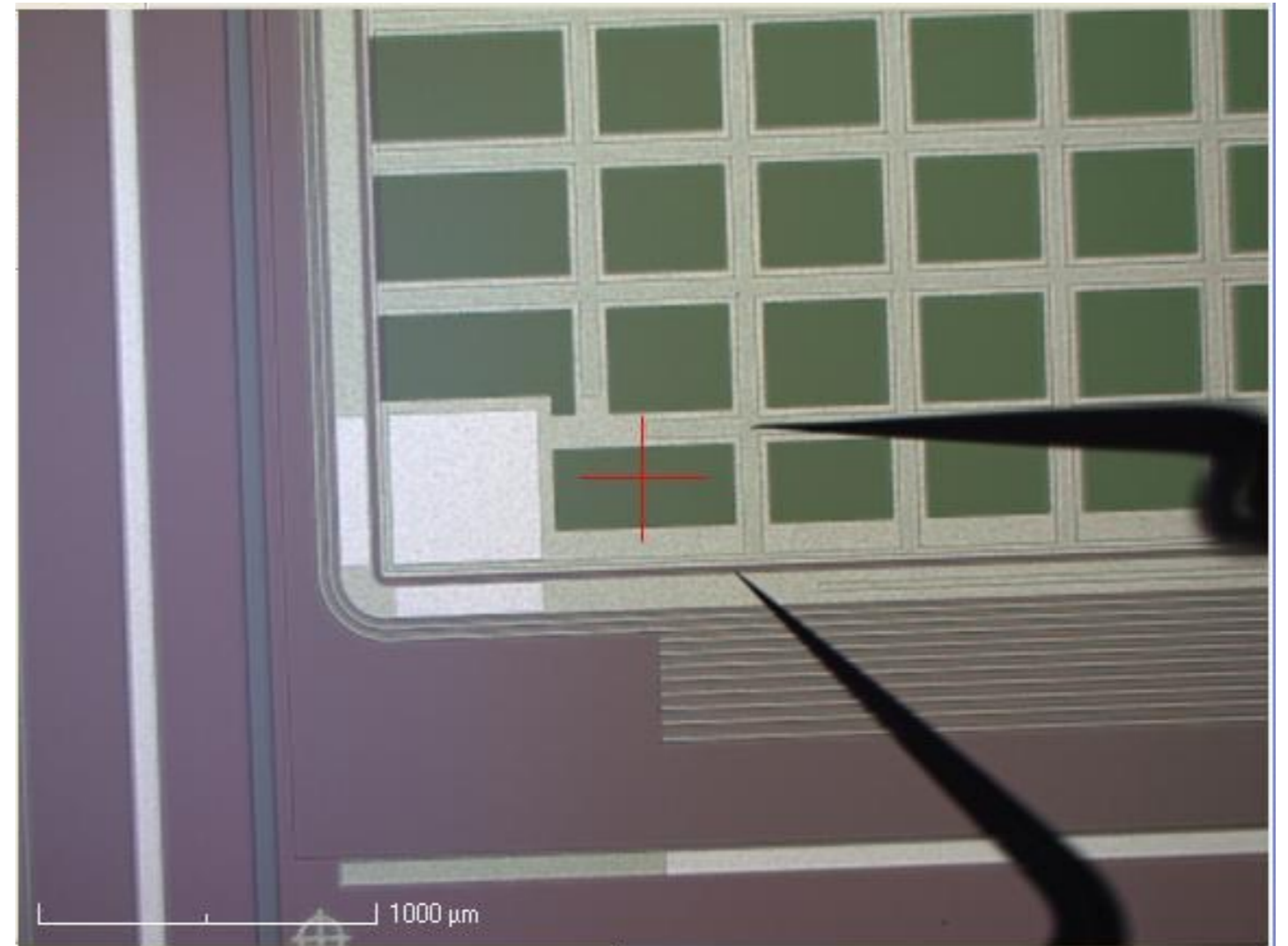
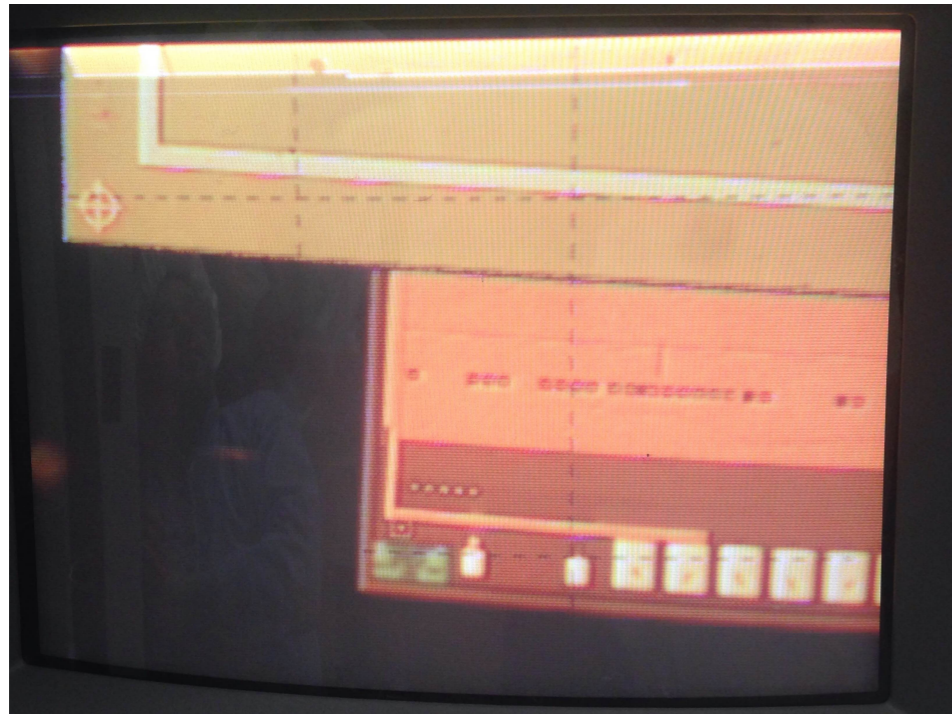
Limiting Factor: Radiation Damage

- 3000 fb⁻¹ over 10 years ⇒ Radiation damage of the previous 10 years in only one year
- Non-ionizing energy loss: fluence up to 2x10¹⁶ cm⁻² n_{eq} for innermost pixel layer
- Surface damage not negligible for pixel region
 - Ionizing dose at 4 cm: 5 MGy
 - Ionizing dose at 50 cm: 110 kGy

Contributions to 1MeV neutron equivalent fluence in Silicon
Integrated luminosity = 3000 fb⁻¹

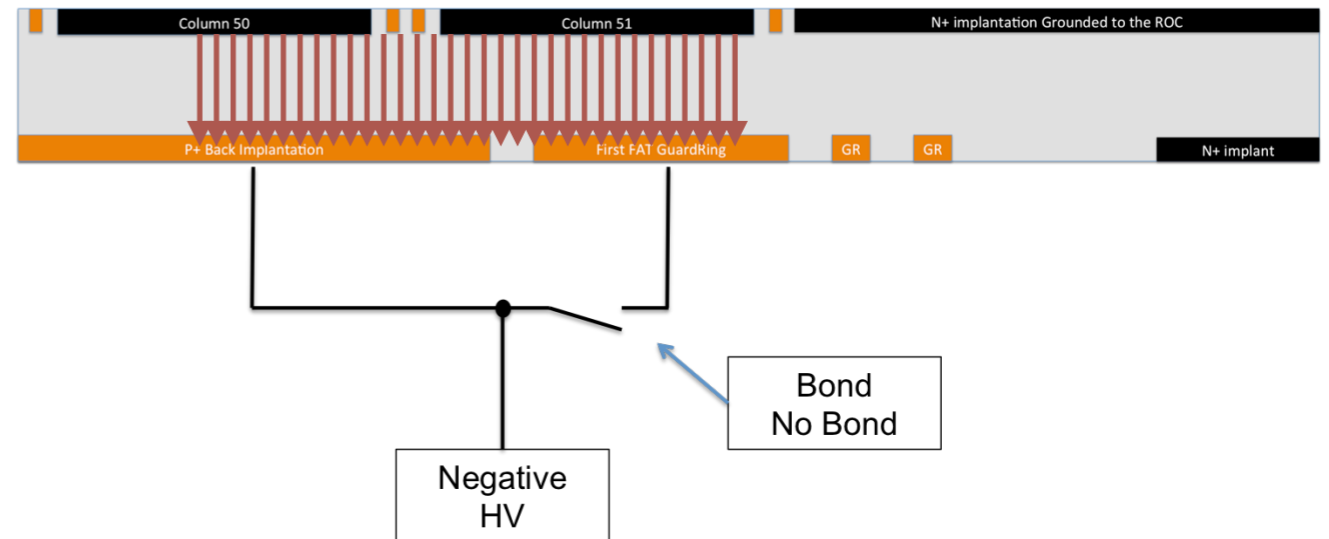
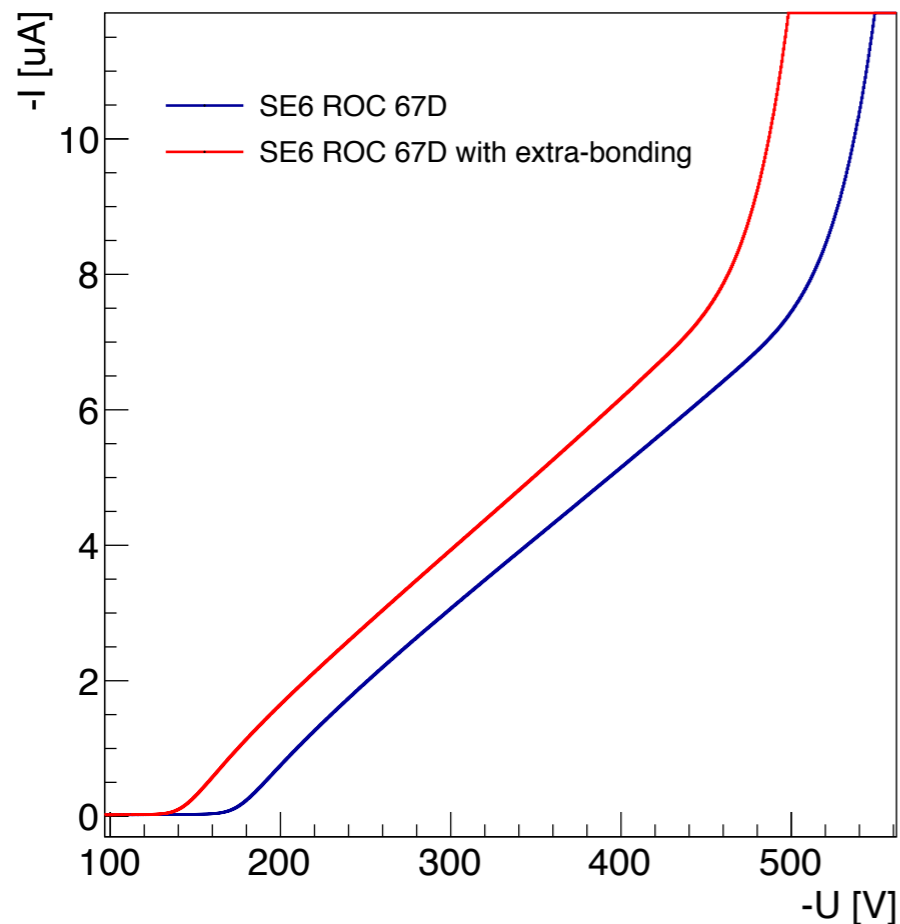


Slim-Edge, some pictures

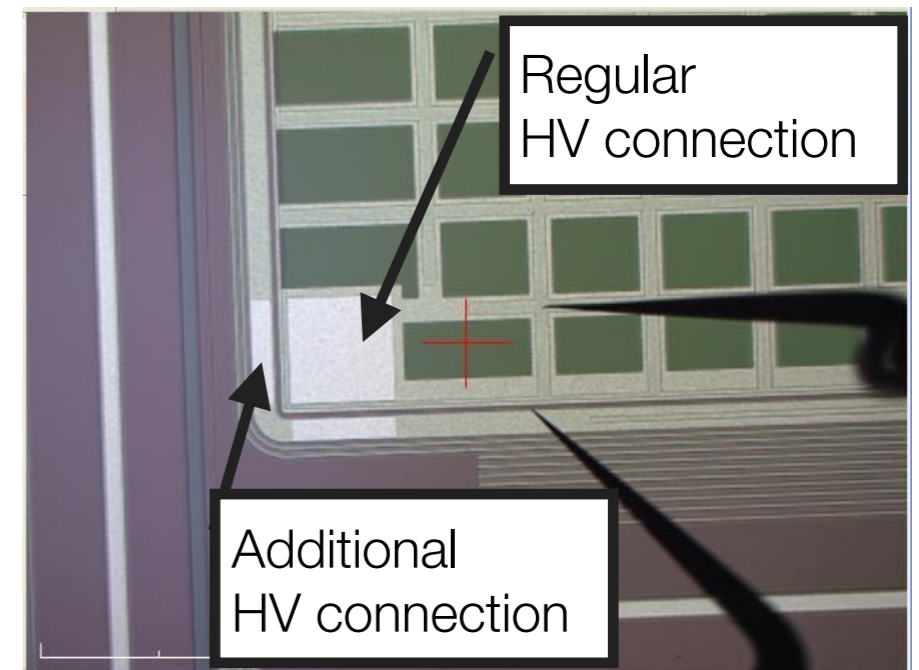


Slim-Edge, adding an extra-bonding

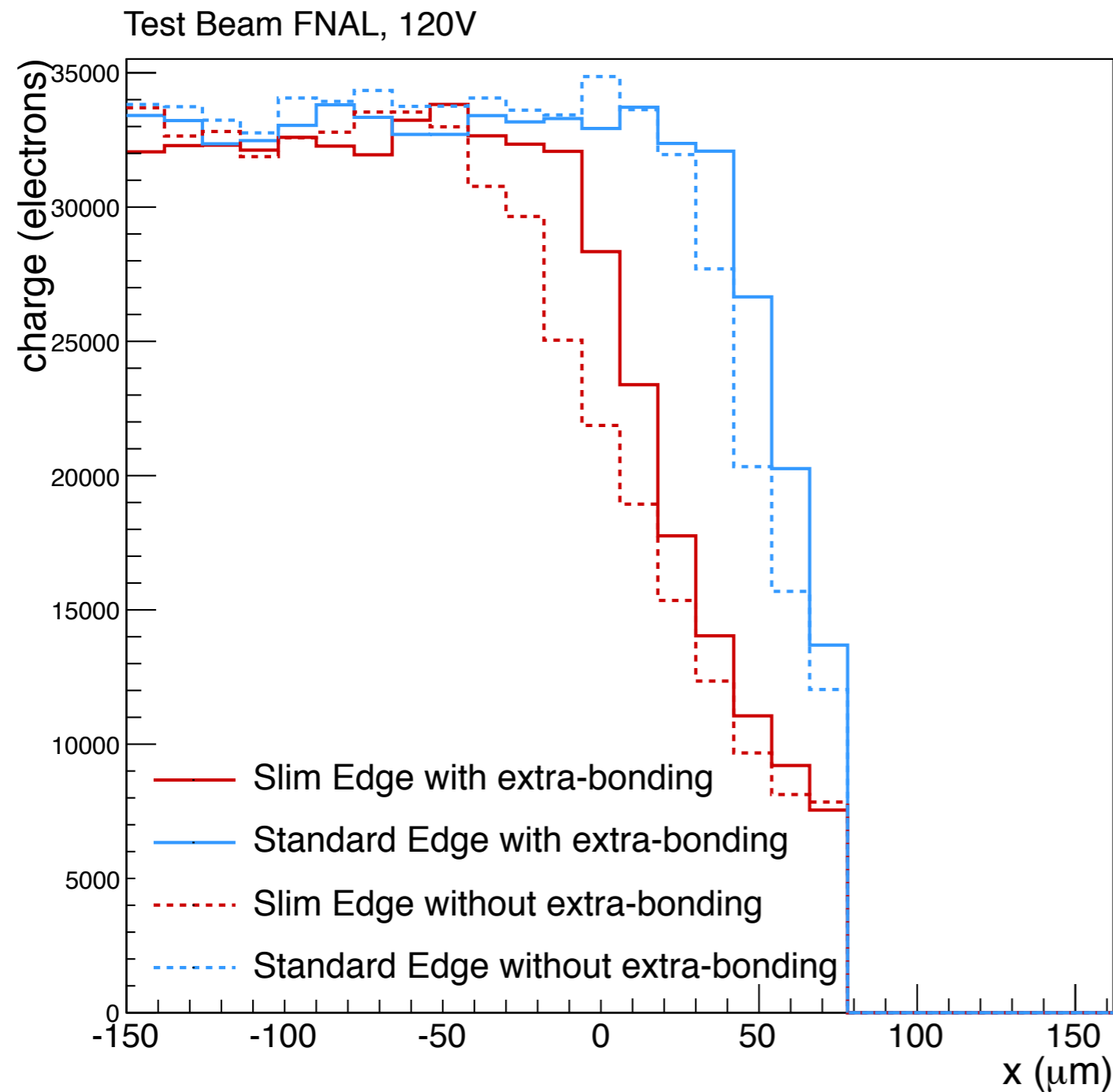
After dicing and bump-bonding there is a new linear component on the I-V curves that is likely associated with the geometry of the slim edge.



Wire bonding of the innermost (fat) guard-ring affects the behavior of the IV curve as it brings the electric field closer to the diced edge

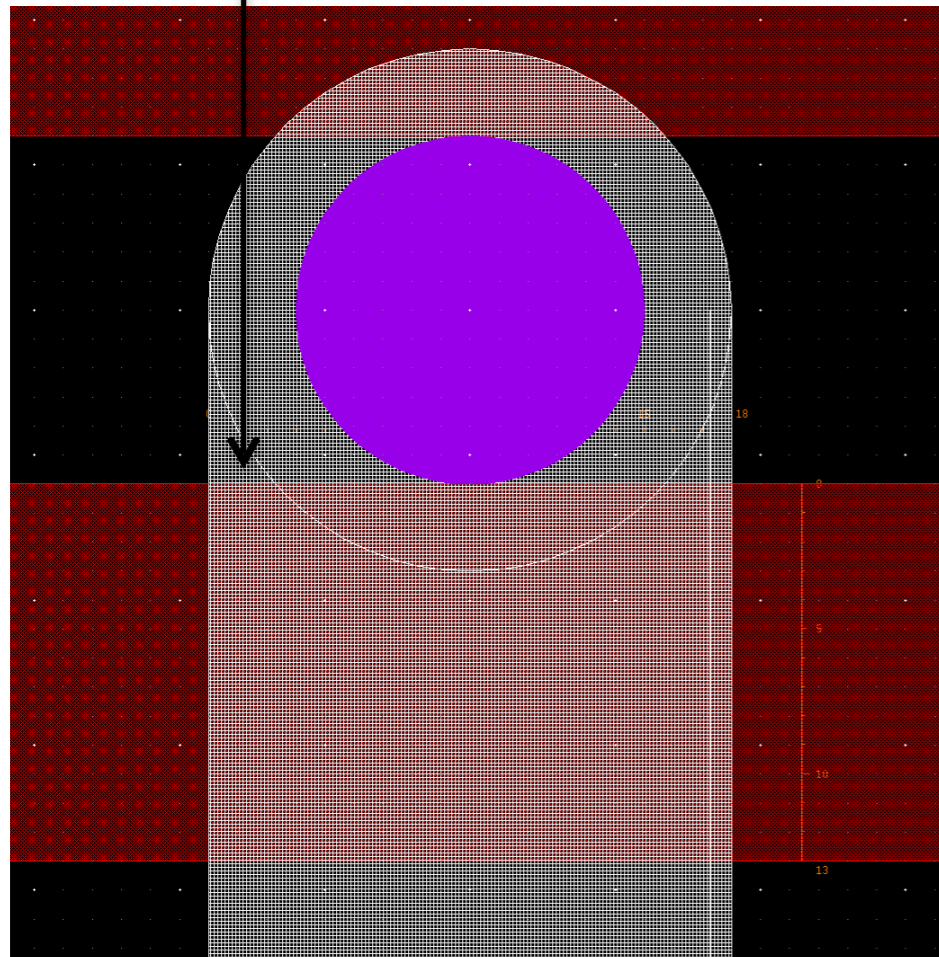
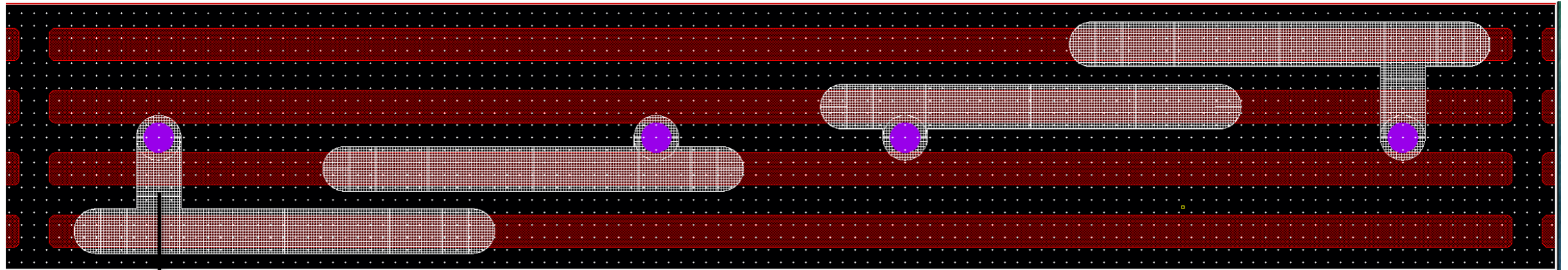


Slim-Edge, charge



- * Slim edge has worse performance
- * Loss of efficiency in charge collection in half of the pixel ($75\mu\text{m}$)
 - * but we recover $950\mu\text{m}$ active area in between pixels
- * The extra bonding helps to recover charge

25x600, closer look at the bonding



18 μm x 13 μm capacitance with an SiO₂ thickness of 900 Å results on ~85 fF

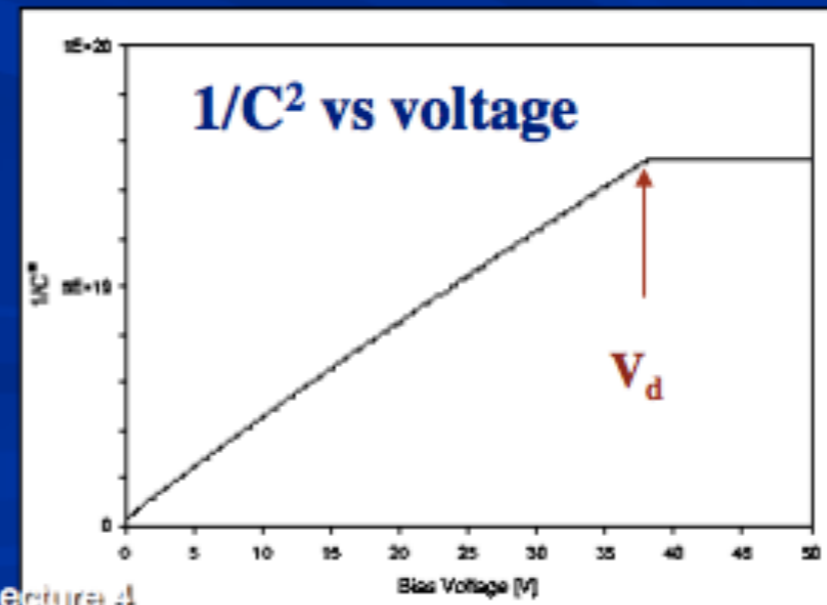
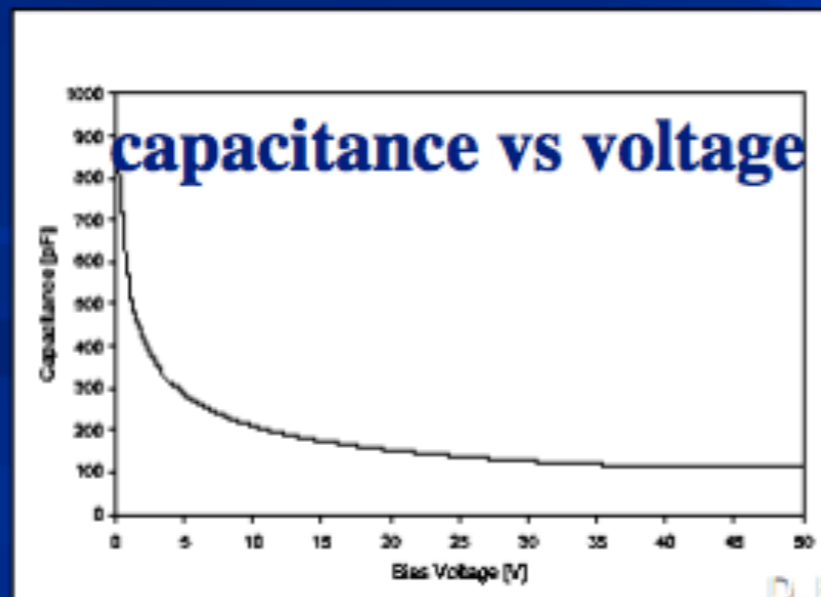
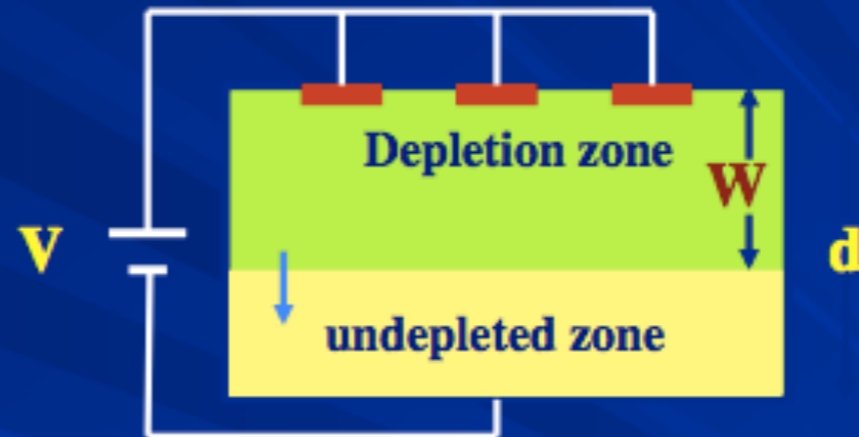
This capacitor can contribute to

- the capacitive load for the preamp
- spurious charge sharing between adjacent pixel

Depletion Zone & Capacitance

- The depletion voltage can be determined by measuring the capacitance versus reverse bias voltage. The capacitance is simply the parallel plate capacity of the depletion zone.

$$C = \frac{\epsilon A}{d} = A \sqrt{\frac{\epsilon}{2\rho\mu V_b}}$$



D. Bortoletto Lecture 4

25